UNIVERSITÄT
DUISBURG
ESSEN

Institute of Ship Technology und Transport Systems
University Duisburg-Essen

ADEL EBADA

INTELLIGENT TECHNIQUES-BASED APPROACH FOR SHIP MANOEUVRING SIMULATIONS AND ANALYSIS

(Artificial Neural Networks Application)

2007

UNIVERSITÄT
DUISBURG
ESSEN

INTELLIGENT TECHNIQUES-BASED APPROACH FOR SHIP MANOEUVRING SIMULATIONS AND ANALYSIS

(Artificial Neural Networks Application)

Von der Fakultät für Ingenieurwissenschaften
Abteilung Maschinenbau der
Universität Duisburg – Essen

zur Erlangung des akademischen Grades

DOKTOR-INGENIEUR

genehmigte Dissertation

von

Adel Ebada

aus

Alexandria, Ägypten

Referent: Prof. Dr.-Ing. Moustafa Abdel-Maksoud

Korreferent: Prof. Dr.-Ing. habil. Mathias Paschen

Tag der mündlichen Prüfung : 29 .05 .2007

Acknowledgment

I hear by record my gratitude to my supervisor, Professor Dr.-Eng. Moustafa Abdel-Maksoud and my co-advisor Prof. Dr.-Eng. habil. Mathias Paschen for their guidance, support, and encouragements, which greatly helped me finish this research in due course. I am also heavily indebted to my colleague Adel Ghetany in the "Norcontrol simulators" and my colleagues in the integrated simulators complex of "Ship Analytic Ship Simulators" of the Arab Academy for Science and Technology and Maritime Transport who readily helped me do the maneuvering experiments of the different ships types.

Last but not least, I wish to acknowledge the financial support of the Arab Academy for science and technology and Maritime Transport for giving me the opportunity to pursue my doctoral degree in Germany.

Adel H. M.A. Ebada

Duisburg, 29th May 2007

Abstract

The aim of this thesis is to establish a reliable, replicable, and consistent Artificial Intelligent (A.I.) system, capable of predicting accurately the turning tracks of ships. The Artificial Neural Networks (ANN) method has been adapted to solve this problem. The physical and operational data of a ship are described and used as inputs into the system in order to predict the turning manoeuvres.

The thesis focuses on both approaches of direct and force models. The ship and controllability data such as underwater hull, rudder and propeller are parameterized and introduced into the system in order to build the direct model for simulating ship manoeuvring motion. The developed method has also been explored in order to include the hydrodynamic forces acting on ships. The initial forces and moments acting on the ship have been described and investigated. The neural system is reinstructed and retuned to solve the prediction problem not only for ensuring more accuracy but also to have deeper insights in the effects of hydrodynamic forces on ship motions, especially the turning manoeuvres. To demonstrate creditability, and confidence in the method used, the results of the program performance were tested against data obtained from ship handling simulators.

Parallel Artificial Neural Networks (PANN) is formulated and implemented in MATLAB (instructed, tuned and trained) in order to predict the manoeuvring behaviour of different ship types with variation of sizes, displacements, speeds and rudder angles. Results obtained from the models are compared with the results generated by two different simulators using different ships. The system accuracy and consistency are quantified by the standard deviation.

Data optimizers with series models have been established and the emphasis came with higher accuracies and better performance than the general model (direct or force model). The prominence of this application leads to wider applications and better abilities to solve multi-problems, related to the focus theme of the research.

The thesis investigates and analyses the diverse results obtained from different prediction models. Thus, it leads to one of the essential points in this research in order to realise the range of the coherence of the applied-based approach. It is essential to study these issues and to analyse the performance of both approaches when applying the environmental conditions in the future to ensure a satisfactory prediction system.

The outcome results indicate that the introduced system is capable of thoroughly analysing ship manoeuvring motion and of comparing different ships' parameters. This system provides the users in advance with the characteristics of transient phases of ship motion. It simulates the real manoeuvring motion before any online training. Further, discussions of recent and future applications are stated in this thesis.

The introduced approach proved to be systematic and valid and can take on a variety of forms. System identification techniques, theoretical prediction methods and regression analysis results from other application techniques are also discussed in this thesis.

Contents

Contents……...I
List of figures…….....VI
List of tables…….....XI
Acronyms and Symbols…….....XII

Preface XXI
Motivation XXI
Operational Manoeuvring Problems Definition……XXII
Human Factor Problems..... XXIII
Previous Related Studies……. XXIII
Present Contributions……...XXIV
Aims and Objectives of the Research XXVI
Methodology XXVII
Organization of the Dissertation XXVII

Chapter 1 1
1 Artificial Intelligence (A.I.) 1
1.1 Introduction 1
1.2 Defining AI 1
1.3 A Brief History of AI 2
1.4 The Disciplines of AI 2
1.4.1 Learning Systems..... 3
1.4.2 Knowledge Representation, Reasoning, Planning and Intelligent Search..... 3
1.4.3 Logic Programming 4
1.5 Soft Computing 4
1.5.1 Fuzzy Logic 4
1.5.2 Artificial Neural Nets 5
1.5.3 Genetic Algorithm 5
1.5.4 Neural Network and Fuzzy Logic..... 5
1.6 Literature Review..... 6

1.6.1 Overview of Previous and the Recent Applications of Artificial Intelligence (A.I)..... 6
1.6.2 Applying A.I. in Marine Control Applications..... 6
1.6.3 Applying Artificial Neural Networks (ANN) in Marine Applications..... 7

Chapter 2 12
2 Artificial Neural Networks..... 12
2.1 Introduction..... 12
2.2 History of the Artificial Neural..... 12
2.3 Neural Network Structure..... 13
2.3.1 Different Network Type Structures..... 14
2.3.2 The Multilayer-Feed Forward Network..... 16
2.4 Training Styles..... 16
2.4.1 Introduction..... 16
2.4.2 Back Propagation Algorithm..... 16
2.5 Supervised and Unsupervised Learning..... 17
2.6 Benefits of Neural Networks and Application Areas..... 18
2.7 The Utilization of ANN in the Thesis..... 19
2.8 Conclusion..... 20

Chapter 3 21
3 Ship Motion Prediction..... 21
3.1 Introduction..... 21
3.2 Equations of Motion..... 21
3.3 Overview of Previous Work..... 25
3.4 Applying of Numerical Simulations Models..... 27
3.5 Turning Circle Manoeuvre..... 28
3.5.1 Turning Motion..... 28
3.5.2 Ship Turning Characteristics..... 29
3.6 The Interface of the ANN as a New Prediction Tool in this Thesis..... 30

Chapter 4 32
4 The Applied Method, Instructing and Tuning ANN..... 32
4.1 Introduction..... 32

4.2 The Main Steps to Create the Model……32
4.3 Generation of the Manoeuvring and Experimental Data 35
4.4 Specifications for Considerations on the ANN Model 39
4.5 Simulative Models using ANN 40
4.5.1 The System's Mathematical Model Architecture 40
4.5.2 Parallel Neural Networks (PNN) Architecture 43
4.5.3 Artificial Neural Networks (ANN) Layers Architecture 45
4.5.4 BPFFNN Architecture 48
4.6 Training and Prediction Procedures 50
4.6.1 Pre Training Procedures 50
4.6.2 Training Procedures 50
4.6.3 Neural Network Predictor 54
4.7 Probability and Accuracy 55
4.8 Improving the Performance of Neural Network Predictor 56
4.9 Decreasing the Limitations of System Prediction 59
4.10 Conclusion 61

Chapter 5 63
5 Neural Hydrodynamic Force Model 63
5.1 Introduction 63
5.2 Propeller-Hull and Rudder Interaction 63
5.3 Ship Resistance and Propulsion 64
5.3.1 Power Estimation and Prognosis 65
5.4 Rudder lift forces 67
5.5 ANN Force Model Prediction Systems 70
5.5.1 Data Generation 70
5.5.2 Data Formation and Structure 72
5.5.3 Force Model Architecture 74
5.5.4 System Validation 75
5.6 Estimation of the Differences in the Initial Side Forces between Port and Starboard Turns 78
5.7 Improving the Performace through Optimizing the Data among Model Series……82
5.8 Conclusion ……88

Chapter 6 90
6 Results and Analyses 90
6.1 Introduction 90
6.2 Turning Circle Limitation 90
6.3 Manoeuvre Tracks 91
6.4 Simulation Results 92
6.4.1 NN Direct Model Results 92
6.4.2 NN General Force Model 96
6.4.3 NN Series Force Models 97
6.5 Prediction Results of using Ship Analytics Ship Simulators Data as another Source of Verification 99

Chapter 7 101
7 Summary and Conclusions 101
7.1 Summary 101
7.2 Conclusions and Implications 102
7.3 Future Directions 105

References 107

Appendices 116
Appendix A 116
A.1 Training and Testing Results of Turning Circle Limitation 116
A.2 Testing Results: Plotting of Turning Circle Limitation 117
Appendix B 119
B.1 Manoeuvres Track Results (performance, goal and epochs) 119
B.2 Manoeuvres Track Results (different ships and rudder angles) 119
B.3 Manoeuvres Track Results (VLCC turning manoeuvre) 121
Appendix C 122
C.1 Simulation Results: Direct Model (performance, goal and epochs) 122
C.2 Simulation Results: Direct Model (different ships and rudder angles) 122
C.3 Simulation Results: Direct Model (port and starboard turn at same δ_r) 124
C.4 Simulation Results: Direct Model (graphes) 125
Appendix D 132
D.1 General Force Model Results (simulation) 132

D.2 General Force Model Results (graphes) 133
Appendix E 135
E.1 NN Series Force Model Results (simulation) 135
E.2 NN Series Force Model Results (graphes) 136
E.3 NN Series Force Model Results (simulation and graphes, Container 2) 138
Appendix F 140
F.1 Training Performance Results “Ship Analytics Ship simulators”..…… 140
F.2 Testing Results of Maximum Advance and Total Diameter
“Ship Analytics Ship Simulators” 142
F.3 Testing Results of Turning Manoeuvre Tracks
“Ship Analytics Ship Simulators” 143
F.4 Simulation Testing Results “Ship Analytics Ship Simulators” 144
Appendix G 145
G.1 Main Ship Parameter and Input Data (Norcontrol Simulators) 145
G.2 Norcontrol NavSim (Models Documontation) 146
G.3 Main Ship Parameter and Input Data
(Ship Analytics Ship Simulators) 146
Appendix H 147
H. 1 Containership 1 (Luna) 147
H. 2 Containership 2 (Jutlandia) 148
H. 3 Bulk Carrier (Norseman) 150
H. 4 VLCC (Nicoline) 151
Appendix I Ship Analytics Ship Simulators Figures 152

List of Figures

Figure 2.1 : Basic Structure of a Single Neuron 13
Figure 2.2 : One technique of black propagation algorithm 17

Figure 3.1 : Surface ship with body axes *O*(*XYZ*) within space- fixed (MSC/Circ.1053) 22
Figure 3.2 : Free running model tests: Optical tracking system 26
Figure 3.3 : Turning circle definition of bulk carrier 29

Figure 4.1 : Block diagram demonstrate the model prediction 41
Figure 4.2 : Parallel Neural Net works Architecture with one decision output in each 43
Figure 4.3 : Parallel Neural Net works Architecture with different decision output in each 44
Figure 4.4 : Parallel Neural Net works Architecture with two decision output in each 44
Figure 4.5 : One single architecture of multiple layers of neurons that constructed in PNN 45
Figure 4.6 : One single architecture of multiple layers diagram 46
Figure 4.7 : Architecture of BPFFNN 49
Figure 4.8 : Error minimization in training process 51
Figure 4.9 : Epochs and goal of one cases set of PNN which is 8.47451*10-5 to get a high training performance 52
Figure 4.10: Results of training goal for the outcome cases set of figure 4.9 which is 8.47451*10-5 52
Figure 4.11: Epochs and goal for other cases set 53
Figure 4.12: Results of training different ships model using various rudder angles to port and starboard side 53
Figure 4.13: Left side trained for 100 000 epochs and goal of 5.42369*10-5 and right side: The outcome results of one case set 58
Figure 4.14: Left side shows 46 989 epochs and goal of 8.47451*10-5 and right side : The outcome results of the same case at figure 4.13 but with different error probability 59

Figure 5.1 : Block diagram of the force model prediction..... 75
Figure 5.2 : Training result using one only of the port side data of Containership 1 as turning to starboard side, rudder 35 degrees and speed 22.1 *knots*..... 76
Figure 5.3 : Training result using the right data of Containership (1) of turning to starboard side, rudder 35 degrees and speed 22.1 *knots* 77
Figure 5.4 : Turning manoeuvre tracks test to starboard side of VLLC, approach thrust = 1642 (speed = 14.7 *knots*) and the initial rudder lift force = 1166 *kN* (δr= 25°)-(Force Model)..... 80
Figure 5.5 : Turning manoeuvre tracks test to port side of VLLC, approach thrust = 1642 (speed = 14.7 *knots*) and the initial rudder lift force = 1280 *kN* (δr= 25°)-(Force Model)..... 81
Figure 5.6 : Turning manoeuvre tracks to port side of tuned initial lift force of VLLC, approach thrust = 1642 (speed = 14.7 *knots*) and the initial tuned rudder lift force = 1395 *kN* (δr= 25°) - (Force Model)..... 82
Figure 5.7 : Block diagram of the force model prediction through optimizing the data between two models series..... 83
Figure 5.8 : Performance and goal of one case of PNN for force model (Bulk carrier and VLCC) series (2) at 50000 epochs..... 87
Figure 5.9 : Results of training goal of 50000 epochs for the outcome case of figure 5.3..... 87
Figure 5.10: Future block diagram demonstrates the force model prediction through optimizing the data among models series……..88

Figure 6.1 : Training results of different ships using various rudder angles to port and starboard side (Direct Model)..... 116
Figure 6.2 : Tests results of turning manoeuvre of different ships using various rudder angles to port and starboard side (Direct Model) 116
Figure 6.3 : Test results of the maximum advance and total diameter using various rudder angles to port and starboard side (Direct Model)..... 118
Figure 6.4 : Difference in the turning manoeuvres limits of VLCC to port and starboard with same rudder angle (Direct Model)..... 118
Figure 6.5 : One case of PNN, the left: Performance, goal and epochs and the right : The results of the one case in the left figure (Direct Model). 119

Figure 6.6 : Turning manoeuvre tracks of different ships at various rudder angles (Direct Model) 121
Figure 6.7 : Turning manoeuvre tracks of VLLC, δr= 25° degrees to both sides (Direct Model) 121
Figure 6.8 : One case of PNN of the direct model, the left side: Performance, goal and epochs and the right side: The results of the one case in the left figure..... 122
Figure 6.9 : Training results of the direct model, prediction of turning manoeuvre motion of different ships using various rudder angles to port and starboard side..... 123
Figure 6.10: Test results of the direct model, prediction of turning manoeuvre of different ships using various rudder angles to port and starboard side 124
Figure 6.11: Test results of the direct model, prediction of turning manoeuvre of containership 2, δr =05 degrees to both sides 124
Figure 6.12: Test results of the direct model, prediction of turning manoeuvre of bulk carrier, δr = 30 degrees to both sides 125
Figure 6.13: Test results of the direct model, prediction of turning manoeuvre of bulk carrier, δr = 10 degrees to both sides 125
Figure 6.14 : Training and test results of the direct model, prediction of the main parameter of turning manoeuvre to the starboard side 128
Figure 6.15 : Training and test results of the direct model, prediction of the main parameter of turning manoeuvre to the port side 131
Figure 6.16 : Testing results of the general force model, simulation of the turning manoeuvre motion of different ships using various rudder angles and speeds to starboard side 133
Figure 6.17 : Test results of the general force model, prediction of the main parameter of turning manoeuvre to the starboard side. 134
Figure 6.18 : Testing results of force model (series 1), simulation of the turning manoeuvre motion of different ships using various rudder angles and speeds to starboard side 135
Figure 6.19 : Testing results of force model (series 2), simulation of the turning manoeuvre motion of different ships using various rudder angles and speeds to starboard side 136

Figure 6.20 : Test results of force model series (1&2), prediction of the main parameter of turning manoeuvre to the starboard side. 137
Figure 6.21 : Testing results of force model (series 1), simulation of the turning manoeuvre motion of containership 2 using same rudder angle to starboard side but different speeds 138
Figure 6.22 : Testing results of force model (series 1), simulation of the turning manoeuvre motion of containership (2) using δ r= 35° to starboard side but different speeds (15.5 *Knots* & 25.5 *Knots*)..... 139
Figure 6.23 : Epochs and performance of two training process for both simulators measured data..... 140
Figure 6.24 : Epochs and performance of two training process for both simulators measured data (second iteration) 140
Figure 6.25 : Results of the training performance of figure 23 Norcontrol Simulators and Ship Analytics Ship Simulators (last four cases of Ship Analytics Ship Simulators)..... 141
Figure 6.26 : Results of the training performance of figure 24 Norcontrol Simulators and Ship Analytics Ship Simulators (last four cases of Ship Analytics Ship Simulators)..... 141
Figure 6.27 : Test results of the maximum advance and total diameter using various rudder angles to starboard side (Direct Model), (Ship Analytics Ship Simulators)..... 143
Figure 6.28 : Test results of turning manoeuvre tracks of containership 2 at two different speeds with same rudder angles (Direct Model) - (Ship Analytics Ship Simulators)..... 143
Figure 6.29 : Test results, prediction of turning manoeuvre of two different ships' types using different rudder angles to starboard side (Direct Model) - (Ship Analytics Ship Simulators)..... 144

Figure H.1.1: Containership 1 (Luna), during cargo operation, MDI (Danish Maritime Institute), simulator mathematical model updated in 2001..... 147
Figure H.1.2: Containership 1 (Luna), ship rudder drawing, MDI (Danish Maritime Institute) 147

Figure H.2.1: Containership 2 (Jutlandia), a stern profile of rudder and propeller, MDI (Danish Martime Institute), simulator mathematical model updated in 2001 148
Figure H.2.2: Containership 2 (Jutlandia), water plan at loaded draft MDI (Danish Martime Institute) 149
Figure H.3 : Bulk carrier (Norseman), a stern, ship profile and plan view MDI (Danish Maritime Institute), simulator mathematical model updated in 2001 150
Figure H.4.1: VLCC (Nicoline), during sailing time, MDI (Danish Maritime Institute), simulator mathematical model updated in 2001 151
Figure H.4.2: VLCC (Nicoline), a stern profile of rudder and propeller MDI (Danish Maritime Institute) 151
Figure I.1 : Containership 2 (Code: C057L), Simulator Ship: GIN505F 152
Figure I.2 : Bulk Carrier (Code: K070L), Simulator Ship: GIN523F 152
Figure I.3 : VLCC (Code: T300L), Simulator Ship: GIN517F 153

List of Tables

Table 4.1 : Ships' start conditions at rudder angles ordered (δ_{RO}) and at time (t_o) 37
Table 4.2 : Sample from the four ships data files at 100 seconds from (δ_{RO}) at (t_o) 38
Table 4.3 : Sample from the four ships data files at 360 seconds from (δ_{RO}) at (t_o) 39
Table 4.4 : Main transient phases' standard deviations of the dircet model predictor for one of the random test selection..... 56

Table 5.1 : Thrust forces and rudder lift forces replaced (δ_r) and (U_G) for containership (1) 71
Table 5.2 : Thrust forces and rudder lift forces replaced (δ_r) and (U_G) for the VLCC..... 71
Table 5.3 : Differences in the initial side force of same rudder angles to both sides port and starboard..... 79
Table 5.4 : Different accuracies between starboard and port turn applying the predictor estimation of the differences in the initial side forces between both sides 81
Table 5.5 : Main transient phases' standard deviations of the NN general force model predictor for one of the random test selection 84
Table 5.6 : Main transient phases' standard deviations of the force model (series 1) predictor for one of the random test selection..... 85
Table 5.7 : Main transient phases' standard deviations of the force model (series 2) predictor for one of the random test selection..... 85
Table G.1 : Main ship parameter and input data (Norcontrol Simulators)……145
Table G.3 : Main ship parameter and input data (Ship Analytics Ship Simulators)……...146

Acronyms and Symbols

Acronyms

A.I	Artificial Intelligence
ANN	Artificial Neural Network
ARMA	Auto-regressive Moving Average
ARPA	Automatic Radar Plotting Aid
ART	Adaptive Resonance Theory
BPFFNN	Back Propagation Feed Forward Neural Network
BPTT	Back Propagation through Time
DNU	Dynamic Neural Unit
DP	Dynamic Positioning
GA	Genetic Algorithm
IMO	International Maritime Organization
ISM	International Safety Management
MIMO	Multi-input Multi-output Model
MLP	Multi-Layer Perceptron
MNN	Memory Neuron Networks
NF	Neuro Fuzzy
NNDL	Neural Network Development Laboratory
NSWC	Naval Surface Warfare Centre
PANN	Parallel Artificial Neural Network
PROLOG	Programming in Logic
RNN	Recurrent Neural Networks
RTRL	Real Time Recurrent Learning
SOLAS	Safety of Life at Sea (International convention)
SOM	Self-Organizing Map
TDNN	Time-Delay Neural Network
VTS	Vessel Traffic Services

Symbols

Latin Symbols

A	Area in general (m^2)
A.C.	Admiralty Coefficient
A_1	Rudder area that faces propeller slipstream (m^2)
A_2	Rudder area that faces speed of advance at ship's stern (m^2)
A_{HL}	Lateral area of the hull (m^2)
A_P	Projected blade area (m^2)
A_R	Rudder area (m^2)
A_{RF}	Flap area (m^2)
A_{RT}	Total rudder area ($A_{RX} + A_{RF}$) (m^2)
A_{RX}	Area of the fixed part of rudder (m^2)
a	Input neurons (ANN)
a_D	Developed blade area ratio A_D / A_O
a_E	Expanded blade area ratio A_E / A_O
$a_H^{'}$	Ratio of the induced force on the hull by the interaction of the rudder to the rudder force
a_P	Projected blade area ratio A_P / A_O
B	Beam or breadth, moulded of ships hull (m)
B	Center of buoyancy (m)
b	Rudder height (span) (m)
c	Chord length (m)
C_B	Block coefficient [$\nabla / (L\ B\ T)$]
$C_D\ (x^{'})$	Drag coefficient due to the cross flow
C_L	Lift force coefficient
c_m	Mean chord length (m)
C_P	Pressure coefficient
C_q	Resistance coefficient ≈ 1
c_r	Chord length at the root (m)
c_t	Chord length at the tip (m)

C_{Th}	Thrust loading coefficient $\left(\frac{8}{\pi} \cdot \frac{K_T}{J^2}\right)$
D	Drag force (N)
D	Propeller diameter (m)
D	Depth, moulded, of a ship (m)
d, T	Draft, moulded, of ship hull (m)
E	Error function (least squares) (ANN)
F	Force (N)
F_n	Froude's number
F'_N	Rudder normal force (N)
f	Activation function (ANN)
G	Centre of gravity, center of gravity of a vessel (m)
$_G$	Subscript ($_G$) denotes the value referred to the centre of gravity
g	Acceleration of gravity (m/s^2)
I	Moment of inertia ($kg\ m^2$)
I_z , I_{zz}	Yaw moment of inertia around the principal axis-z ($kg\ m^2$)
i	Neurons in the input layer are labelled with the subscript (ANN)
J	Propeller advance coefficient ($V_A\ /\ nD$)
J_{zz}	Added moment of inertia about midship, axis-z ($kg.m^2$)
j	Index of output neuron (ANN)
j	Labelled subscript of the Hidden neurons (ANN)
$j\ net$	Input for the activation function of neuron j in the hidden layer (ANN)
K	Keel reference
k	Labelled subscript of the output neurons (ANN)
K_Q	Propeller torque coefficient ($T / \rho\ n^2\ D^5$)
K_T	Propeller thrust coefficient ($T / \rho\ n^2\ D^4$)
L	Length (m), Length of ship (m), Length of waterline (m)

L	Lift force (N)
L	Total rudder lift force (N)
V	Displacement volume (m^3)
L_1	Rudder lift force at A_1 (N)
L_2	Rudder lift force at A_2 (N)
LOA	Length, overall (m)
LPP	Length between perpendiculars (m)
M	Midships
M	Moment of forces (Nm)
M	Momentum ($Kg.m/s$)
m	Mass (kg)
m'_y	Dimensionless hydrodynamic mass in the y-direction
N_A	Aerodynamic moment in acting to z-coordinate (Nm)
N_H	Hull moment acting to z-coordinate (Nm)
N_P	Propeller moment acting to z-coordinate (Nm)
N_R	Rudder moment acting to z-coordinate (Nm)
N'_r	Added moment of inertia about midship
n	Rate of revolution, propeller rotation speed, rotational speed (rps)
o_{pj}	Represents the actual output at that node (ANN)
p	Angular (rotary) velocity around body axis-x ($1/s$, $degree/s$)
P	Pressure (N/m^2)
P	Propeller pitch (m)
P	Pattern index (ANN)
P	Power (W)
P_B	Brake power (W)
P_D	Delivered power at propeller (W)
P_E	Effective power (W)
P_I	Indicated power (power required at engine) (W)
P_S	Shaft power (W)

P_t	Total pressure (N/m^2)
P_T	Thrust power (W)
Q	Torque P_D / ω (Nm)
QPC	Quasi -Propulsion coefficient
R	Propeller radius (m)
R	Resistance force (N)
R ,r	Radius (m)
$R.P.M$	Propeller revolution per minute ($1/min$)
$R.P.S$	Propeller revolution per second ($1/s$)
R_F	Frictional resistance of a body (N)
R_n	Reynolds number
R_P	Pressure resistance (N)
R_R	Residuary resistance (N)
R_T	Total resistance (N)
R_V	Total viscous resistance (N)
R_{VP}	Viscous pressure resistance (N)
R_W	Wave making resistance (N)
r	Angular (rotary) velocity around body axis-z ($1/s$, $degree/s$)
r	Propeller slipstream radius in rudder position (m)
$\dot{r}$	Yaw acceleration, angular acceleration about body z-axis (rad/s^2, $degree/ s^2$)
r_∞	Theoretical slipstream radius far behind the propeller (m)
r_o	Half of the propeller diameter (m)
S	Area of hull wetted surface (m^2)
S	Propeller span length (m)
S_j	Hidden layer output for a neuron (ANN)
T	Propeller thrust (N)
T	Period (s)
T, d	Draft, moulded, of ship hull (m)
t	Iteration number (ANN)
t	Thrust deduction fraction

t	Time (s)
t_o	Time at process start
t_{pj}	Target output for pattern p on node j (ANN)
U	Actual ship velocity (m/s)
u	Advance velocity (m/s)
u, v_x	Velocity component indirection of x-axis (m/s)
u_p	Effective relative inflow velocity in axial direction to propeller
$\dot{u}$	Advance acceleration, surge acceleration, linear acceleration along body x-axis (m/s^2)
u'	Non dimensional velocity in x-direction
$\dot{u}'$	Non dimensional acceleration in x-direction
$\dot{v}$	Advance acceleration, sway acceleration, linear acceleration along body y-axis (m/s^2)
v'	Non dimensional velocity in y-direction
$\dot{v}'$	Non dimensional acceleration y-direction
V	Velocity, ship speed (m/s)
V	Undisturbed fluid velocity (m/s)
V	Weight matrices (*output weight matrices of input W*) (ANN)
V_A	Local fluid velocity (m/s)
V_A	Propeller advance speed, speed of advance (velocity behind ship), speed of water passing propeller (m/s)
V_{corr}	Mean value of the axial speed component over the slipstream cross section, it is corrected according to the momentum theorem (m/s)
V_{KN}	Speed in knots (kn)
V_x	Mean axial speed of the ship stream at rudder position (m/s)
V_∞	Mean axial speed of the ship stream far behind the propeller (m/s)
v, v_y	Velocity component indirection of y-axis (m/s)
$_y$	Subscript ($_y$) denotes the value referred to the y-coordinate
W	Weight matrices (ANN)
W	Wake fraction
X	Measured force in the x-direction (N)

X	Distance of the respective position behind the propeller plane (m)
X	Input vector (ANN)
X_A	Aerodynamic force in x-coordinate direction (N)
$X^{'}$	Dimensionless force of force coefficient in x-direction
X_H	Hull hydrodynamic force in x-coordinate direction (N)
X_P	Propeller force in x-coordinate direction (N)
X_R	Rudder force in x-coordinate direction (N)
$X'(u)$	Dimensionless hull resistance in straight ahead motion
X'_{RO}	Dimensionless rudder resistance in straight ahead motion
X'_{rr}	Coefficients due to resistance increment which are mainly caused by the motion, theoretically corresponds to $m'_{y}\ \alpha'$
$X'_{vr}, X'_{vv}, X'_{rr}$	Coefficients due to resistance increment which are mainly caused by the motion
$X'_{\dot{u}} = m'_x$	Dimensionless hydrodynamic mass in the x-direction
x'_H	X-coordinate of the application centre of the induced force acting on the hull due to the interaction by the rudder
x'_R	X-coordinate of the application centre of normal force of the rudder
x_i	Absolute displacement of the ship at the reference point i = 1, 2, 3: surge, sway, and heave respectively
x'_P	Donates the x-coordinate of the propeller position
x	Subscript ($_x$) denotes the value referred to the x-coordinate
Y	Force y in Y direction
Y_A	Aerodynamic force in y-coordinate direction (N)
Y_H	Hull hydrodynamic force in y-coordinate direction (N)
Y_P	Propeller force in y-coordinate direction (N)
Y_R	Rudder force in y-coordinate direction (N)
Y'	Force coefficient in Y direction
$Y'_{\dot{v}}$	Dimensionless added mass in the y-direction (m'_y)
$Y'_{\dot{r}}$	Dimensionless added mass about midship, theoretically correspond to ($m'y\alpha'$)
$y_i(t)$	One arbitrary unit activation at time t in a recurrent network

$Y_{\dot{u}}^{'} = m_{y}^{'}$	Dimensionless hydrodynamic mass in the *y*-direction
Z	Number of propeller blades
$_{z}$	Subscript ($_z$) denotes the value referred to the *z*-coordinate

Greek Symbols

α	Angle of attack (*rad. or degree*)
α	Momentum (*Kg.m/s*)
$\alpha^{'}$	*X*-coordinate of the centre of $m^{'}_{y}$
Λ	Rudder aspect ratio
Δr	Added value to potential slipstream radius because of the increasing in the slipstream diameter with increasing *X* due to turbulent mixing with the surrounding fluid (*m/s*)
$\Delta^{'}$	Non dimensional displacement
Δ	Displacement (buoyant) force g $\rho \nabla$ (*N*)
∇	Displacement volume $\Delta / (\rho$ g) (m^3)
β	Drift angle (angle between *U* and the *x*-coordinate) (*rad. or degree*)
β	Angle of drift or side-slip (*rad. or degree*)
δ_{RO}	Rudder angle ordered
δ_{r}	Rudder deflection angle (*rad. or degree*)
η	Learning rate
η	Efficiency
η_m	Mechanical efficiency
η_T	Transmission efficiency
η_D	Propulsive efficiency
η_H	Hull efficiency
η_O	Open-water propeller efficiency
ρ	Density of the fluid (M/L^3 *mass/unit volume*)
ρ	Mass density (kg/m^3)
$\rho V^2/2$	Dynamic pressure (N/m^2)

$1/2\,\rho\ V_{corr}^2$	Stagnation pressure (N/m^2)
ψ	Angle of yaw, heading or course (*rad. or degree*)
$\dot{\psi}$	Yaw velocity, angular velocity about body *z*-axis (*1/s, degree/s*)
$\ddot{\psi}$	Yaw acceleration, angular acceleration about body z-axis ($1/s^2$)
σ	Standard deviation

Preface

Motivation

Today combinations of traditional and modern ships sailing all over the world and have completely different manoeuvring characteristics. New global researches have found a large margin in manoeuvring behaviour between traditional ships and modern designs. The large margin is not only for the new developments of the container ships, but also for the other types such as RoRo, RoPax, Ferry and Cruise vessels. For maintaining a high safety factor level, it needs to clarify the safe mode of navigation and ship manoeuvrability behaviour in different circumstances.

Ships' manoeuvrability is the main factor to construct the approaches to the ports, channels as well separation skim and generally the manoeuvring areas. In addition to the human factors such as ships' crew, pilots, Vessel Traffic Services (VTS) and shore operational warnings and advices are constructed operational problems.

IMO regulations and recommendations issued by the Maritime Safety Committee and the other publications attained a good level of safety but they did not provide the ship's Master till now with an easy computerized solution in order to predict in advance the ship motions for his identified ship in different conditions. IMO recommendations and the criteria stated in Resolution A.601 (15) for all new ships subject to the requirements of the 1974 SOLAS Convention, as amended, regarding to the pilot card, wheelhouse poster and manoeuvring booklet in addition to the other IMO requirements are mainly based on sea trails in ballast condition and calculated loaded conditions which do not actually represent the real world. Such criteria provide only a general unified boundary of ship manoeuvring behaviour.

The International Safety Management (ISM) Code and its guidance for safe operation of ships and for pollution prevention is a good step forward but its policy is poor to apply an intelligent technique which could enhance the emergency manoeuvring procedures for solving the ambiguity area of manoeuvring behaviour for any specific condition.

Operational Manoeuvring Problems Definition

In the last decade new ship designs have been innovated and thus their dynamic characterization change rapidly. The mirror sterns are commonly built to optimize calm water resistance and to increase the cargo capacity, the bow flare is often increased to allow for additional cargo capacity. The result is a different behaviour in ship motion.

Changes in designs, speeds and size will be increasing in the future. Consequently, ship's Master and crew on board will have difficulties to judge the consequences of these developments and it becomes difficult for them to correctly identify the ship's track and motion in terms of manoeuvring prediction. Some of the large container ships recently suffered form high momentum and were in danger of collision or undefined track. These phenomena have already happened. But appropriate guidance on how to avoid these situations is in general not available. Therefore, the ships may face dangerous phenomena or situation which may require identifying the ship's track and all different transient phases of ship motion against the time factor.

Ships sail in different loading conditions, speeds, drafts, trims and dissimilar stability conditions that have a different manoeuvring behaviour not stated in pilot card, wheelhouse poster and manoeuvring booklet. Consequently, ships will be subject of behaviour ambiguity before decision making-especially in emergency situations and that could lead to their damage or loss.

The main factors formulating the operational manoeuvring problems are not only related to ship motion but, also extend to the sailing area and the environmental conditions. It is multi-problems which may need specific manoeuvre and emergency procedures to ensure safety in dangerous situations (Cockcroft and Lameijer, 1999).

The ship's Master and other officers till now depend on their experience to expect in advance the motions of the ship in the different conditions. Each type of ships has different behaviour as well as the different size. Every ship has its own individual dynamic behaviour with each displacement, trim and stability. Up to

now ships' Masters have to face all these challenges without having adequate system or tools to evaluate the individual ship manoeuvring performance that sail in different circumstances. In addition, ships' Masters need evidence to prove their decisions and that evidence cannot be well clarified without demonstrating the ship dynamic behaviour in all stages of the voyage. These issues formulate one of the most important problems in sea operation.

Human Factor Problems

Studies of the human mind show that the cognitive attitude of ship Master/Human falls short to cope with multi-variable problems and the human mind always tends to simplify complicated problems in order to find a solution such as predicting the ship's motions in different conditions. This fact can be easily traced when ship Master handles a ship in different operational and environmental conditions (Turban, 1993).

The majority of the maritime community believe that reducing speeds in traffic or when entering a narrow channel is a safer action for sailing although it is not the correct action in many cases, especially with some modern vessels and ship's Master needs evidence in order to verify his decisions. Consequently, maintaining high safety factor level needs to clarify the safe mode of navigation and the ship manoeuvrability behaviour in different circumstances. Thus, a reliable system is required to be on board in order to enhance the experience of the ship Master and crew.

The meaning of the field interaction between people and machines is rapidly growing in maritime applications. Decision support and expert systems on board ships need an intelligent system technique to be integrated and user friendly especially in ship motion.

Previous Related Studies

In the previous work that applied ship motion models were never exhaustive enough to cover all possible sailing and environmental conditions. The success of

the previous work in manoeuvring motions prediction depends on the accuracy of the used hydrodynamic derivatives. The main methods to achieve that task are based on model tests or numerical models. These methods are described in chapter three.

In addition to some A.I. applications have been done in motion area of a predictor/controller to dynamic positioning of offshore structures. There are scattered works for specific submarines and ships for special prediction purposes. This motivated the research to give an effort in this new application area. Obviously, complex mathematical models were constructed to simulate ship-motions. The applied methods in this thesis have emerged as a practical technology executing successful manoeuvring motions applications. The thesis methods are different in many phases from the domain of the recently field applications as clarified and discussed in the following chapters.

Present Contributions

The major contributions of the present work can be summarized as follows:

- Artificial Neural Networks models have been developed as a predictive tool of manoeuvring motion simulations. Parallel Neural Networks simulations have been created using different ships and operational data with MATLAB implementation. The work demonstrates that the predictive system exhibit an ability to be robust and accurate when there is a short time needed to make decisions such as in emergency situations. The models' architectures enable the models to simulate the manoeuvring motions of different ship types with any controllability action that is not included in the system. Moreover, the prediction applications could be used as users' familiarization training or on-line application.

- Three approaches that are adopted to solve the manoeuvring motion prediction problems are the direct model, the force model and the series model. The direct model relies on figuring out the visual description based on the ship parameters and the controllability actions. The force model is

applying the main hydrodynamic forces of the rudder and propeller to estimate the ship manoeuvring motions. The series model can be used as a direct or force model to predict ship manoeuvring motions for a specific optimised domain of input data. These three approaches will cover wider applications with the available data. One model could predict the manoeuvring motions without applying the hydrodynamic forces while the other model could.

- The incorporation of the different approaches has the supremacy to solve many manoeuvring motion prediction problems with adequate efficiency such as correcting the data noise and even estimate the missing data.

- The applied methods as applications on-line are faster than the incremental training and predicting mode during the on-line application. Therefore, adequate level of redundancy in the future will be addressed with a built-in off-line predictive system with wider domain of application than the domain of specific data of one unit. Then the main system as off-line training and on-line application will be more effective to enhance the incremental mode of prediction.

- Moreover, the criteria that drive the mechanism of damping the errors tolerance towards the realistic errors of the different manoeuvring motions' variables could be applied to train the system in sailing duration (refer to chapter four). Thus, the measured and stored manoeuvring motion variables from the automatic multiple fusions on board the ship could be inserted into the system prediction. The system would be able with the driving criteria to train immediately as off-line mode. These additional successive experienced data with regard to the same unit would increase the predictive ability of the system in different conditions.

- The data optimization among model series increased the efficiency of the stored exemplars-based learning algorithms. Consequently, in terms of the generalization domain, the computational efforts were decreased dramatically with fast execution time and were gained better ability to detect

the decision boundaries for different manoeuvring motion conditions.

- Regarding to the design and regularity aspects, the applied methods offer an opportunity to analyze the motion performance of different ship types. To integrate the intelligent techniques in this thesis with towing tank application would have many advantages. Some of these advantages are developing the outcome accuracies, better management of time factor and lower the costs. An additional assistance is to verify the IMO manoeuvring requirements in the design stage.

- The intelligent system is practical, easy to handle and of simple application. It could be integrated with other navigation systems such as Auto pilot, ARPA …..etc. in the context of bridge integrated system to support the ship's Master decision. This is not only making for the optimum mode of navigation but also to enhance in the situations of short time needed to make a decision or the system itself can react immediately.

Aims and Objectives of the Research

The main goal of this thesis is to develop new practical mathematical models to be friendly methods for accurate ship manoeuvring motions simulation.

The research hypothesis adapted nonlinear concept to solve the problem in consideration. The work started in the first stage with an initiative to apply intelligent technique as a tool to simulate the ship manoeuvring motion. The second stage of the research focuses on utilizing ship handling simulator to generate different manoeuvring experiments to test the hypothesis through exploring the predicted limits of turning circle manoeuvres as a maximum advance and total diameter. The third stage was devoted to build a mathematical model to solve the problem of ship turning tracks. The fourth stage focuses on developing manoeuvre summation prediction of turning tracks at any rudder angles. In the final stage (the fifth stage), the work was extended to include the hydrodynamic forces influencing the equation of motion for wider applications.

Methodology

Formulating the research strategy commences with research in the related previous and recent work in the perspective of relevant research by means of research development; as preference is exhibited in Chapters 1 and 2.
Understanding and investigating the different topics of A. I. approaches in context helped to select a suitable method for ship motion prediction. In subsequent stages, Artificial Neural Network (ANN) is selected for the application presented in this thesis as a new practical tool. The method is integrated with the tools in MATLAB to simulate the turning manoeuvring motion.

A Navigation simulator was used to generate the data required for the training and validation of the system; the study was further carried out for different types of ships (two containerships, a bulk carrier and a tanker); the ships in the simulator which had been selected were real ships commercially sailing, where the motion in the simulator simulates real ship motion.
Data files of more than hundred experimental manoeuvres were recorded and documented. About two thirds of such data files were provided to the system for training, a second set of the rest of the data files which representing blind manoeuvres were used for validation.

The developed Parallel Artificial Neural Network (PANN) mathematical model captured ships various contributions to motion behaviours through several learning methods related to their physical parameters, control devices and parameters that explain the turning motion. The applied methods have been tested later in another integrated simulators complex of American Ship Analytics Ship Simulators for validation.

Organization of the Dissertation

The dissertation comprises seven chapters as follows:
Chapter 1 discusses previous and recent applications of artificial intelligence (A.I.) and (ANN) in the field of ship operation in addition to research problems.
Chapter 2 explains the artificial neural networks structures, types, training styles

and the choice of ANN to be applied in this research.

Chapter 3 addresses ship motions and manoeuvres in addition to current prediction methods.

Chapter 4 demonstrates and discusses the applied methods and the technique of applying Back Propagation Feed Forward Neural-Network (BPFFNN) and extends to apply the Artificial Parallel Neural-network (APNN) with the different patterns of the transient phases of turns.

Chapter 5 explains the application of applying the hydrodynamic forces on different models. It also discusses the results obtained from the different models and their advantages.

Chapter 6 presents the results and discusses the standard deviation of each variable predicted as one of the characters in transient phases of all predicted turns. Finally,

Chapter 7 presents the conclusions and the original contribution and major achievement of this research work, in addition to the recommendations relating to exploring future research work associated with this dissertation.

Chapter 1

Artificial Intelligence (A.I.)

1.1 Introduction

This chapter provides a brief overview of the disciplines of Artificial Intelligence (AI) and Soft Computing. It also highlights the different topics of A.I. and presents an overview approach to the Artificial Neural Networks (A.N.N).

The subject of A.I. deals with symbolic processing and numeric computation. Knowledge representation, reasoning, planning, learning, intelligent searching and uncertainty management of data and knowledge are the common areas covered under A.I.

The chapter generally discusses the applications of (A.I.) and (ANN) as practical advanced tools in many significant complexity areas of engineering problems in addition to ship motion application and other marine applications.

1.2 Defining A.I.

Three decades ago, John McCarthy has coined the phrase A.I. to refer to the artificial intelligence (Bender and Edward, 1996). Relevant definitions are concerned with comparing the performance of the machine with human ability (Haugeland, 1985), (Kurzweil, 1990). Other definitions of similar concepts were established but none of these definitions has been universally accepted. The main reason at that time was the use of the word “intelligence”, which is by nature an immeasurable quantity or an abstract not subject to analysis.

Later on, much formalization came out to clarify the term “intelligence”. One approach related to Psychologists and Cognitive theorists is that intelligence helps in identifying the right piece of knowledge at the appropriate instances of decision making (Konar, 1994), (Newell and Simon, 1972).

A.I. is a system model which can think and plan (Ling, 1999). It has the ability to compute in the models that can think and act rationally (Luger, *et al.*, 1993). Moreover, it can act rationally to execute the right action at the right time; a prospect which added pragmatic significance to the engineering practical world.

1.3 Brief History of AI

The world has seen powerful computational devices and programming languages only in the last half of the twentieth century. Buchanan stated that the turning point in the history of A.I. was a published paper in the philosophy journal *Mind* in 1950. The paper crystallizes ideas about the possibility of programming an electronic computer to behave intelligently, including a description of the landmark imitation game that we know as "Turing's Test". Buchanan said that Edward Feigenbaum and Julian Feldman's book "*Computers and thought"* published in 1963 was the first book to collect descriptions of working A.I. programs.

Another turning point came with the development of knowledge-based systems in the 1960s and early 1970s. Subsequent steps with many contributions of knowledge representation and information processing have been done (Nilsson, 1980).

The modern era starts from the latter half of the 1970s to the present day. When the expert system that deals with real life problems became one of the main innovations in this period (Buchanan, 2005), in addition to many applications mentioned in this chapter.

1.4 The Disciplines of A.I.

The subject of A.I. spans a wide horizon. It deals with the various kinds of knowledge representation schemes, different techniques of intelligent search, various methods for resolving uncertainty of data and knowledge, different schemes for automated machine learning and many others. Among the application areas of A.I., we have: Expert Systems, Game-Playing, and Theorem-Proving, Natural Language Processing, Image Recognition, Robotics and many others. The

subject of A.I. has been largely enriched through incorporating a wide discipline of knowledge gained from Philosophy, Psychology, Cognitive Science, Computer Science, Mathematics and Engineering. The outlines contained in the field of A.I. subject could be summarized as follows:

1.4.1 Learning Systems

The concept of learning is illustrated here with reference to the problem of berthing a ship by a pilot. A pilot practical learning of ship handling usually starts with other senior pilot in order to see how the ship can be manoeuvred and berthed safely in a relative short time. Each time, the skill system passes through an adaptation cycle and the best performance and results are saved by the learning process. This learning problem is an example of the well-known **parametric learning**, where the adaptive learning process adjusts the parameters of pilot skill system autonomously to keep its response close enough to the "*sample training pattern*".

1.4.2 Knowledge Representation, Reasoning, Planning and Intelligent Search

One of the important fundamentals of engineering knowledge is the knowledge organization. A variety of knowledge representation techniques is in use in Artificial Intelligence.

A complete and organized storehouse of knowledge needs minimum search to identify the appropriate knowledge at a problem state and thus, yields the right next state on the leading edge of the problem-solving process (Wilkins, 2000). Reasoning problem is mainly concerned with the testing of the satisfaction ability of a goal through a given set of data and knowledge.

One of the significant areas of A.I. that well contacts with knowledge base is the planning process. The planning problem, on the other hand, deals with the determination of the methodology by which a successful goal can be achieved from the known initial states (Bender and Edward, 1996).

Automated acquisition of knowledge by machine learning approaches, including generation of new pieces of knowledge from given knowledge base, is an active area of current research in Artificial Intelligence (Mark, 1995).

1.4.3 Logic Programming

For more than a century, mathematicians and logicians were used to design and develop various tools to represent logical statements by symbolic operators. Logic Programming has recently been identified as one of the prime areas of research in A.I. Building architecture for PROLOG machines; a hot topic of the last decade (Aliello and Massacci, 2001).

1.5 Soft Computing

Generally, it is a collection of computing tools and techniques, shared by closely related disciplines that include fuzzy logic, artificial neural nets, genetic algorithms, mobile and stationary agents, belief calculus, decision trees, swarm optimization and some aspects of machine learning like inductive logic programming. The scope of Fuzzy logic, artificial neural networks and genetic algorithms as tools in the broad spectrum of A.I. is outlined below.

1.5.1 Fuzzy Logic

Fuzzy logic deals with fuzzy sets and logical connectives for modelling the human-like reasoning problems of the real world. A fuzzy set-unlike conventional sets-includes all elements of the universal set of the domain but with varying membership values in the interval [0, 1]. Many researchers introduced the concept in systems theory, and later extended it for approximate reasoning in expert systems. Among the pioneering contributors to fuzzy logic, it is found the work of Tanaka as presented in the stability analysis of control systems; and Pedrycz in fuzzy neural nets. Pattern classification has been always one of the hot areas of Fuzzy Logic such as supporting vector machines for pattern classification (Abe and Inoue, 2002).

1.5.2 Artificial Neural Nets

An Artificial Neural Network (ANN) is either a hardware implementation or a computer program, which strives to simulate the information processing capabilities of its biological exemplar. ANN is typically composed of a great number of interconnected artificial neurons. Artificial neurons are simplified models of their biological counterparts (refer to Chapter 2).

1.5.3 Genetic Algorithm

A genetic algorithm (GA) is a mathematical algorithm that imitates the natural process of biological evolution. It follows the principle of ***Darwinism***, which rests on the fundamental belief of the "***survival of the fittest***" in the process of natural selection of species. The evolutionary cycle in a GA consists of the following three sequential steps (Michalewicz, 1992): a) Generation of population (problem states represented by chromosomes); b) Genetic evolution through crossover followed by mutation; and c) Selection of better candidate states from the generated population.

The integration of two or more types of A.I. is also possible to increase the capability of solving complicated problems.

1.5.4 Neural Network and Fuzzy Logic

The results obtained by researches have shown that neural network and fuzzy modelling can be more accurate than traditional analytical methods especially for complicated processes. Furthermore, with respect to the steps forward following the work in the domain area of ship manoeuvring, it was found that ANN mathematical models could be successful after improving the performance of these models in order to solve the motion prediction as well as the motion simulation as the most complicated problems in ocean engineering. This represents the main drive of this investigation to concentrate on ANN.

1.6 Literature Review

1.6.1 Overview of Previous and Recent Applications of Artificial Intelligence (A.I)

The previous and recent applications of A.I. introduce the topics covered under the heads of intelligent systems and demonstrate the scope of their applications in real significant complex engineering problems (Stankovic, *et. al*., 2003) and (Deng and Visonneau, 1998).

Recently, A.I. has strongly emerged as a practical technology, capable of executing successful applications in many fields. In addition to the applications mentioned above, A.I. has been gaining momentum as an effective strategy; especially in areas that need intelligent systems such as: Forecasting electricity demand and optimizing power supply, etc. Some of the important areas in which A.I. can be applied are speech and image understanding, expert systems, pattern classification and navigational planning of mobile robots.

1.6.2 Applying A.I. in Marine Control Applications

In recent years, extensive attempts have been directed to apply fuzzy logic controllers to surface ship path control. It has been shown that fuzzy logic controllers have many advantages and can perform better than traditional controllers based on mathematical modelling of the dynamic processes.

Neuro Fuzzy (NF) systems have increasingly attracted the growing interest of many researchers in various scientific and engineering areas due to the increasing need for intelligent systems in marine applications, in that they Provide control actions for diverse areas such as: Auto pilot, propulsion, electrical and power applications (El-Sharkawi, 1995), (Charytoniuk and chen, 2000), (El-Tahan, 1999), (Fukuda and Shibata, 1 1992), (Lin and Su, 1999), (Mamdani, 1977) and (Wu, *et. al.*, 2002), in addition to some applications that have attained well results in motion area as a predictor/controller to dynamic positioning of offshore structures.

More progress has been achieved in that regard by using the fuzzy logic autopilot (Sugeno type), which is augmented by the capability of adjusting its scaling factors. The proposed adaptive fuzzy autopilot emerged as a viable practical alternative for coastal sailing, where track keeping is of vital importance in all circumstances. An adaptive fuzzy autopilot for ship track-keeping is developed in order to solve the problem of track-keeping the manoeuvre of way-point turning and ship guiding through a complex path (trajectory) especially in coastal areas (Velagica, *et. al*., 2001).

Applying mathematical models is never exhaustive enough to cover all possible sailing and environmental conditions. However, in near-coast regions where change of the depth under keel is often experienced and consequently ship's dynamics can be changed from course stable to course unstable. Approaches have taken attempts to overcome the need for ship's mathematical model(s) by using more than one methods and disciplines of A.I.

Some researches were conducted in the area of fuel consumption in Darmstadt University of Technology, Institute of Automatic Control; where the researches investigated different applications, through utilizing neural networks for modelling and control of diesel combustion engines.

1.6.3 Applying Artificial Neural Networks (ANN) in Marine Applications

In general, the application areas of ANNs are: Robust and associative pattern recognition, filtering, data segmentation, data compression, adaptive control, optimization and modelling complex functions. The most common application of an artificial neural net is in machine learning. In this respect ANN can be extended to the marine applications.

In previous years, literature related to predicting commercial ships motion by means of artificial intelligence such as artificial neural-network or fuzzy-logic, is hardly found compared to the other traditional methods. As a matter of fact, there are not much related to the manoeuvres predictions of different types of ships (size and displacements condition) except for some limited manoeuvres predictions for specific ships or submarines. Recently, some momentum was gained in the area of

dynamic positioning of offshore structures and ships travelling in restricted waters (El-Tahan, 1999) and in environmental effects (Koushan, 2004). Neural network controllers have also been applied to ship manoeuvring controls. Neural network approaches used to design course-keeping autopilots, track-keeping controllers and automatic berthing systems (Hearn, *et. al*., 1997).

Yusong Cao, Zhengquan Zhou and William S. Vorus provided a brief description of the proposed neural network prediction/controller, during "Dynamic Positioning Conference" 17 – 18 October, 2000, under the topic of "Advances in Technology". Obviously the accuracy of the neural network prediction is verified and the effectiveness of the neural network controller for dynamic positioning of a ship is demonstrated with numerical simulations.

In terms of "dynamic positioning", there exist researches describing an auto-regressive moving average (ARMA) functional-link neural network predictor/controller for the dynamic positioning of offshore structures. The ARMA neural network predictor acquires the knowledge about the system through an online training using a small number of samples of the latest system status measured on board of the structure. A mathematical model of the nonlinear ship manoeuvring motion is used as a Multi-input Multi-output (MIMO) system to validate the neural network predictor/controller. The results of the work were very promising and encouraging (Cao, *et. al.*, 2000) and (Lee, *et. al.*, 2001).

Koushan and Mesbahi (1998) introduced both conventional and artificial neural networks empirical methods for the prediction of rudder force. They also discussed features of saving energy of integrated propeller-rudder system. The development costs for ANN method were about one tenth of development costs for conventional methods.

The manoeuvring and control division at the David Taylor Model Basin in USA along with applied simulation technologies have been developing and applying neural networks for problems of naval interest. The research describes the development of ANN applying feed forward neural network (FFNN) predictions of four-quadrant thrust and torque behaviour for the Wageningen B-Screw Series of propellers (Robert, *et. al.*, 2006).

The Neural Network Development Laboratory was established at the Naval Surface Warfare Centre (NSWC) in 1995 with the directive to apply neural network technology as a predictive tool of problems of interest to the Navy. The subsequent development of a Recurrent Neural Network RNN-based simulation tool for submarine manoeuvring was documented in (Faller, *et. al*., 1997) and (Faller, *et. al*., 1998*a*). RNN simulations have been created using data from both model and full-scale submarine manoeuvres. In the latter case, incomplete data measured on the full-scale vehicle, were augmented by using feed forward neural networks as *virtual sensors* to estimate the missing data (Hess, *et. al*., 1999). The creation of simulations at both scales permitted the exploration of scaling differences between the two vehicles, as described in (Faller, *et. al*., 1998*b*). An initial formulation of the problem using an RNN model for use with ships is described in (Hess, *et. al*., 1998). A technique was further developed for the accurate prediction of tactical circle and horizontal overshoot manoeuvres (Hess and Faller, 2000).

Many data files of one submarine model were provided to the researching participant groups in order to develop time-dependent nonlinear equation systems that relate input control variables to output state variables. A *recursive* network is one that employs feedback; namely, the information stream issued from the outputs is redirected to form additional inputs to the network using the RNNs to predict the time histories of manoeuvring variables of a model submarine executing submerged manoeuvres. The input data consists of the initial conditions of the vehicle and time histories of the control variables: Propeller rotation speed, and rudder and stern plane deflection angles. As the simulation proceeds, these inputs are combined with past predicted values of the state variables (outputs) to estimate the forces acting on the vehicle. The resulting outputs are predictions of the time histories of the state variables: Linear and angular velocity components, which can then be used to recover the remaining hydrodynamic variables required to describe the motion of the vehicle.

An additional effort has been extended and the description of the implementations and techniques to predict the submarine manoeuvres was published in a paper in the "24th Symposium on Naval Hydrodynamics" in Fukuoka, JAPAN, (8-13 July 2002) by Hess and Faller. Their paper describes the methods that were used and

the predictions that were submitted by the Neural Network Development Laboratory (NNDL) at the Naval Surface Warfare Centre (NSWCCD) through using Recursive Neural Networks (RNNs). Some times as in the former applications especially with the submarine, it is difficult to find a set of training patterns to predict the manoeuvring motions in specific environmental conditions. Therefore, this problem is required feedback as an on-line training using evolutionary computation.

The previous well - appreciated research work represent scattered investigations for specific ship or submarine for special prediction purposes as mentioned above. The inputs into the system as well the outputs were for a specific unit. In incremental mode the aspects of consistency and generalization are not an easy task, however, that it has a long way to go before it can safely and accurately solve the desirable manoeuvring motion prediction in the real world conditions for different ship types. In incremental mode the performance of standard architecture selection strategies are not optimal for learning and predicting. It tends to underestimate the complexity of the optimal architecture. Learning is affected mainly by the overall network topology and function performed by the nodes.

Studying and investigating the previous work was the drive of this present study with the objective of extending the prediction task in order to have more reliable accuracy. In the neural network community, it is held that batch training is more correct and faster when it used as a predictive system during the on-line application than the incremental training and predicting mode during the on-line application. Thus, it is necessary to provide an adequate level of redundancy with built-in off-line predictive system as a main system in addition to any other mode prediction.

Other phase for the off-line training is the main advantage of the generalization performance. The generalization algorithm performance will be affected when certain areas of the expert input patterns are ignored. Then, the proof must be extended to cover a broader spectrum of learning algorithms. Smart generalization entails the tight interrelation among prior knowledge, learning and reasoning.

The generalization capability of ANN regarding ship motion depends firstly on the ability to categorize factors that affect the motion in the existing condition. It

depends only on the knowledge experienced during the training process; in addition to the deviation of the predicted future situations from the situations already experienced. The relation between prediction requirements and ANN advantages are clarified in this thesis in chapters four and five.

Further derivation of the present study is to predict the manoeuvring motions of different types of ships. Predicting different ships needs another strategy to build the system prediction and to formulate the inputs and the outputs in order to execute the required task. The following chapters explain and demonstrate in depth such issues. In terms of predicting ship motion that applies intelligent techniques, many contemporary researches are currently under progress and racing in this area. The choice of ANN in this thesis is determined after realizing the relation between prediction requirements and advantages, as well as for seeking ways to extend this relation for different vessels in one general model rather than for a specific vessel.

This general overview of applying A.I. and ANN in marine applications and its limitations in ship motion application has motivated this research work as an extra effort in this new application area. The next chapter focuses on the different ANN structures, learning categories and their advantages, in addition to the prediction ability of the proposed applied method.

Chapter 2

Artificial Neural Networks

2.1 Introduction

In its most general form, a neural network is a machine that is designed to model the way in which the brain performs a particular task or function of interest. The network is usually implemented by using electronic components or is simulated by software on a digital computer.

Basically, three characteristics are contained in the ANN. The first is the network topology, or interconnection of neural 'units'. The second is the characteristics of individual units or artificial neurons. The third is the strategy for pattern learning or training.

This chapter highlights the different network type structures and the utilisation of ANN in context of its multi benefits regards to the thesis application.

2.2 History of the Artificial Neural

In the decade of the first electronic computer the history of the ANNs started in 1940s. Rosenblatt introduced the first innovated neural model, the perceptron in 1957 for a pattern recognition tasks for biological visual systems. A multi-layered perceptron model (MLP) was derived in 1960 and it was complicated by the lack of a suitable learning algorithm. Many improvements have been done till Minsky and Papert (1988) added another innovation and showed that multilayer perceptrons were required to solve non-linear problems. Another good step forward was done by Widrow-Hoff who introduced an algorithm based on the so-called *delta rule* to train the network as a theory of brain learning, “Hebb Rule” (Elliott and Shadbolt, 2002). The problem of efficient algorithm capable of providing training for complex nonlinear problems solved later by the innovation of back propagation algorithm and that has been done by Rumelhart and Mclelland (Chauvin, Rumelhart, 1995).

Carpenter and Grossberg in 1983 introduced an Adaptive Resonance Theory (ART). Afterwards, the development of ART has continued and resulted in the more advanced ART II and ART III network models. Later in 1988, Broomhead & Lowe introduced Radial Basis Function (RBF) networks and their work in this area opened a new border in the neural network community. It would be suitable to mention here the Self-Organizing Map (SOM) that introduced by Kohonen in 1982 and it was a unique kind of network model.

2.3 Neural Network Structure

Basically, a neural network (NN) consists of connected neurons. These neurons can be considered as nodes, which get input signals from neurons and pass the information to other neurons (Reed and Marks, 1999). Each neuron in the first hidden layer receives information represented by weights, bias and the incoming input information x_i and passes the sum *net* to an activation function *f*. The bias is an additional input, which does not come from another neuron. Biases are inputs that allow desired non-zeroes values come out of *net* even if all the inputs x_i are zeroes. The use of a bias also helps the network to find relationships between input and output more easily. It is linear or nonlinear function and many activation functions could be used (refer to Chapter 4). The neuron output is the output of the activation function) (*net f*) of this neuron.

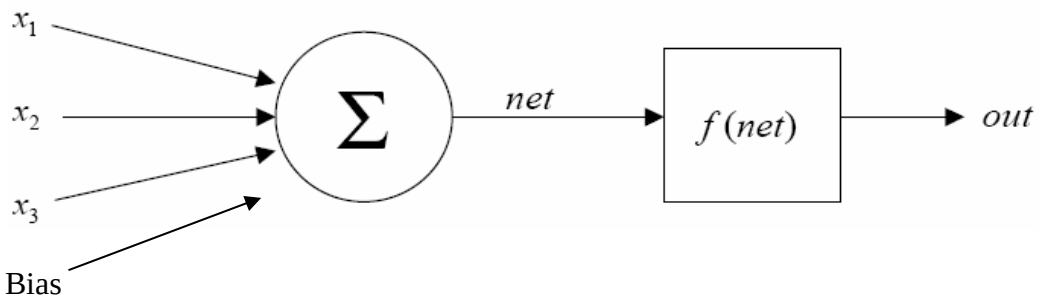

Figure 2.1 Basic Structure of a Single Neuron

Figure 4.1 shows a single neuron with input set coming from three different neurons. The corresponding neuron output is called *out* and is computed by equation (4.1) and directed to each neuron in the following hidden layer.

$$\text{Out} = f\left(\sum_i x_i + b\right) \qquad (4.1)$$

A group of neurons instructs one layer or more and can increase the power of a network extremely.

2.3.1 Different Network Type Structures

The best architecture of the ANN depends on the nature of the problem to be represented by the network. For a simple problem, one layer might be enough. The more neurons in a hidden layer, the more powerful are the networks (Demuth and Beale, 1998).

It is essential to realize the relation between each type of ANN and its application as long as the research applies this type of technique. Moreover, it is essential to realize the limitation of each type and if there is an innovated idea to extend this limitation.

Some applications could use learning time sequences. There are many tasks that require learning a temporal sequence of events. These methods in many tasks include tapped delay lines (Time-Delay Neural Network (TDNN)); context units (e.g. Elman Nets, Jordan Nets) Back Propagation through Time (BPTT) and Real Time Recurrent Learning (RTRL).

In Recurrent Networks, the network has probably an additional connection from the hidden unit to itself or from the output to the input layer, etc. Recurrent networks have been used in associative memories as well as for the solution of optimization problems (Hopfield, 1982) and (Yu, *et. al.*, 2006). The network behaviour is based on its time history and hence the problem is to solve the task assuming that the pattern presentation is a function of time, (Kolen and Kremer, 2001). For an arbitrary unit in a recurrent network, it now defines its activation at time t as: $y_i(t) = f_i(net_i(t\text{-}1))$. These networks can be used to model many new kinds of problems; however these nets also cause many new difficult issues in training.

A recent model addressing this problem used Long Short-Term Memory. The Long Short-Term Memory Model is an attempt to allow the unit activations to retain important information over a much longer period of time than specific steps which is the limit of RTRL or BPTT models. In brief, the hidden units of a conventional recurrent neural network are replaced by memory blocks.

In terms of “Memory Neuron Networks (MNN)” each neuron is associated with a memory neuron whose single output summarizes the history of the past activations of the neuron. These memory neurons represent the trainable dynamical elements of the model. Since the connections between a neuron and its memory neuron involve feedback loops, the overall network is now a recurrent one (Sastry, *et. al*., 1994). Another approach introduces a neuron model called the dynamic neural unit (DNU) (Rao, 1993).

The following are different type structures to distinguish between their structures and applications. A layer could be fully connected network model where each neuron is laterally connected to all neighbouring neurons in the layer (refer to Hopfield network). Other type presents the initiative of the Adaptive Resonance Theory (ART) network; the layers in this model are connected to both directions. Other more type is the network type exhibits the theory of the Self-Organizing Map of Kohonen where, each neuron in the network contains a so-called feature vector. As a pattern is presented to the network, it 'resonates', a certain number of times between the layers before a response is received from the output layer. According to the training data, the neuron whose feature vector is closest to the input vector is activated. The activated neuron is called the best matching unit (BMU) and it is updated to reflect input vector causing the activation. The neighbouring neurons are updated towards the input vector or away from it according to the learning algorithm in use to achieve the process of updating the BMU (Hodju and Halme, 1999). The neurons in this ANN model are grouped in layers which are connected to the direction of the passing signal from left to right in this case (refer to the perceptron network).

2.3.2 The Multilayer-Feed Forward Network

The multilayer feed forward network classifies in its name the network structure. First of all, it consists of more than one layer.

In practice, multilayers feed-forward networks have been used successfully in pattern recognition problems (Widrow B. *et al*., 1988) and identification the uncertainties in data classification (Karayiannis, 2006). From a systems theoretic point of view; multilayer feed-forward networks represent static nonlinear maps with the elements of the weight matrices as parameters, while recurrent networks are represented by nonlinear dynamic feedback systems.

Constructing and tuning parallel networks in different methods that can utilize the benefit properties of different modelling are discussed in Chapter 4 and 5.

2.4 Training Styles

2.4.1 Introduction

Once the network is implemented and the architecture is given and fixed, it needs to be trained. Training is the process of presenting data (patterns) to the network in order to store the relationship between input and output in its weights. There is more than one style of training (refer to Chapter 4 and 5). If the results test of NN is able to give reasonable answers to new patterns and the testing is successful, the NN is able to compute outputs for given inputs similar to the trained patterns. The presentation of completely different patterns will mostly lead to high errors between targets and NN outputs.

2.4.2 Back Propagation Algorithm

The most commonly applied training algorithm is called the back propagation algorithm which is used in this thesis.

The back propagation algorithm is used for supervised learning with input/target pairs, whereby the network is adjusted, based on a comparison between outputs and targets, until the network output matches the target. There are many techniques of the back propagation algorithm (refer to 4.4 and 4.5 in Chapter 4). Chapter four is clarifying the use of steepest descent technique of back propagation learning that updates the network weights and biases.

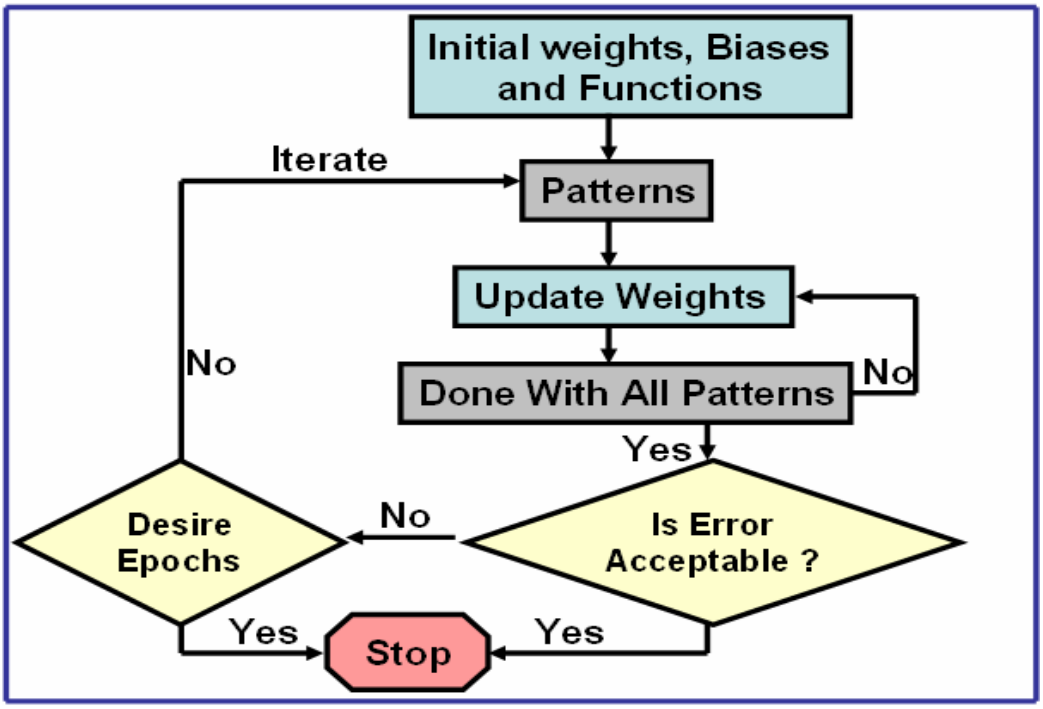

Figure 2.2: One technique of black propagation algorithm

2.5 Supervised and Unsupervised Learning

Learning rules fall into two main broad categories: Supervised learning, and unsupervised learning. ANN of the supervised-learning type, such as the multi-layer perceptron, uses the target result to guide the formation of the neural parameters. The supervised learning algorithms realized with ANN have been successfully applied in control (Narendra and Parthasarathi, 1990) and automation.

In unsupervised learning, there are no target outputs available. The weights and biases are modified in response to network inputs only. They categorize the input patterns into a finite number of classes. Most of these algorithms perform clustering operations. This is especially useful in such applications as vector

quantization and self- organizing map to cluster the input data and find features inherent to the problem. Knowledge acquisition and planning analogue to digital conversion of data are applied in unsupervised learning. Another new approach is applied for objective video quality assessment (Le Callet, *et. al*., 2006).

In this thesis the models have been built depending on the supervised training where the targets are the desired ship motion to enable the prediction of this motion under all circumstances. Since the correct ship motion corresponding to the given inputs is required for the training the supervised training is necessary.

2.6 Benefits of Neural Networks and Application Areas

It is apparent that a neural network derives its computing power through, first, its massively parallel distributed structure and second: Its ability to learn and therefore generalize. The use of neural networks offers the following useful properties and capabilities:

The ANN has the capability to solve the **nonlinear** relation problems. An artificial neuron can be linear or nonlinear. Nonlinearity is a highly important property, particularly if the underlying physical mechanism responsible for generation of the input signal (e.g., speech signal) is inherently nonlinear.

The **input-output mapping** is function of the ANN comes after realizing the relation of the both sides' equation or it is so called balancing the relation as input and output by applying a set of labelled training samples or task examples. Each example consists of a unique input signal and a corresponding desired response. Naval Surface Warfare Centre and Applied Simulation Technologies researchers in USA investigated the uncertainty present in the input vector that propagates through a trained network onto the output vector. This uncertainty is determined in the process of using the matrix of partial derivatives related to the change in each output with respect to the different inputs (Hess, *et. al.*, 2006).

Moreover, the **property of adaptively** is added to the input-output mapping that means if the neural network trained to operate in a specific environment can be easily retrained to deal with minor changes in the operating environmental

conditions. Neural networks have a built-in capability to adapt their synaptic weights to changes in the surrounding environment.

Evidential response is one of the benefits of ANN that comes after learning algorithm. In the context of pattern classification a neural network can be designed to provide information not only about which particular pattern to select but also about the confidence in the decision made. This latter information may be used to reject ambiguous patterns should they arise and thereby improve the classification performance of the network.

Every neuron in the network is potentially affected by the global activity of all other neurons in the network. The knowledge is represented by the structure and activation state of a neural network and the operation is dealt as **contextual information.**

The system could have a limited inherently **fault tolerance** which is acceptable due to the implementation of the neural network in hardware form and it is still capable of robust computation in the sense that its performance degrades gracefully under adverse operating conditions. Consequently, the system can obtain many patterns containing errors which are acceptable in the accuracy range.

The massively parallel nature of a neural network makes it potentially fast for the computation of certain tasks. This same feature makes a neural network well suited for implementation using **very-large-scale-integrated (VLSI)** technology.

Basically, neural networks enjoy universality as information processors so they are **uniformity of analysis and design**. Neurons in one form or another are represented an ingredient common to all neural networks. Modular networks can be built through a seamless integration of modules. The design could be different from one to other with unlimited structures depending on the application.

2.7 The utilization of ANN in the thesis

Many difficulties faced the applied methods in describing more than inputs

formation into the system that have ship physical and controllability meaning. To solve the problems of ship turning manoeuvre predictions, it demanded more extensive computational efforts in developing parallel neural-network simulation models.

The first problem was the dissimilarity of the dimensions of the motion variables' characteristics (e.g., velocities, distance travel, yaw rate, drift angle, number of revolutions per minute of the propeller and speed rate). Each individual variable had completely different nonlinear curves with the other variable running in same time.

The four-selected ships are completely different from one another in all factors which control the motion. In addition, the standard deviation to detect the accuracy of each factor is different from one another.

The artificial neural-networks built different system identification strategies for each networks group regards to the different variables that simulate the motion in order to build the system models for high performance training. Each network in the group has specific accuracy to handle the training case with suitable economic computational efforts.

The ability and utility of multi-applied programs running in parallel to compute the prediction or simulate ship motion are able to overcome a lot of obstructions and difficulties such as different accuracies of the measured data. The methods and results that came out of that work can be seen in Chapters 4, 5 and 6.

2.8 Conclusion

The studying and investigation of the different AI topics was essentially to realize different suitable applications of each and to recognize the limitation of each type. Many features and benefits of the ANN are applicable to be used in the application of this thesis. Moreover, the system has the ability and flexibility to extend its limitation with innovating methods to be appropriate for the type of the problems of the ship manoeuvring motion. The next chapters clarifying this fact in context of the interface between the ability of ANN and the prediction of ship manoeuvring.

Chapter 3

Ship Motion Prediction

3.1 Introduction

Manoeuvring is addressing ship behaviour in the horizontal plane (surge, sway and yaw motions). Sea keeping and stability are addressing ship behaviour in the longitudinal and transverse planes (mainly heaving, pitching and rolling motions).

These are three important areas to determine the safety of ship: First one is ships designs. Second one is ship approval. Third one is ship operation which is the topic of this thesis.

3.2 Equations of motion

It is preferred to highlight the equations of the motion of the ship. It is vital for identifying the nature of the relation between inputs and outputs in the equations of motion to be an essential basic for building the ANN models. It is also an important issue to realise the limitation of applying each ANN model.

The equations of motion, which describe the hull fixed coordinate system are referred to the origin at the centre of gravity or at the midship. The equations have more than one form. The coordinate system in figure 3.1 is used. The equations of motion referred to the centre of gravity, are represented by equations (3.1-3.3) as follows:

$$m\,(\dot{u} - v_G\, r_G) = X_G \qquad (3.1)$$

$$m\,(\dot{v} + u_G\, r_G) = Y_G \qquad (3.2)$$

$$I_{zz}\,\dot{r_G} = N_G \qquad (3.3)$$

Where, m is the mass of the ship, I_{zz} is the moment of inertia of ship in yaw motion. The subscript G denotes the value referred to the centre of gravity. The notation of u_G, v_G and r are velocity components at centre of gravity of ship (*C.G*).

U is the actual ship velocity measured relative to the fluid. It can be decomposed in an advance velocity component *u* and a transversal velocity component *v*. *X*, *Y* and *N* represent the hydrodynamic forces and moment acting on ship's centre of gravity. The transverse velocity *v* has been chosen rather than the drift angle β for wider application.

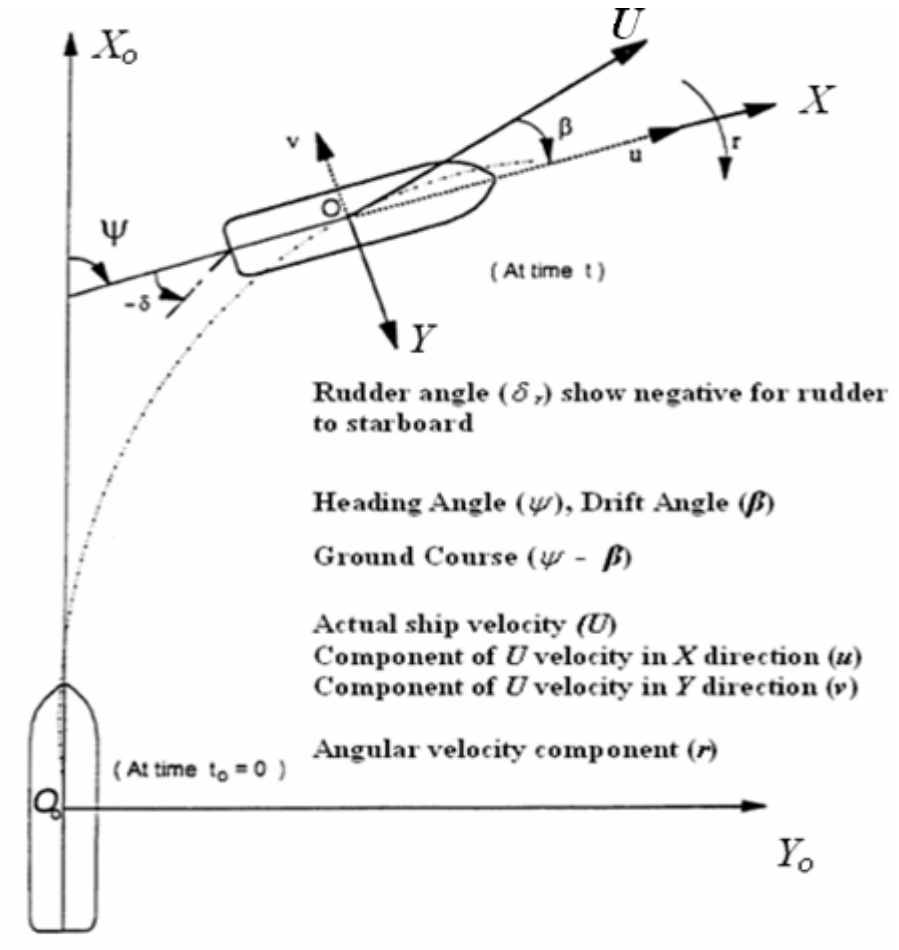

Figure 3.1: Surface ship with body axes *O*(*XYZ*)
within space-fixed (MSC/Circ.1053)

In this research all figures of ships plotting and motion simulations are referred to the origin at midship. They stated that the hydrodynamic forces can be described in the coordinate system referred to the origin at the midship to be more convenient for applications (see Equations 3.4-3.6). The main abbreviations are explained in the following, while the rest are listed in the nomenclature.

$$m\ (\dot{u} - vr - x_G\, r^2)\ =\ X\ =\ X_G \qquad (3.4)$$

$$m\,(\dot{v}+ur+x_G\,\dot{r}) = Y = Y_G \tag{3.5}$$

$$(I_{zz}+m\,x_G^2)\,\dot{r}+m\,x_G\,(\dot{v}+ur) = N = N_G+Y_G\,x_G \tag{3.6}$$

Where, $u = u_G$, $v = v_G - x_G r_G$, and $r = r_G$, with x_G representing the *x*-coordinate of the centre of gravity (due to the symmetry of the ship $Y_G = 0$).

The following stage is to express the forces and the moments to the body coordinate system *X*, *Y* and *Z*. Ogawa and Kasai (1978) have stated the manoeuvring motion forces with the help of Taylor series expansion. The high order terms are ignored in the Taylor series expansion and only the linear terms are considered in the following equations. The forces *X* and *Y* are expressed in equations (3.7) and (3.9) in sequence; the moment *N* is described in equation (3.10).

$$X' = \frac{X}{\frac{1}{2}\rho L^2U^2} = X'_{\dot{u}}\,\dot{u}' + \left(X'_{vr} - Y'_{\dot{v}}\right)v'r' + X'_{vv}\,v'^2 + X'_{rr}\,r'^2 + X'(u)$$

$$+(1-t)T'\left(\frac{u_p}{nD}\right) + X'_{RO} - F'_N\sin\delta \tag{3.7}$$

$$T' \quad = \quad \rho n^2 D^4 k_T \frac{\left(\frac{u_p}{nD}\right)}{\frac{1}{2}\rho L^2U^2} \tag{3.8}$$

Where, the bare-hull terms are grouped in the first five terms in Equation 3.7. The effects of the propeller and the rudder terms are presented in the last three terms.

X' : Non dimensional Force coefficient in *X*-direction

$X'_{\dot{u}} = m'_x$: Non dimensional hydrodynamic mass in the *x*-direction

$Y'_{\dot{u}} = m'_y$: Non dimensional hydrodynamic mass in the *y*-direction

$X'_{vr}, X'_{vv}, X'_{rr}$: Hydrodynamic coefficients due to resistance increment which are mainly caused by motion, X'_{rr} theoretically corresponds to $m'_y\,\alpha'$.

(*1- t*) : Thrust deduction factor

t	: Thrust deduction fraction
u_P	: Axial velocity of the propeller
n	: Speed of propeller revolution
D	: Propeller diameter
T'	: Non dimensional propeller thrust
$X'(u)$	: Non dimensional hull resistance in straight ahead motion.
X'_{RO}	: Non dimensional rudder resistance in straight ahead motion.
F'_N	: Non dimensional rudder normal force.

The force Y and the moment N are described as follows:

$$\begin{aligned} Y' &= \frac{Y}{\frac{1}{2}\rho L^2 U^2} = Y'_{\dot{v}}\dot{v}' + Y'_{\dot{r}}\dot{r}' + Y'_{v}v' + (Y'_{r} + X'_{\dot{u}}\dot{u}')r' \\ &\quad + \int_{-1/2}^{1/2} (v' + x'r')\left|v' + x'r'\right| C_D(x')\,dx' \\ &\quad - (1 + a'_H)F'_N \cos\delta \end{aligned} \tag{3.9}$$

$$\begin{aligned} N' &= \frac{N}{1/2\rho L^3 U^2} = N_{\dot{v}}\dot{v}' + N'_{\dot{r}}\dot{r}' + N'_{v}v' + N'_{r}r' \\ &\quad + \int_{-1/2}^{1/2} (v' + x'r')\left|v' + x'r'\right| x' C_D(x')\,dx' \\ &\quad - (x'_R + a'_H x'_H)F'_N \cos\delta \end{aligned} \tag{3.10}$$

In the equation (3.9) and (3.10) the first four terms represent the linear terms based on the added mass and the lift, the integral terms in both equations which are nonlinear based on the cross flow concept, and the last term in both equations is the force and moment induced on the hull by the rudder, respectively. The two equations terms and abbreviations are explained in the Acronyms and Symbols in this thesis.

In fact the hull wake has tremendous effects on the manoeuvring performance. The concept for the straight course which has long been established in the fields of propulsive performance may partly be helpful. When the ship is surging with straight course, it will be under thrust, drag and weight forces. Whenever, the

rudder angle changes, new forces will appear such as rudder lift force and drag force which are the components of a so-called rudder normal force. Consequently, the ship bow will yaw to the opposite side of this force and other forces will be changed and created such as hull drag and lift forces. In other words the hull, propeller and rudder interaction will be changed and these will simulate the fluid dynamic motion (Orgawa and Kassa, 1978).

The right side of Newton's Equations (3.11, 3.12 and 3.13) can be written as follows:

$$\text{Surge} : \quad m.(\dot{u} - vr) = X_H + X_P + X_R + X_A \qquad (3.11)$$

$$\text{Sway} : \quad m.(\dot{v} + ur) = Y_H + Y_P + Y_R + Y_A \qquad (3.12)$$

$$\text{Yaw} : \quad I_Z.\dot{r} = N_H + N_P + N_R + N_A \qquad (3.13)$$

The sub indexes stand for: *H* is hull, *P* is propeller, *R* is rudder and *A* is aerodynamic. *X* and *Y* are the external forces. *N* is the external moments acting on the ship referred to the moving reference *x*, *y*. The first term in the three equations in the right side concerns the ship resistance; the second term concerns the propeller force, the third is rudder force and the fourth is aerodynamic forces. All forces have components in *X* and *Y* direction, while the moment is acting with respect to the ship's reference point.

Based on the above mathematical description, the inputs of the ANN are defined. The task of the ANN in this thesis is to develop an alternative prediction model to describe the ship motion without detailed knowledge about the complicated structure of the ship in this approach stage of the research.

3.3 Overview of Previous Work

The success of the previous work is attributed heavily of determining the hydrodynamic coefficients. The main methods to achieve that task are the experiments with model tests, full scale sea trials and system identification techniques, theoretical prediction methods and regression analysis results from similar designs.

The first and simplest method is to base the prediction on experience and existing data, assuming that the manoeuvring characteristics of the new ship will be close to those of similar existing ships. The second method is to base the prediction on results from model tests. The most two commonly techniques are the free-running test and the other is captive model tests.

The first model test is a **"free-running model"** moving in response to specified control input such as rudder and propeller (see Figure 3.2). A scale model has been established to simulate the full scale ship to reduce costs by avoiding the manufacture of a special model for manoeuvring tests, such tests may be carried out with the same model employed for resistance and self-propulsion tests. Manoeuvres such as turning circle, zig-zag and spiral tests are carried out with the free-running model. Recently, more efforts have been made at deriving the coefficients of mathematical models from tests with free-running models parameter identification methods to predict the manoeuvring characteristics of the ship.

Figure 3.2: Free running model tests: Optical tracking system
(VBD Towing Tank, Duisburg, Germany)

The second model test is a "**captive model".** The main types of the captive models test are straight line tests in a towing tank, rotating arm test, planar

motion mechanism tests, and oscillator tests. The force measurements on the model will be recorded. The analysis of the measurements provides the coefficients of a mathematical model, and then specific equations are used for the prediction of the ship's response to any control input. The diameter in the second type will be varied for each test. The hydrodynamic coefficients related to ship turning as well as to the combination of turning and drift will be determined by this method. Additional tests often have to be conducted in a towing tank in order to determine the hydrodynamic coefficients related to ship drift. Then, the prediction will take place by means of a mathematical model using these obtained coefficients.

Generally, we can say that model tests suffer from scale effects and corrections must be introduced in the analysis of the results.

As mentioned above determining the different coefficients depends mainly on the free-running test and the captive model tests. Then, the mathematical model is a set of equations which can be used to describe the dynamics of a manoeuvring ship after applying these measured coefficients.

3.4 Applying of Numerical Simulations Models

Mainly there are two types of basic mathematical models using the numerical simulations. The first is called "Motion Models" or "Coefficient Models"; it solves the equations of motions after formulating the terms into coefficients which are obtained from the model test for certain manoeuvres as mentioned above in 3.3. The second is called "Force Models"; it is calculating the coefficients theoretically and solving the equations after determining all forces acting on the ship. Velocity and track are calculated by integrating the accelerations to solve the kinematical parts. To solve the dynamic parts of the equations, introducing the mass and the hydrodynamic mass with the accelerations to obtain the forces acting on the ship is required. The chosen method is based on a model developed by Söding (1984).

CFD methods can be used now to carry out a complete simulation of the ship motion in viscose flow (Xing-Kaeding, 2006).

It should be mentioned here that the neural network method which is applied in this thesis is a numerical application (refer to Chapters 4 and 5).

3.5 Turning Circle Manoeuvre

3.5.1 Turning motion

Manoeuvring is changing in ship's course or speed or both of them. The word turning circle manoeuvre or tactical circle diagram tells the ship Master the manoeuvre at maximum rudder angle.

Turning circle tests are performed to both port and starboard at approach speed of at least 90 per cent of the ship's speed corresponding to 85 per cent of the maximum engine output with a maximum rudder angle as per IMO requirements. For the purpose of this research the rudder angles tested to both port and starboard within a range of maximum and small angles to achieve the purpose of predicting the ship motion in addition to different approach speeds.

The essential information of the turning manoeuvre to the ship Master is the maximum advance and the total diameter to determine the limitation of the motion in case of emergency situations (see Figure 3.3). These limitations of the motions lead the ship Master to determine the safe speed mode and the safe distance from other targets. The data that define the motion of the manoeuvring ship are shown in Figures 3.1.

The ship also has a rotation velocity with respect to the *z*-axis. This axis is normal to the *XY* plane and passes through the reference point (midship in this thesis). β is the angle between *U* and the *x* axis and it is called drift angle. Ψ is the ship heading angle and (δ_r) is the rudder angle. Surge acceleration is ($\dot{u}$), sway acceleration is ($\dot{v}$), angle of yaw is (ψ), angular velocity about body *z*-axis is ($\dot{\psi}$). The accelerations are denoted similarly like the velocities but with a dot above the letter to indicate a time derivative. Trajectory is defined as (*x* and *y*).

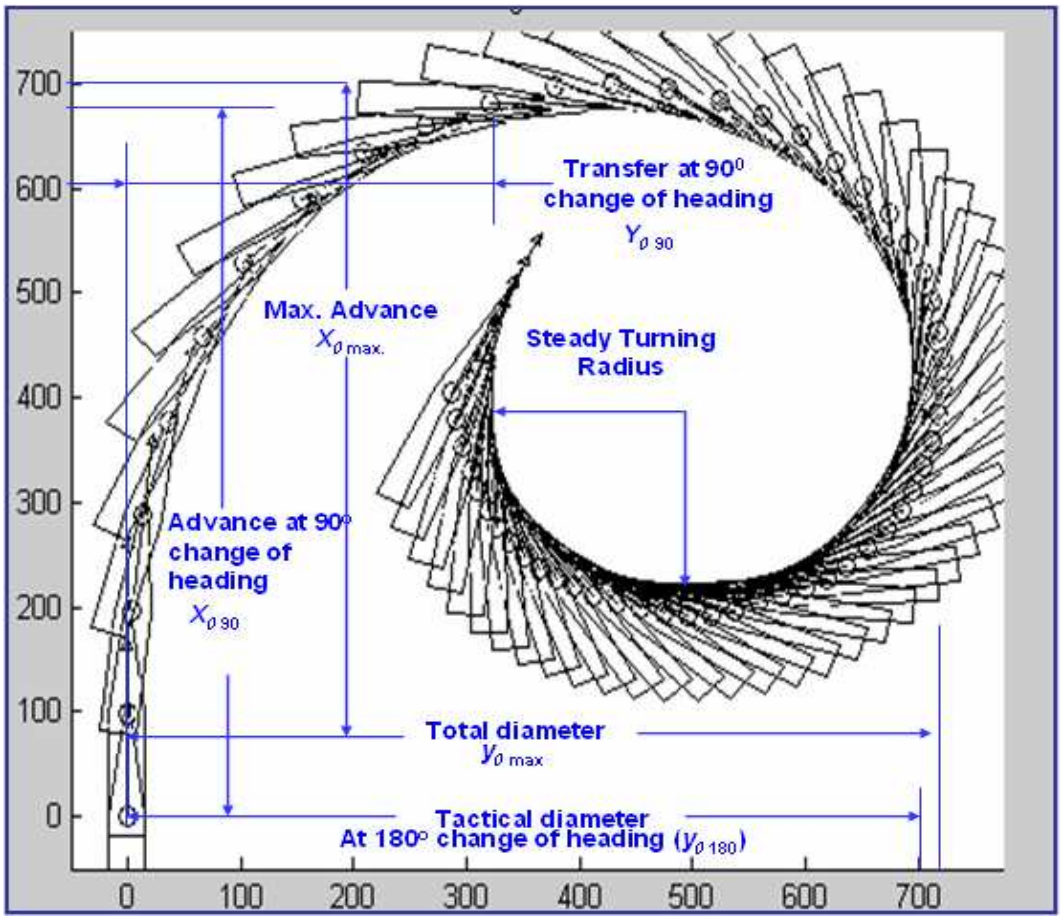

Figure 3.3: Turning circle definition of bulk carrier, *L.B.P.* = 219 m., $\delta_r = 35^{o}$ to starboard side
One of the experimental simulator turning manoeuvres

3.5.2 Ship Turning Characteristics

The most fundamental ship manoeuvre is the turning manoeuvre. The behaviour of the ship during the manoeuvre turn is the consequence for the resulting forces and moments, which are produced by the flow on the rudder, hull and propeller. The turning manoeuvre can be divided into three phases (Lewis, 1989).

At the beginning, the rudder angle is zero and the ship has a steady course and speed. In this case, there are no resultant forces since the propeller thrust counteracts the total drag of the ship. The first phase begins when the rudder executes to deflect to port or starboard. The first phase has the initial transient due to rudder forces which will direct ship's astern e.g. to port side, whereas the turn will eventually be to starboard. This is because the rudder position at the ship' astern and whenever the rudder deflect to starboard side then the rudder lift force will act to

port side. As a result of the high transverse acceleration ($\dot{v}$) and the angular acceleration ($\dot{r}$), a quick raise of the drift angle (β), and the rotation velocity (r) take place (see Figure 3.3). With the introduction of these parameters, the ship enters the second phase of turning. In this phase all parameters change dramatically. Surge, sway and yaw accelerations will occur. Finally in the third phase, the turning ends with the establishment of the final equilibrium of the forces and moments and the ship settles down to a turn of constant radius as shown in Figure 3.1. In the last phase of the turning manoeuvre, the transversal velocity (v) and turn velocity (r) as well as the drift angle (β) will be constant. The transverse acceleration ($\dot{v}$) and the angular acceleration ($\dot{r}$) equal zero and the path of the ship is circular. Figure 3.2 shows a definition diagram for the turning path of a ship. Generally, it is characterized by four measured values: Advance, transfer, tactical diameter, and steady turning radius.

The midship is decided to be a reference point because it is a fixed point easy to detect and is not as the pivot point which has a variable positions depending on the motion direction and different forms of ships.

3.6 The Interface of the ANN as a New Prediction Tool in this Thesis

The coefficient and force mathematical models can predict the manoeuvring behaviour of similar ships with satisfactory accuracies. Whenever, the models are tied to particular equations, this could cause a low accuracy of the outcome predication for other dissimilar ships. The capability of the coefficient models to predict ship manoeuvring motions depends on the accuracy of the input coefficients. Assuming that a good mathematical model is available, the problem is to determine the coefficients with sufficient accuracy.

The models prediction based-approach neural networks are trained to simulate the motion of different ship types contained all in one model. One of the major advantages, that the process-dependency is a black box approach models. The neural networks proved their capability to solve the black box inputs into the system with satisfactory accuracies in the horizontal plane. Consequently, the computational prediction time is relatively short.

Other significant interface that the NN model prediction has high ability to classify the date in groups depends on the fault tolerance. The procedures to damp the tolerance toward the realistic errors are explained in chapter four. This mechanism is extended to the main variables that demonstrate the manoeuvring motion to improve the predictor performance.

Chapter 4

The Applied Method, ANN Direct Model Prediction

4.1 Introduction

The aim of this chapter is to investigate the use of Back Propagation Feed Forward Neural Networks (BPFFNN) and Parallel Artificial Neural Networks (PANN) for providing a new practical method for an accurate prediction of ship manoeuvring motion during the operation time. Consequently, it will be required to predict the manoeuvring performance of the ships at different displacements with different speeds and rudder angles.

Different ships (two containers, bulk carrier and tanker) are considered in this chapter. The direct model is trained for the different parameters of these four ships without applying the hydrodynamic forces which are applied in chapter five. The system is developed to predict the turning track limitation as maximum advance and total diameter, ship trajectory and ship turning track simulation.

The prediction included different parameters which describe the characteristics of different phases of turning manoeuvres and time dependent values such as: Turning track information, velocity, distance, propeller revolution per minute, angle of attack, course of ship's path, course of ship's head and acceleration.

Afterwards, the method is extended to include other ships' data files from another source of "American Ship Analytics Ship Simulators". This step was taken forward for more verification and validation of the NN system prediction. The results obtained form the training process and the testing of blind manoeuvres are discussed in this chapter and in Chapter 6.

4.2 The Main Steps to Create the Model

MATLAB provides many and high-level functions to enhance the designer to build a suitable model structures of the desire applications. Many algorithmic

development and analysis were made through the mathematical computations that were created in the neural network tool box in MATLAB.

Recognitions of needs are the first stage to draw the main aims with their objectives. Then, it is necessary to create a design of dialogue structures to draw these objectives in a MATLAB programming language and to determine the categories of the main objectives.

MATLAB has more than one data type. Data formalization must be defined in the system to a suitable type to prepare the model and to simplify the programming. A further step is to confine the information flow structure and configuration to simplify dialogue. A structure is a MATLAB array that divides its contents up into fields. The fields of a structure can contain data types which are different from one another considering the bandwidth of the application related to the data files. Then, the following stage is to organize these networks according to its functions.

Understanding the problems of the manoeuvring motions as an expert task is the stage before mathematical concepts interact. Then, the following step is coding the initial mathematical computations in a real programming language.

The main problem was the large number of outputs; it is difficult to train the ANN to give all outputs with high accuracy at the same time. Parallel ANNs are used to receive the same inputs at the same time. Then, each ANN will give only one output, or a number of outputs with similar characteristics. Despite the necessity for a complicated construction and significant efforts, this increases the accuracy considerably. The efforts and the complicated constructions were done because the problem arises strongly when the outputs are of different nature. In other words, when the characteristics of the outputs are dissimilar for a large number of outputs, it will be difficult to use only one ANN for all outputs. The weights and biases between the input layer and the first hidden layer, for example, will be common for the next layers and thus for all outputs. This creates some limitations in the capability of the ANN in the training phase.

The states of all nodes are determined and stable as soon as signals from the input nodes have had time to propagate through the network without feedback loops.

This study was exclusively concerned with developing and characterizing algorithms for setting the connection strengths by "training" a network on a set of representative input/output mappings. However, it is possible to describe dynamic behavior using static NNs with the proper choice of outputs. The output sequence has to be related to the inputs with the same dynamics of the original system. In other words, the output of the ANN represents a sequence of values for the variables that explains the dynamic variation of these variables depending on the applied inputs. Therefore, it is required to establish response periods criteria and to design a dialogue to compute the data configuration that responses in the defined time step. The collections of the variables which are necessary to describe the system at a particular time relative to the objectives of the study define one state of the system. The power of the system is to simulate the out come of the other variables in the defined prediction domain which are not experienced prior. The MATLAB tool box provides possibility of “Simulation with concurrent inputs in a Dynamic System”. It has also the possibility of “Simulation with Sequential Inputs in a Dynamic Network”.

The major stage is to set up the simulation dialogue with testing procedures to evaluate the model. To access the stage of the system’s prediction stability, it is necessary to improve the predictor performance and its accuracy. Improving the predictor performance and its accuracy concentrates on using the differential equation which gives the step size toward the desired goal and the binary functions in the nods. The prior stage could be accomplished if the right momentum defined from error function as least squares.

The controlling stage was to export the analytic training results to the investigation domain. Important investigations came out from the Network/Data Manager to investigate the basic ingredients of a control system. These can be described by the objectives of the control, control system components, and results. The objectives can be identified with actuating signal input patterns and so control variables are the results. The elements of the control system have the central role to achieve the objectives with controlling the outputs in some prescribed manner by the inputs.

The main role of the control in this stage is to damp the errors to be closer to the realistic errors and to damp the differences between the two data sets as a first data

set and second data set. The first data set are the differences between the outputs of the training data and measured data while the second data set are the differences between the outputs of the blind Manoeuvres results and the measured results. The analytical results, graphics and plotting are analysed in the way for damping the goal errors. These procedures would enhance improving the initial system. These events will be applied to all networks and the subsystems. It is compulsory that the entities of the subsystems act and interact together towards the accomplishment of the main system's objectives and aims.

The following items will deliver more precise clarification and explanation of the system which so far has only been highlighted prior.

4.3 Generation of the Manoeuvring and Experimental Data

A Navigation simulator was used to generate the data required for the training and validation of the system. The study was carried out for different ship types which have variable parameters. These selected parameters were reasonable to match the ability of the training process of the neural network.

The Norcontrol Navigation Simulator used to train marine officers and masters and the investigated ships were navigated in the same way as a real ship. This fact has been checked several times in calm sea and weather during the manoeuvring exercises in the simulator bridge (refer to Norcontrol models documentation in Appendix G.2).

All trials and the experimental data files have been obtained taking into consideration the IMO requirements and maritime safety committee (Resolution MSC.64 (67), adopted on 4 December 1996) and (MSC/Circ.1053, December 2002). IMO MSC/Circ.1053 has provided in the explanatory notes to the standards for ship manoeuvrability, the information necessary to assist those responsible for ship operation to evaluate ship manoeuvrability.

Data files of eighty-two experimental manoeuvres have been recorded and documented. Fifty-nine of these data files were provided to the system for training.

A second set of twenty three data files that represent blind manoeuvres were used for validation.

There were many difficulties in obtaining high accuracies for the manoeuvring data files. The four selected ships are completely different from one another in manoeuvring behaviour. Ship handling and manoeuvring using the simulator in order to complete a set of data files for the purposes of this research was not a straightforward task. This task necessitates a high skill of ship handling, manoeuvring and professional engineering knowledge in order to fulfil the implementation of motion prediction and simulation requirements (refer to MSC/Circ. and Resolution mentioned above).

The main purposes of the manoeuvring data files were to create a system able to provide limitations of turn manoeuvres for the tactical turn or any rudder angle turn, manoeuvring tracks and manoeuvring simulation predictions for the motion of the set of the blind manoeuvres.

For recognizing the parameters variation among the selected ships, it is important to clarify some of the different main parameters of the investigated ships: Lengths overall (L.O.A) were varied from 234 meters to 322 meters and the displacements were varied from 73 096.0 tonnes to 269 869.0 tonnes. The main parameters of the different ship types are in Appendix G (Table G.1). An essential part of the inputs into the system in addition to the experimental data depends on the main dimensions and main ratios of the investigated ships (Schneekluth and Bertram, 1998).

Trajectory is defined as (x and y). Total speed (U) is measured relative to the fluid. Control data that propel and direct the vessel are propeller rotation speed (n) or it can so called ($R.P.M$), rudder deflection angle (δ_r); it is negative to starboard side and positive to port side, rudder area (A_R). The time of rudder angle ordered (δ_{RO}) is considered and named (t_o). The trim angle is negated due to the even keel loaded condition. Draft, block coefficient and displacement have been modified to meet the actual load condition.

Table 4.1: Ships' start conditions at rudder angles ordered (δ_{RO}) and at time (t_o)

		Investigated ships			
Recorded Data	Unit	Container Ship 1	Container Ship 2	Bulk Carrier	V.L.C.C.
t	s	0 s	0 s	0 s	0 s
X	m	0	0	0	0
Y	m	0	0	0	0
U_G	*knot*	24.7	25.5	13.1	14.7
R.P.M	*1/min.*	91	101	99	74
δ_r	*degree*	00	00	00	00

In each experiment, the ships began with constant heading run as steady course ahead without any rate of turn to port or starboard side($\dot{\psi}$). The rudder had no angle to any side. Then, the action of the rudder angles ordered (δ_{RO}) at time (t_o) and at the same time the ships position were recorded and all the essential data for these types of manoeuvres were recorded as mentioned above (see Table 4.1). The measured data files were documented using two methods, one by the printer files and the other by the plotter files. About two thirds of these data files were provided to the system for training. A second set of about one third of the data files, represent blind manoeuvres used for validation.

The surface motions are presented by the longitudinal axis *x* and it is positive towards the bow, *y* is the transverse axis and is positive to starboard and the angular motion around the axis *z*.

For each manoeuvre, the data set contained complete time histories until the manoeuvre ended. The time interval between each two successive readings varies in the range of 5 seconds to 10 seconds and in some cases extended to be more, when it is suitable and required e.g. slow ship's speed. The main recording data at each time simulation were: Simulation time (t), starting position as latitude and longitude of manoeuvring begin action, ground speed (U_G), sea speed (U), propeller revolution per minute ($R.P.M$), ship's ground course ($\psi - \beta$), ship heading (ψ), turn rate ($\dot{\psi}$), rudder angle (δ_r), distance travelled, and speed rate.

The drift angle was obtained from ship's ground course (ψ - β) and ship heading (ψ). The initial conditions have been taken with high consideration for obtaining the accurate outcomes as mentioned above (see Tables 4.2 and 4.3).

Table 4.2: Sample from the four ships data files at 100 seconds from (δ_{RO}) at (t_o)
(Ships had different approach speeds similar as in Table 4.1 and different δ_r)

		Investigated ships			
Recorded Data	Unit	Container Ship 1	Container Ship 2	Bulk Carrier	V.L.C.C.
t	*s*	100 s	100 s	100 s	100 s
X	*m*	1047	1095	614	750
Y	*m*	488	395	128	26
U_G	*knot*	22.3	21.3	11.3	14.6
R.P.M	*1/min*	91	94	95	74
δ_r	*degree*	12	30	20	06
$\dot{\psi}$	*1/min*	48.0	51.0	37.3	10.4
$\dot{u}$	*knot/min*	- 0.6	- 3.3	- 2.0	- 0.2
ψ	*degree*	067.5	069.2	046.1	009.6
ψ - β	*degree*	059.5	057.5	034.9	006.7
β	*degree*	8	11.7	11.2	2.9

The heading of the ship changed in response to rudder deflection. The rate of turn increased gradually until it reached a constant rate of turn. All the data recorded until the manoeuvre ended after one complete turn which is 360 degrees on the track course plus the drift angle at least.

The environmental conditions for calm weather were applied; rate of current and true wind speed were zero, which is an ideal condition for all manoeuvre details.

Table 4.3: Sample from the four ships data files at 360 seconds from (δ_{RO}) at (t_o)
(Ships had different approach speeds similar as in Table 4.1 and different δ_r)

		Investigated ships			
Recorded Data	Unit	Container Ship 1	Container Ship 2	Bulk Carrier	V.L.C.C.
t	*s*	360 *s*	360 *s*	360 *s*	360 *s*
X Y	*m* *m*	162 419	1430, 2627	995 1212	1071 1200
U_G	*knot*	16.3	22.6	8.7	8.0
R.P.M	*1/min*	82	99	89	69
δ_r	*degree*	20	05	10	25
$\dot{\psi}$	*1/min*	49.1	30.4	24.6	24.5
$\dot{u}$	*knot/min*	- 0.18	- 0.18	- 0.6	- 0.8
ψ	*degree*	306.8	159.6	142.8	148.0
ψ - β	*degree*	295.8	153.0	132.1	134.0
β	*degree*	11	6.6	10.7	14

4.4 Specifications for Considerations on the ANN Model

For wider applicability, the following limitation and simplifying assumptions are made for the present:

- Applying manoeuvring motion of single screw ship has right handed propeller for all ships.
- Ship motion is dealt with calm sea condition and the flow around the hull is free from uncontrollable forces such as wind and current. Moreover:
- The hull was free from other hydrodynamic forces such as shallow water and passing ship effects as so called semi-controllable forces.

The specific features of the ANN mathematical model are aimed at fulfilling the following:

- The numerical terms of the model should be as much related to the physical meaning as possible.
- Each term must have the ability to be evaluated experimentally or theoretically.
- The ANN model must be formed logically in order to develop the model for wider predictive applications.
- The model design must have the ability and flexibility to accept and predict the motion of different controllability actions.
- The constructed model is based on the consideration to make it rational and handy for practical use.
- The constructed model can be improved to enhance the manoeuvre prediction in the ship design stage. Moreover, it could improve to check the current IMO manoeuvre requirements as well to achieve the owner desires.

The discussions to fulfil these features and to find out a correlate technique to rationalize the ANN models will come later in this and the following chapter.

4.5 Simulative Models using ANN

4.5.1 The System's Mathematical Model Architecture

The model's architecture is structured as a training ANN set built on the selected inputs that have the ability to reach the desired decision outputs. A predictor system was produced and generated from the trained ANN. The predicting system has the ability to receive new desired ships' patterns and predicts the manoeuvring limitations, ships' tracks and simulates ships' motions.

The inputs described the ship's trajectory as different positions of the ship's track during its motion. The controllability's devises such as propeller and rudder are fed to the system with initial control action. Ship's parameters with different transient phases of motion at specific time interval depend mainly on ship speeds built in concrete patterns to construct an initially trained ANN system. An effort has been done to built the final training ANN as a PNN, each built with Multi-Layer

Networks after finding out a correlate technique to rationalize the ANN mathematical model, see the block diagram figure 4.1.

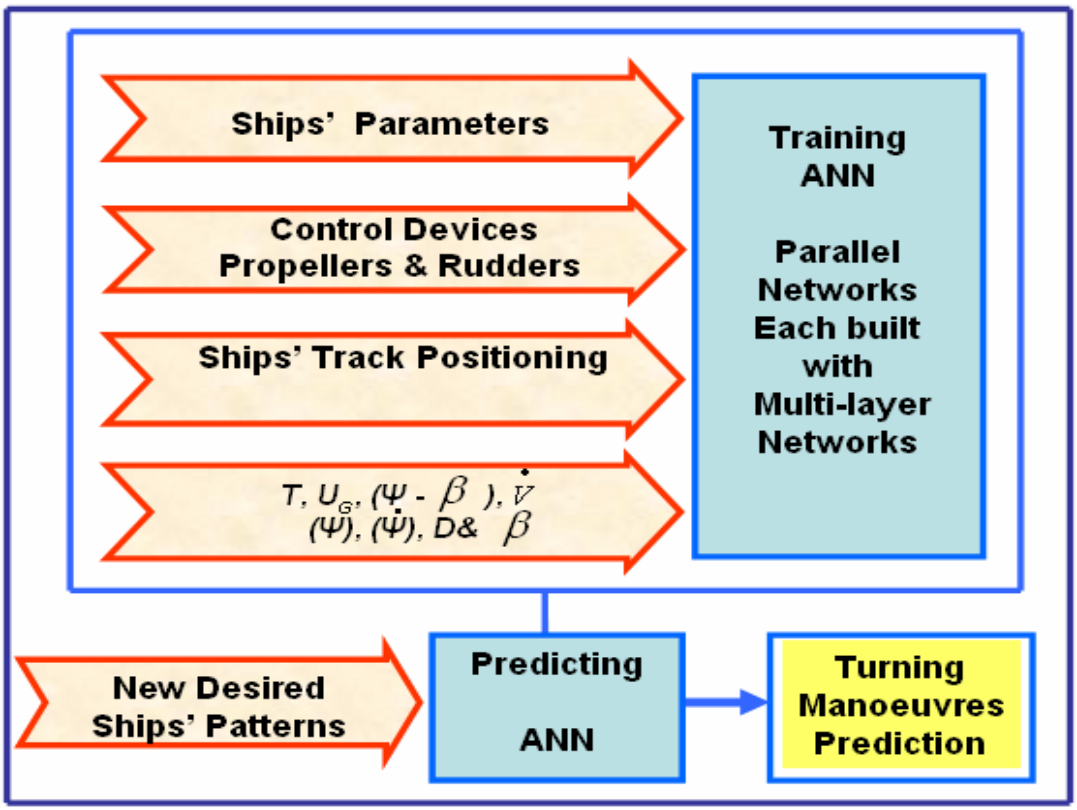

Figure 4.1 : Block diagram demonstrate the model prediction

The system's success depends on observing and measuring the system's behaviour to learn the neural network from the measured data. The future behaviour of the system can be detected from the learning steps.

The high performance of the mathematical neural network model prediction is conducted concretely with some important issues such as computational effort, training sample size, and ability to generalize. Moreover, in the case of on-line training and predicting, other issues are so important, one of them is a memory effect of the time-evolving system. This means that the output of a system depends not only on the current input but also on the system outputs at previous time steps.
The computational effort depends on the number of the layers, the number of nodes on the layers and the number of the training samples. In general: The networks have better system emulation if these numbers are increased. Obviously,

the computational effort dramatically increases with increased training samples, layers numbers and nodes numbers. The computational efforts have certain limits and any increase may negatively affect the predictive accuracy and could reach computationally prohibitive levels.

The size of the training samples should be enough for the purposes required. The way of samples choice and the large number of the samples help the system s' behaviour to be sufficiently captured. The samples chosen depend on investigating the problems of the applied application.

Deep knowledge of the problems involved in ocean engineering, naval architecture, computer science and manoeuvring practice of ship motion in addition to the skills required to build the models system.

Moreover, the sufficient sample numbers depends on understanding the neural network process and how the network will be trained and used. In this work, off-line training has been used, and that means a large number of training samples are needed. It has been reported that the number of the required samples for control of marine vessels could be in range of about 1000 to 10000 or even more (Cao, *et. al*., 2000). In the off-line training, the network only needs to train once to predict the future behaviour of the system. Generally, the prediction of the needed pattern comes immediately and in some cases with a shorter time compared to the other prediction methods, and the coefficients will stay unchanged in the prediction of the future behaviour of the system.

The superior off-line training gives prediction for situations not experienced in the training and that depend on the knowledge mentioned above. In other words: The ability to generalize is differing from network to other. If the networks succeed to realize the different patterns with suitable type of training, the further increase in the size of the training data could give a better generalization till a certain limit which would not be necessary to increase the networks' ability to generalize.

4.5.2 Parallel Neural Networks (PNN) Architecture

Many numbers of ANNs are used in parallel to describe the different parameters of turning manoeuvres for each individual ship and each manoeuvre. The numbers of ANNs which describe the ship track and the different manoeuvrability transient phases depend on the travel distance, travel time, plotting track and the application purposes; see figures (4.2-4.4).

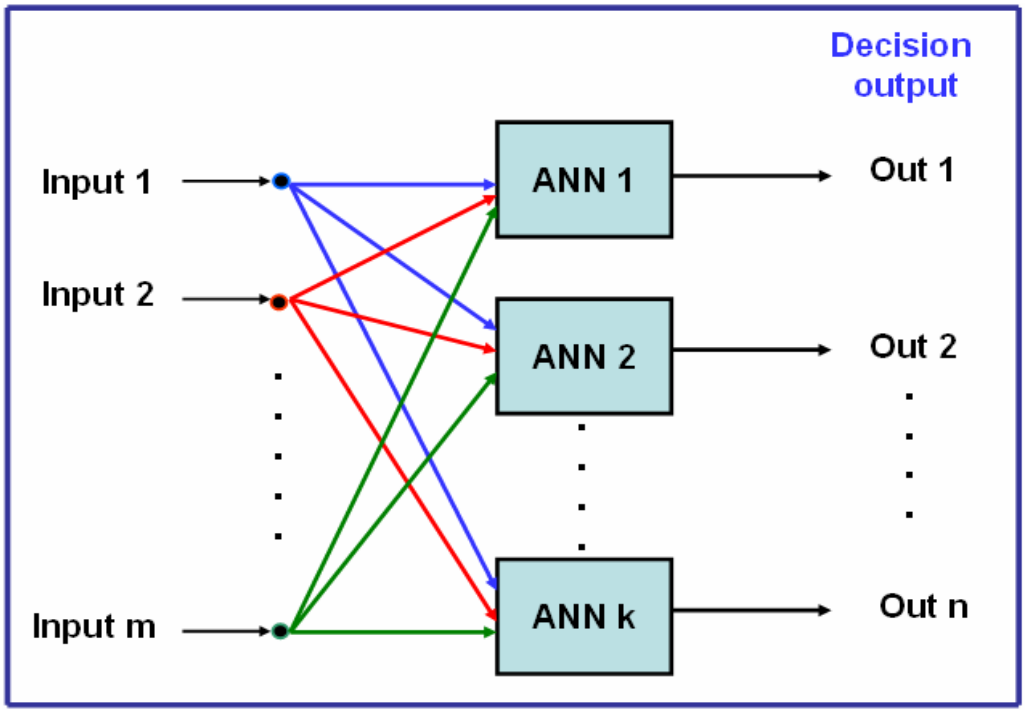

Figure 4.2 : Parallel Neural Networks Architecture with one decision output in each

Parallel ANNs describe the ships' trajectories as different positions of the ships' tracks during their motions with any rudder angle, similar techniques are applied to the other variables of interest that describe the different characteristics of a ships' turning motions to both sides (port and starboard). The architectures of ANNs number which were used in the PNN were different from each others.

Multi-layers in parallel are constructed for the variables that simulate the motion as shown in the parallel neural networks architecture (figure 4.2) that gives one decision output. Other architecture gives more than one decision output as in figures 4.3 and 4.4.

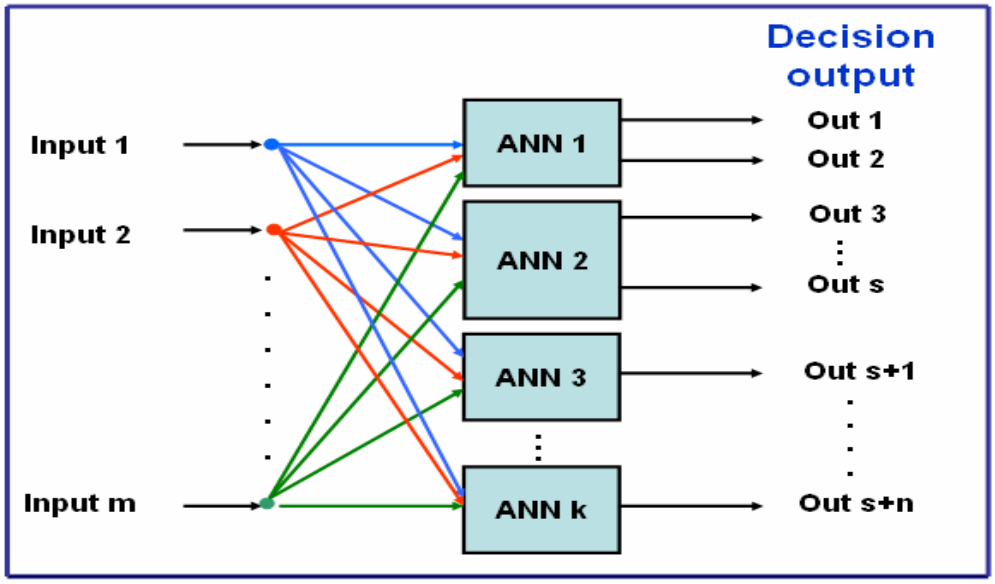

Figure 4.3 : Parallel Neural Networks Architecture with different decision output in each

The use of PNN gives better performance and accuracies. Each variable has a different nonlinearity characteristic and that causes performance ambiguities in some stages of the training. The nonlinear characteristics of the variables have different behaviours. One variable could increase or decrease smoothly while the other variable is sharply running at the same time. The techniques of structuring the APNN are built in such a way as to overcome all these problems, and to refine the standard deviation, and ending with better performance.

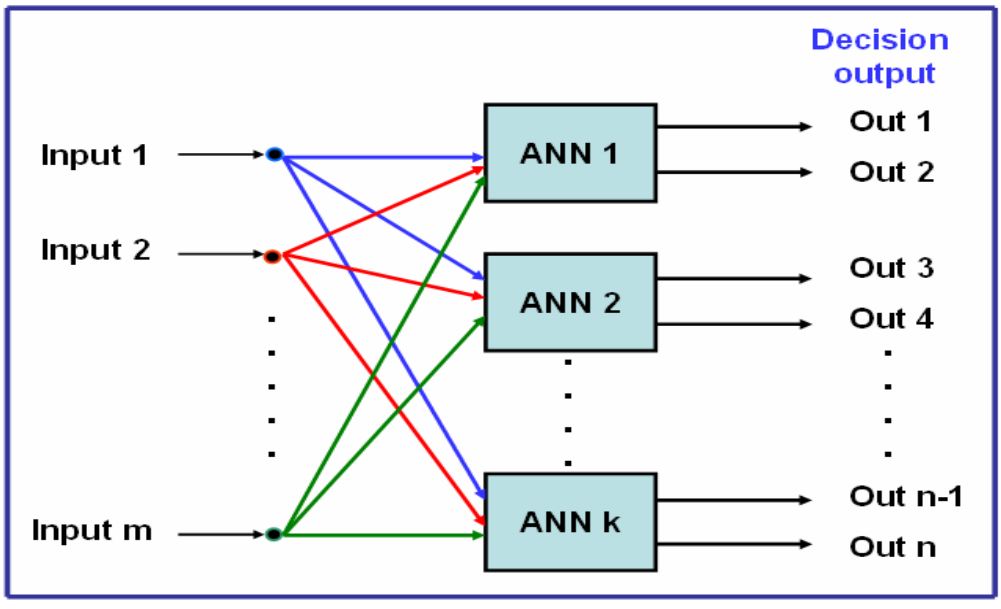

Figure 4.4 : Parallel Neural Networks Architecture with two decision output in each

4.5.3 Artificial Neural Networks (ANN) Layers Architecture

Multilayer network technique is applied. Each layer in the network has its own role and functions (see Figure 4.5). A layer that produces the network output is called an output layer. All other layers are called hidden layers except the first layer which is defined as an input layer. The layers are built of multilayer networks technique which have the ability to play different roles. Some researchers refer to the inputs as a layer number one. This work uses the input layer as a designation for the inputs fed to the neurons constructed before the first hidden layer.

The sequences in one network architecture are that of a node in each layer which receives signals from nodes in the layer on the left, and passes the modified (or weighted) signals to the nodes in the layer on the right. It is obvious that the design of the network is to determine the weights so that the system output from the network structure predicts as closely the output of the real system. The future predictive behaviour of the system can be detected from the learning steps as in following paragraph.

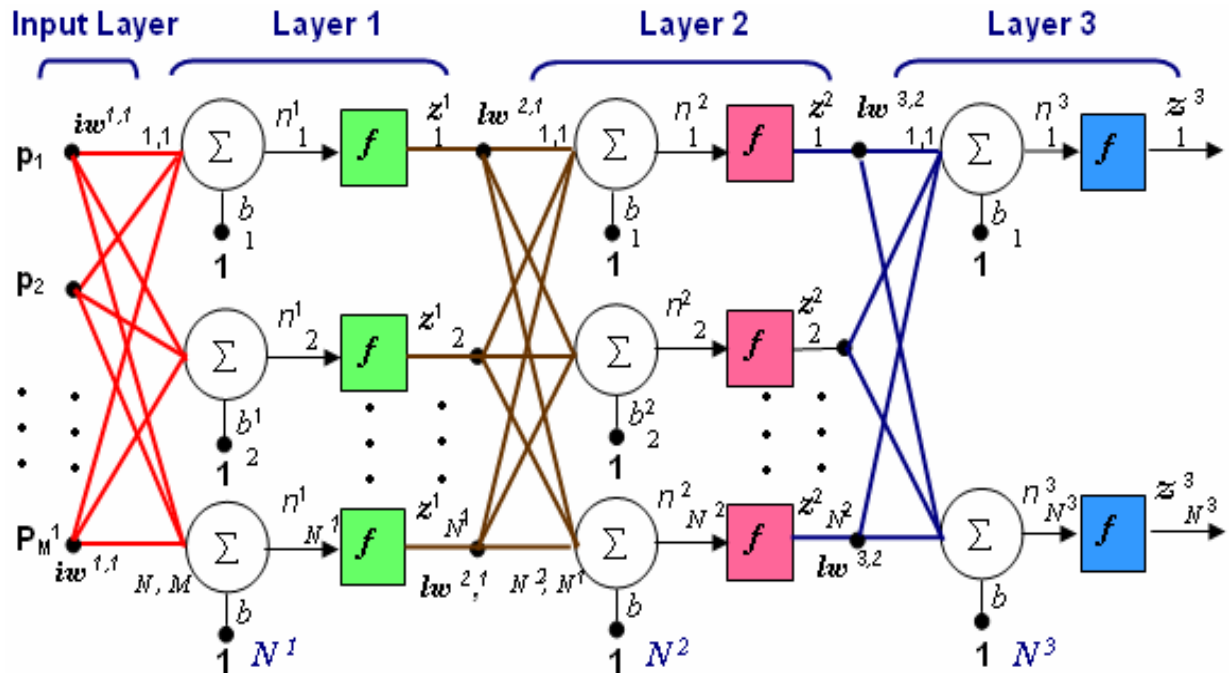

Figure 4.5: One single architecture of multiple layers of neurons constructed in PNN

Figure 4.5 shows in detail the architecture of one of these numbers that are contained in the PNN and uses the back propagation feed forward neural network form. While figure 4.6 shows the layers diagram of other architecture for different output decision.

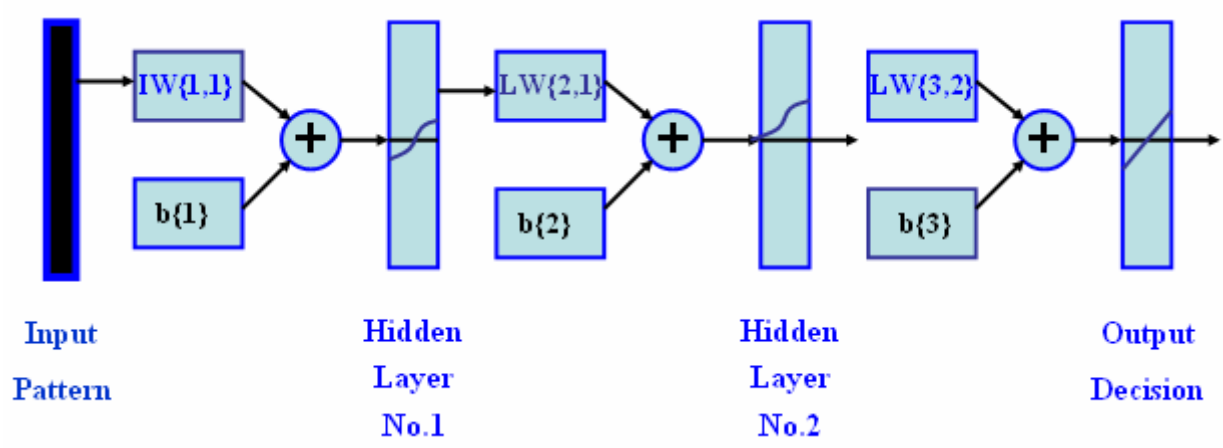

Figure 4.6: One single architecture of multiple layers diagram

The structure here is four layers as one of the structures have been built in this research (one input layer, two hidden layers and output layer). The inputs are fed to the neurons which were constructed before the hidden layer number one. Each layer has a weight matrix *W*, *a* bias vector *b*, and an output vector *a*. To distinguish between the weight matrices, output vectors, etc., for each of these layers in the built system, the number of the layer has been appended as a super script to the variable of interest shown the following figure and in the equations 4.1, 4.2 and 4.3; general form is in equation 4.4.

The nodes in the input layer serve as a summation to couple the inputs to the designed net. The calculations are performed in the hidden layers and the output layer. The nodes in the four layers are fully connected by weighted links. Most nodes have a bias and this is implemented as an additional input multiplied by the weight associated with the link and then summed along with the other inputs to the node, further details can be found out, see (Hirose, 2003).

The network mentioned above has M^1 inputs that could be so many inputs for wider applications of motion prediction. For the investigated ships in this study, the inputs into the system prediction are represented in appendix G. The network in figure 4.5 has N^1 neurons in the first layer, N^2 neurons in the second layer, etc. The numbers of neurons in this application have been changed in each hidden layer and the output layer forms one to twenty one. A constant input of one is fed to the biases for each neuron so as to reflect the correct magnitude with any decision output value applying the sigmoid form of activation function. Obviously, the outputs of each intermediate layer are the inputs of the next layer. One of the intermediate layers such as layer two can be analyzed as a one-layer network. The vectors and matrices of layer two can be identified as N^1 represents the inputs; N^2 is the neurons in this layer. The multiplication of N^2 and N^1 are the weight matrix W^2 while the input to layer two is z^1 and the output is z^2. The three layers of notation can be articulated by the following equations [4.1-4.3]:

$$z^1 = f^1 (IW^{1,1} \; p + b1) \tag{4.1}$$

$$z^2 = f^2 (LW^{2,1} \; z^1 + b2) \tag{4.2}$$

$$z^3 = f^3 (LW^{3,2} \; z^2 + b3) \tag{4.3}$$

Equivalent of z^3 is as follows:

$$z^3 = f^3 (LW^{3,2} \; f^2 (LW^{2,1} \; f^1 (IW^{1,1} \; p + b1) + b2) + b3) \tag{4.4}$$

Each layer contains neurons, which contain a nonlinear transfer function that processes the input to the node and produces decision outputs. The binary sigmoid functions used for this work to produce the decision outputs are defined by:

$$g = f(net) = \frac{A}{1+e^{(-\lambda \; net)}} - D \tag{4.5}$$

Where: A can be equal 2 or 1 and D is equal 0 or 1 that depends on the pattern problems and the desired decision outputs. f is a non-linear function, λ is constant and net is a neuron input.

4.5.4 BPFFNN Architecture

The primary objective here is to explain how to use the back propagation technique to train feed forward neural networks to solve specific problems (see Figure 4.7).

The term back propagation refers to the manner in which the gradient is computed for nonlinear multilayer networks. There are a number of variations on the basic algorithm that are based on other standard optimization techniques, such as conjugate gradient and Newton methods.

Back propagation was created by generalizing the Widrow-Hoff learning rule to multiple-layer networks and nonlinear differentiable transfer functions. In this thesis the technique a gradient descent algorithm is implemented in back propagation learning. In the Widrow-Hoff learning rule, the network weights are moved along the negative of the gradient of the performance function. One of the iterations of this algorithm can be written as follows:

$$x_{k+1} = x_k - \alpha_k g_k \qquad (4.6)$$

Where x_k is a vector of current weights and biases, g_k is the current gradient, and α_k is the learning rate.
There are many stages in the training process that could be summarized in mainly four steps. Generally, the first step is gathering the training data; the second is creating the network object; the third is training the network and the fourth is simulating the network response to new inputs. For more information on the subject of back propagation can be found in (Hagan, *et. al.*, 1996).

The method used in this thesis implements the batch mode as a batch steepest descent training function. In batch mode, the weights and biases of the network are updated only after the entire training set has been applied to the network. The gradients, calculated at each training pattern, are added together to determine the change in the weights and biases.

The learning rate is multiplied times the negative of the gradient to determine the changes of the weights and biases. The larger the learning rate, the bigger the step

and vice versa. If the learning rate is too large, the algorithm becomes unstable. If the learning rate is too small, the algorithm takes a long time to converge.

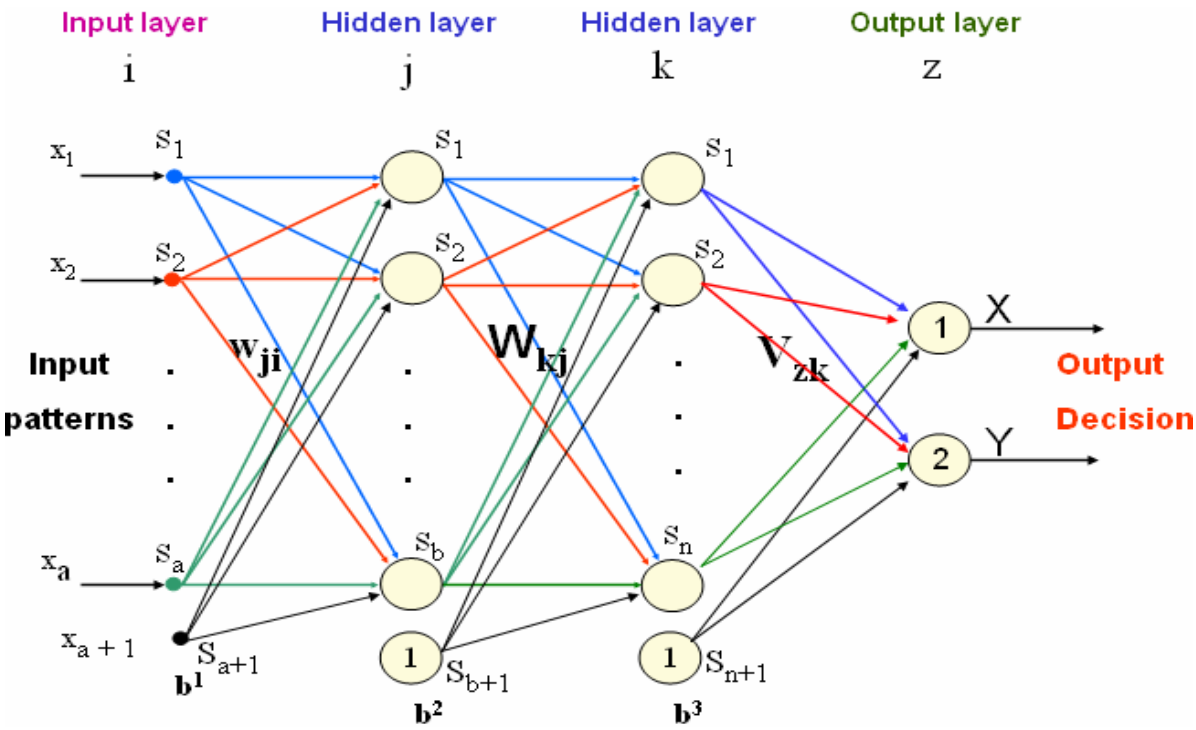

Figure 4.7: Architecture of BPFFNN

The basic feed forward network structures often have one or more hidden layers of sigmoid neurons followed by an output layer. The feed forward network illustrated schematically in Figure 4.7 consists of four layers (groupings of nodes); an input layer, two hidden layers and an output layer. The outputs of each layer represent the inputs to the next layer and feeding forward from left to right.

The network shown in Figure 4.7 has (x_a) inputs, S_a neurons in the first layer, S_b neurons in the second layer and S_n in the third layer, etc. It is common for different layers to have different numbers of neurons. A constant input 1 is fed to the biases for all neurons. Each layer has a weight matrix (w_{ji}, W_{kj} and V_{zk}) and an output vector (a) that depends on the transfer function (can be nonlinear) and the inputs to the layer as shown in the figure. For further details see (Hirose, 2003).

4.6 Training and Prediction Procedures

4.6.1 Pre Training Procedures

Before training the ANN, it is common to normalize all variables (inputs and outputs), which gives two advantages: To deal with dimensionless variables and to overcome the problem of changing the variables in a very wide range. One approach is to replace the existing variables by alternative dimensionless ones as in (Lewis, 1889) to designate the non dimensional form shown in following example:

$$\Delta' = \frac{\Delta}{\frac{\rho}{2}L^3} \quad ; \quad v' = \frac{v}{V} \quad ; \quad \dot{v}' = \frac{\dot{v}L}{V^2} \tag{4.7}$$

Another method is to combine two or more inputs together to form one input after normalization, which has the advantage of reducing the number of inputs taking their effect on the results into account.

The effect of the mentioned above inputs is studied in details and formed in relatively small number of inputs in the order of nine and increased gradually to reach twenty one inputs so as to have broad and friendly applications. Those inputs that have low effect on the specific three types (four ships) are ignored to simplify the analysis and to get fast results with almost the same accuracy.
It is also common to define and insert into the system the inputs after normalization depending on their maximum and minimum values.

4.6.2 Training Procedures

The inputs of the network are processed in successive steps through the non-linear sigmoid functions after multiplication by the weights to get outputs from each node until they arrive at the output layer of the network. The difference between the target and predicted output is a measure of the error of the prediction (see Equation 4.8).

$$E_p = \frac{1}{2}\sum_j (t_{pj} - o_{pj})^2 \qquad (4.8)$$

Where:

E : Error function (least squares)

P : Pattern index

j : Index of output neuron

t_{pj} : Target output for pattern p on node j

o_{pj} : Actual output at that node

The purpose of training is to gradually reduce the error in subsequent iterations. The training algorithm used in this work is defined in section 4.4.4. The weights could be updated using the delta rule, which is used to minimize the error from hidden-to-output neurons (see Figure 4.8 and the following equation).

$$\triangle w_{ij}(t) = -\eta \frac{\partial E(t)}{\partial w_{ij}(t)} + \alpha \triangle w_{ij}(t-1) \qquad (4.9)$$

Where $-\eta$ is the learning rate, α is the momentum and t is the iteration number.

The elements are interconnected so that the input to each node is determined by the outputs of some or all of the other nodes, and the whole accomplishes some useful "computations". Such a computational approach is often called "parallel distributed processing".

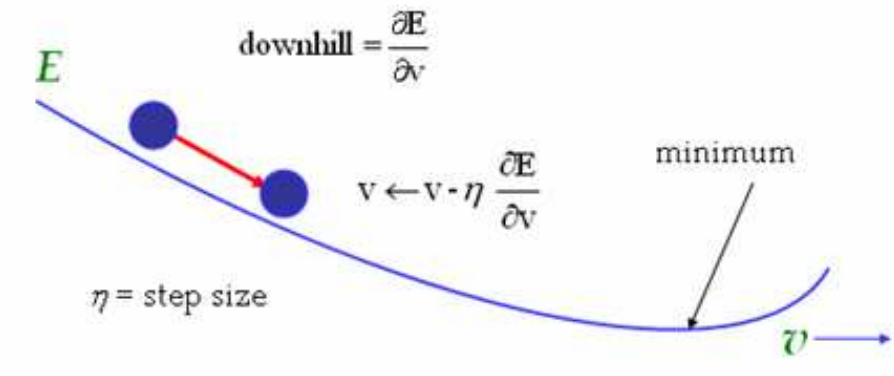

Figure 4.8: Error minimization in training process

To achieve the results shown in figures (4.9 & 4.10), the ANNs needs about 89603 epochs to reach the specific goal, which is about $8.5*10^{-5}$ for some manoeuvring positions. The epoch is defined as: The presentation of the time series for the inputs and outputs for one specific NN result in the training set.

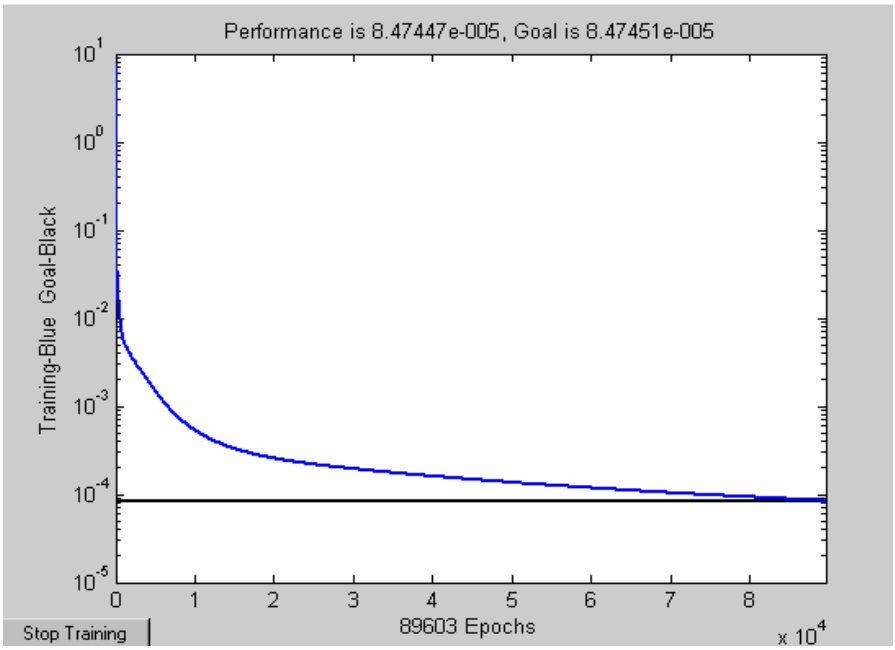

Figure 4.9: Epochs and goal of one cases set of PNN which is $8.47451*10^{-5}$ to get a high training performance

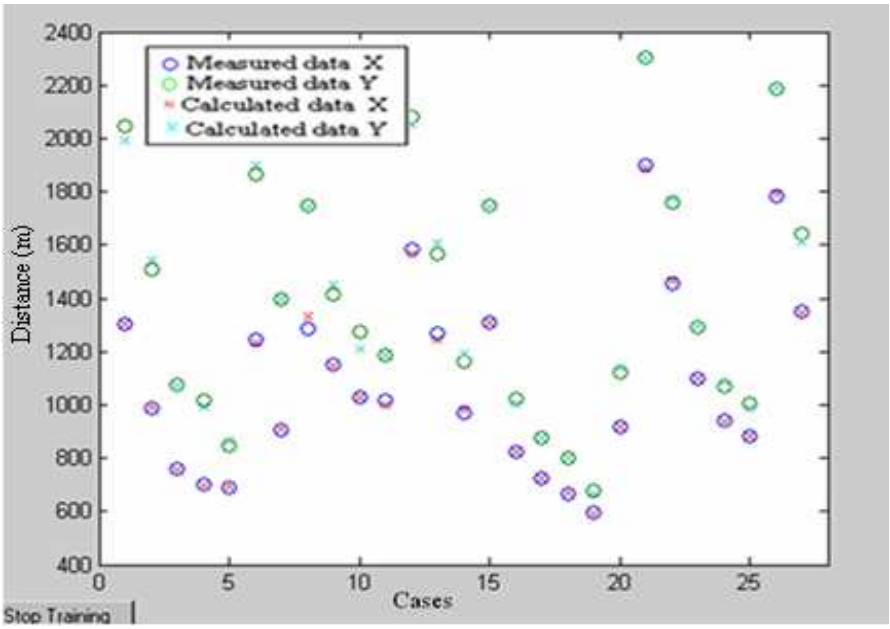

Figure 4.10: Results of training goal for the outcome cases set of figure 4.9 which is $8.47451*10^{-5}$

Other networks were trained for 135117 epochs as a selected epoch for best performance, see figure 4.11. The training goal was about $4.364*10^{-5}$.

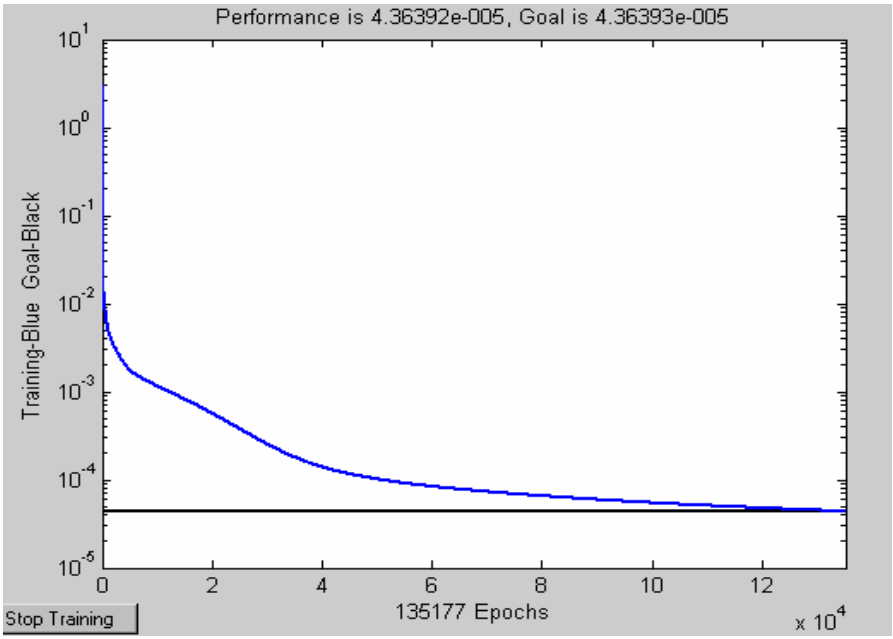

Figure 4.11: Epochs and goal for other cases set

The selected epochs and the defined goals are chosen to avoid over learning to all process. Over learning in the training process gives outstanding results and prediction failures. The training procedures were accomplished successfully and achieved high accuracy as shown in Figure 4.12.

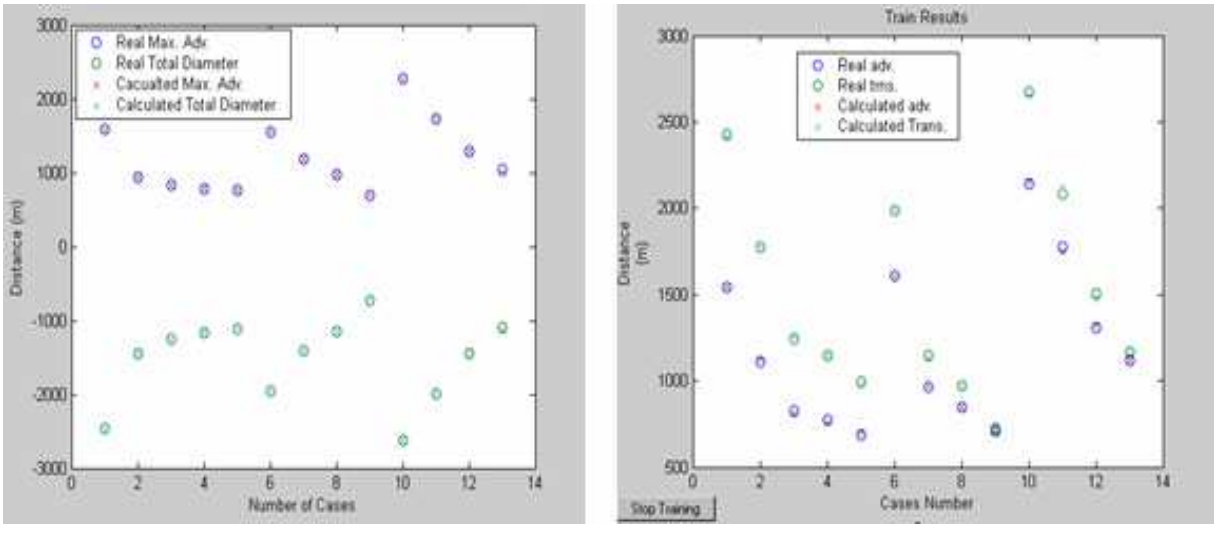

Figure 4.12: Results of training different ships model using various rudder angles to port and starboard side

For the application mentioned above, the ANNs needs about 6148 to 150000 epochs to reach the specific goals for the different PNN. The numbers of training epochs for the networks are chosen depending on realistic and probabilistic aspects according to the worst condition. The worst condition is the case where the error caused by the ANN is added to the measurement error and hence the overall error is maximized, i.e. the two errors have the same sign. The results in this case have to remain within an acceptable level to increase the reliability of the process.

The network is trained using the above mentioned cases with specific epochs for best performance. The net is tested for its ability to generalize during the training process by pausing the training process every 200 epochs and saving the weights to a data file. The process is carried out until the final stopping epoch or the defined goal is reached.

4.6.3 Neural Network Predictor

The training results of the system applying PANN mathematical models disentangle the nonlinear relation between the input data and the ship manoeuvring prediction. Many coefficients are represented by weights and biases that can be used to determine the different impact of dissimilar data inputs to the system on the behaviour of ship turning manoeuvres.

Increasing the number of layers and the number of nodes in the layers will support the predictor with large numbers of weights/constants. In some applications, it could be important to increase such weights until the limit of the highest prediction accuracy. In a simple application this will lead to poor prediction ability. Consequently, it differs from one predictor application to the other in addition to whether the training process is carried out in the on-line mode or in the off-line mode.

The capability of the neural network predictor to estimate the turning manoeuvring behaviour of new unknown patterns was tested extensively. Once the input signals of unknown patterns are received, they are then modified and passed continuously on until the signals reach the last layer (output layer). This flow of signals through a network of nodes is similar to the flow of signals passing through the human

neural systems. The human neural system gives analogue decisions and the ANN system here gives digital output decision.

The processes of training and testing have been repeated several times with different random selection of the test patterns to prove the satisfactory accuracy of the applied prediction method for more validation.

Weights and biases between two layers in one model can be used in other similar constructed architecture of predicting model depending on understanding the application area and the environmental problems.

4.7 Probability and Accuracy

A further important step is to evaluate system accuracy. Generally, a measure of the variability of the data about the mean is expressed as the standard deviation. One of the useful information deriving from the mean is the standard error. The equation that expresses the range of variation as variance or standard deviation is given as follows:

$$\text{Standard deviation} = \sqrt{\frac{\sum_{i=1}^{n} d^2}{n-1}} \qquad (4.10)$$

Generally, each data in the samples in equation 4.10 differs from the mean by an amount called the deviation (*d*). In this thesis, the system evaluation is to find the standard deviation of the calculated data from the measured data. Consequently, it is necessary to find each *d* value and then add all the d^2 values. Where *n* is the number of sample. We can then obtain the standard deviation which is the square root of the variance divided by the square root of the value (n-1). The value (n-1) is accepted as standard and necessary practice. The equation that expresses the standard deviation of the trajectory is as follows:

$$\sigma_X = \sqrt{\frac{1}{n-1}\sum_{i=1}^{n}(X_T - X_C)^2} \qquad (4.11)$$

$$\sigma_Y = \sqrt{\frac{1}{n-1}\sum_{i=1}^{n}(Y_T - Y_C)^2} \tag{4.12}$$

$$\sigma_{Position} = \sqrt{\sigma_X^2 + \sigma_Y^2} \tag{4.13}$$

Where: σ_X is the standard deviation of the *X* value in the *XY* plane, σ_Y is the standard deviation of the *Y* value in the *XY* plane, $\sigma_{Position}$ is standard deviation of the position, the notation (*T*) added to *X* and *Y* is the measured data and the notation (*C*) is the calculated data.

The same technique is applied to the other variables of the different transient phases that represent ship's motion to find out the standard deviation. Table 4.1 shows one of the results of the random test selections to predict the main variables that describe ship motion. Where, *L.O.A.* in the table is the main length over all of the four investigated ships.

Table 4.4: Main transient phases' standard deviations of the direct model predictor for one of the random test selection

Variable	Standard deviation	Unit		Variable	Standard deviation	Unit
U_G	0.36	*knot*		ψ	3.11	*degree*
R.P.M	1.3	*1/min*		ψ - β	3.15	*degree*
$\dot{\psi}$	0.87	*1/min*		β	0.34	*degree*
$\dot{u}$	0.089	*knot/min*		(*x*, *y*)	0.15*L.O.A* 41.96845	*m*

4.8 Improving the Performance of Neural Network Predictor

One of the most powerful advantages found in this study is that the ANN mathematical model can check the accuracy of the given data through the training

and testing random processes and realize the correct accuracy value of the data files. Consequently, the model has the ability to detect the errors of the data.

In the training process the errors of the different variables must be defined to the system. During the experimental manoeuvres in the simulator, great care has been taken to considering the limitation of the error sources. The probabilities of machines, human and aids to navigation errors are considered as “initial errors estimation”.

The initial estimated errors are applied as initial goals in the training processes. All the variables initial errors are defined to the system before the training procedures.

The training processes performance and the results of the system are analysed. The accuracy of the trained data is examined through the random training and testing processes. As a result of this operation, new defined errors are inserted into the system for better performance and more accurate prediction.

The data variability for specific variable such as speed, acceleration, courses, etc. has been estimated separately. Moreover, in some periods of the manoeuvres, the data of a specific variable in such periods were added together and delivered to one of the PNN as a training case to get better accuracy. In other words, the manoeuvre data of the different transient phases were grouped in the most meaningful way and the outcome is connected using the PNN to have the optimum training performance completed with better result accuracies.

The final intended goals are estimated from these processes. Both of the training process and neural network predictor were guided to the “final errors estimation” which considered as “realistic errors”, both designations are used in this thesis.

Consequently, the predictor provides higher accuracy than the prediction that only depends on the initial approximation errors for the unknown patterns. In order to elucidate that, two cases studies are presented with number of epochs, goals and outcome results.

The numbers of the iterations are required to estimate final measured data errors for the different variables depend on the initial errors estimation. This fact can be

clarified by illustrating the two cases studies. The first case is the example shown in figure 4.13 and the second case is the example shown in figure 4.14 as a case set of grouping data to predict the ships' trajectories.

In the first case: The system trained to achieve a dimensionless goal of $5.42369*10^{-5}$ following the initial errors estimation procedures (see Figure 4.13). The outcome were 100 000 epochs and the training errors were generalized in the worst conditions which means that the errors of different sources will be added with same sign. The error is generalized for each of the trajectory components (*X* and *Y*).

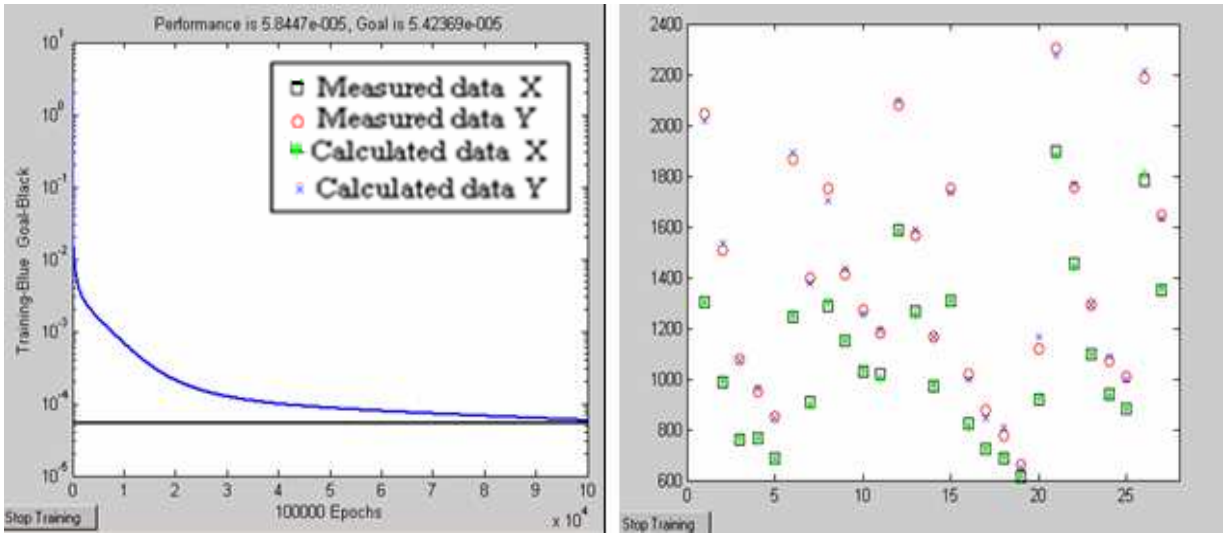

Figure 4.13: Left side trained for 100 000 epochs and goal of $5.42369*10^{-5}$ and right side: The outcome results of one case set

In the second case, more than one random tested process is evaluated and the system is trained to achieve dimensionless goals, which ended with $8.47451* 10^{-5}$ as an optimum data error for that group of the same case. This optimization is produced from the ANN system mathematical model. The results of the ANN predictor dramatically improved the generalization ability of the system for the blind cases and provided better accuracies. The training epochs are reduced from 100 000 to 46 989 and the computational period is dramatically decreased. The difference between the first operation which applies the dimensionless goal of $5.42369*10^{-5}$ and ANN optimum operation which applies the dimensionless goal

of $8.47451*10^{-5}$ is only six meters added to the error that comes out from the initial errors estimation to get optimal ANN goals.

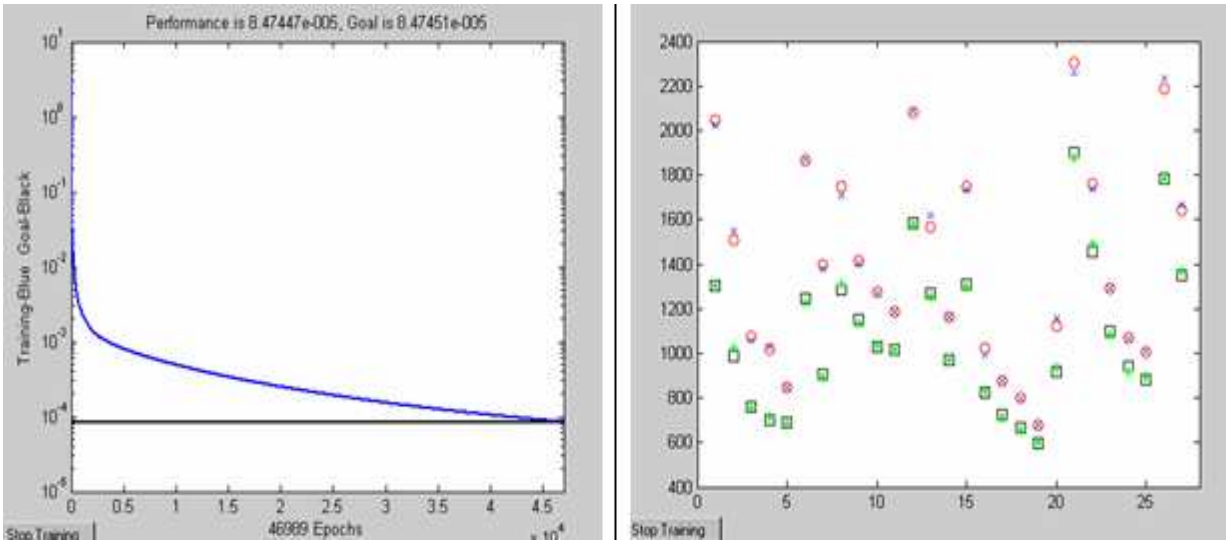

Figure 4.14: Left side shows 46 989 epochs and goal of $8.47451*10^{-5}$ and right side: The outcome results of the same case at figure 4.13 but with different error probability

This technique is applied to the others variables for more precision for the measured data errors. The prediction results of the manoeuvrings limitation, the ships' trajectories and ships' motions simulations are described and illustrated in chapter six.

4.9 Decreasing the Limitations of System Prediction

This system is trained to predict nonlinear motion problems. It is also trained for the manoeuvre controllability actions of engine and rudder for different speeds and rudder angles for four different ship types. The ANN mathematical model succeeded in recognizing complex problems of the motion for different transient phases' characteristics of each individual ship.

Motion prediction for other types of ships needs more training to introduce other variables as inputs. The expert's task is to build these variables in the patterns for the first layer. This is an essential step in order to simulate the manoeuvres for other unknown ships. As the ANN system was trained for different speeds and rudder angles, it needs to be trained for the other variables of different

displacements, ships' forms, trims and, etc. The system needs to understand the other nonlinear variables characteristics with sufficient number of patterns otherwise, the prediction results will be inaccurate and the prediction will be poor grades.

Further investigations were carried out to check the generalisation of the models. Thus, other ships' data files from another source into the system. The ANN-based mathematical models have been tested in another integrated simulators complex of "American Ship Analytics Ship Simulators". Sixteen experimental data files were collected for another four ships (two containerships, a bulk carrier and a VLCC) in the "American Ship Analytics Ship Simulators". All manoeuvres considered of altering courses to starboard. The four selected ships differ from the four ships of the "Norcontrol Simulators" in their parameters and behaviours (see Appendix G). Only the simulation periods of the sixteen experiments were compressed to reduce the simulations' cost. Only ten experimental data files of "Ship Analytics Ship Simulators" were inserted into the ANN training system in addition to the "Norcontrol simulators" data files. The rest of the six blind manoeuvre experiments of the "Ship Analytics Ship Simulators" in addition to the blind manoeuvres of the "Norcontrol simulators" data files were used to test the system validation.

Integrated Norcotrol simulators and Ship Analytics Ship Simulators used together in one system prove the property of adaptively of ANN mathematical model and the ability of the system to be retrained to deal with other changes in patterns that have different parameters. Neural networks have built-in capability to adapt their synaptic weights to change with the different patterns that have different nonlinear characteristics that match these different inputs to the system (refer to Fig. 6.23, 6.24, 6.25 & 6.26 in Appendix F.1). The plotted circle and square shapes are represented the measured data, where the star shapes are represented the calculated data.

The results of the blind manoeuvres for both systems had high accuracies in the limitation of ships' turning manoeuvres and ships' tracks (refer to Fig. 6.27& 6.26 in Appendices F.2 & F.3). The results of the motion simulation for both systems confirmed the investigated fact mentioned above. Thus, the Norcotrol patterns in

the system were enough to solve the different transient phases' characteristics with their motion simulations. On the other hand, patterns in Ship Analytic were not enough to solve the simulation problems with sufficient accuracies. In addition to the problems arose from compressed the simulation periods, the discussion of these problems are in chapter six (see Figure 6.29 in Appendix F.4 that shows the fair accuracies). Generally, one or two points diverging from the other points that describe the nonlinear characteristics of different ships' parameters are not enough to define the nonlinearity function. Therefore, unknown nonlinearity function needs to be recognised by the system through adequate training patterns. Then, the system would be able to predict the other unknown ships' patterns. In other words, to solve different ships' forms and types which have different parameters and conditions, a good wide expert choice of patterns is required. The application of ANN mathematical models series in chapter five facilitates this hypothesis by optimizing the data among Model Series (see Chapter 5 in 5.7 and 5.8).

4.10 Conclusion

Parallel Artificial Neural Networks (PANN) used the techniques of Back Propagation Feed Forward Neural Networks (BPFFNN), was trained and tested using different ship data. The results of the training process and the blind manoeuvres test proved that the proposed system is a practical method and it is able to predict the ship turning manoeuvres with sufficient accuracies during the operation time (see the results in Chapter 6).

The ANN mathematical model has the ability to check out the errors in the data files and to correct the initial estimated errors. The procedures and the mechanism of damping the tolerance to word the realistic errors are extended to all variables to improve the predictor performance.

The main system consists of subsystems employ different styles of generalization to support broad and complex areas of prediction applications. The dynamic system is operating the topology of these subsystems synchronously and in parallel to predict the manoeuvring motions.

The results of these procedures allow increasing the efficiency in learning and reasoning as aspects to be intelligence. The integration of these aspects may lead to more powerful models and very large scale integrated implementability. This feature is not only in the individual multilayer architecture but also in each subsystem and in the main system.

Afterwards, the method is extended to include other ships' data files from another source of "American Ship Analytics Ship Simulators" to decrease the limitations of the system prediction. This step was also taken forward for more verification and validation of the ANN system prediction. The results and the discussions of this extension and verification are given in chapter six.

Chapter 5

Neural Hydrodynamic Force Model

5.1 Introduction

This chapter describes different hydrodynamic models as practically applied methods. The aim of development is to apply the hydrodynamic's forces on the manoeuvring ship as inputs into the system, with respect to the requirements of ANN. The advantage of this model is making the applied method applicable for a wider application range of manoeuvres. Another aim was to improve the accuracy of the applied method. A discussion about this goal will come later in this chapter. Moreover, application of the hydrodynamics forces will dramatically decrease the number of delivered training manoeuvres to the system.

It is necessary to investigate the propeller-hull and rudder interaction, resistance problems, and powering problems before inserting the hydrodynamic forces. The target is to estimate thrust forces and rudder lift forces as essential inputs into the system.

Regarding the different hydrodynamic models, a step has been taken forward by improving the system performance through optimizing the data among models series.

5.2 Propeller-Hull and Rudder Interaction

A summery of the interaction among hull, propeller and rudder is given in Volker (2000). The ship stern form has strong influences on propeller inflow and cavitation. The stern shape affects the viscous resistance, wake flow and vortices strength.

The single screw propeller causes different pressure reductions on the port and starboard sides of the ship. The interaction of the upward component of the wake

field and the direction of rotation of the propeller will influence the pressure distribution on the ship stern.

The propeller excites a complicated combination of forces and moments acting at the propeller hub and fluctuating pressure acting over the stern surface.

The investigation of the interaction between the rotating propeller and the stationary ship shows an inherently unsteady nature of the problem especially when applying the controllability of rudder and engine. The problems of including viscous forces and complexity of the geometry increase the difficulty of investigating the interaction among all these factors (Abdel-Maksoud, *et. al*., 1998).

Testing work performed at SSPA for MARINEX (Olofsson, 1991) resulted in a 34% difference in required power for two designs having relatively minor differences in stern geometry. Also, stern forms in both full load condition and ballast condition affect the required power.

5.3 Ship Resistance and Propulsion

The estimation of the resistance of a full scale vessel is based on model test data (Lewis, 1988*b*), (Deng and Visonneau, 1998) and (Masuko, 1988). The ship resistance is required to determine the effective and installed power to propel a vessel at its required service speed. The estimation of the effective power requirement involves the estimation other resistance of appendages such as shafting, shaft brackets, rudders, fin stabilizers, bilge keels, etc. In addition, the hull above water causes air resistance. The result of the main physical components is the resistance that contains pressure and shear force over the hull (Dawson, 1979). According to Froude, the total resistance of a ship is consisting of the following components:

$$R_T = R_F + R_R \tag{5.1}$$

Where:

R_F Frictional resistance as a function in Reynolds number (R_n)

R_R Residuary resistance (wave making resistance, form effect and viscous pressure) as a function in Froude's number (F_n)

Each of the resistance components given above adheres to a different set of scaling laws. Each resistance component and the ratio among these components depend on the ship shapes and speeds. For example, the approximate breakdown of resistance components for the tanker (VLCC) and the bulk carrier is about 60-65% frictional resistance, 30% viscous pressure resistance and 5-10% wave resistance. While for the two containerships are 45-50% frictional resistance, 10% viscous pressure resistance and 40-45% wave resistance. The symbols of the resistance components are in the "Acronyms and symbols".

5.3.1 Power Estimation and Prognosis

The powering problem could be divided into three main areas. The first is the estimation of effective power; the second is the estimation of Quasi-Propulsion Coefficient (*QPC*) or (η_D) and the last is the estimation of required power margins.

Effective horsepower (P_E) is the power required to move the ship hull at a given speed in the absence of propeller action. The following equation defines the effective power:

$$P_E = R_T \times V_S \tag{5.2}$$

Where:

P_E Effective power (*W*)
R_T Total resistance (*N*)
V_S Speed of ship (*m/s*)

To join installed power and effective power requires calculating the Propulsive Efficiency (η_D) and Transmission Efficiency (η_T); in addition to margin estimation. This is known as the design power margin (to allow for increases in fouling, bad weather, etc.).

Propulsive efficiency (η_D) is the ratio between the effective power (P_E) and the delivered power (P_D), and forming the Quasi-Propulsion Coefficient (*QPC*). In contrast, the transmission efficiency is the ratio between the delivered power (P_D) and the brake power (P_B).

$$\eta_D = \frac{Effective\,Power}{Delivered\,Power} = \frac{P_E}{P_D} \tag{5.3}$$

$$\eta_T = \frac{Delivered\,Power}{Brake\,Power} = \frac{P_D}{P_B} \tag{5.4}$$

P_B is the power output at the shaft coming out of the engine before the reduction gears and P_D is the power required to be delivered to the propulsion unit at the tail shaft after the losses in the shaft horsepower.

The basic principle is that the effective power required to drive the ship is less than the power delivered to the propulsion device. The power delivered to the propulsion unit will exceed the effective power by the efficiency of the propulsion unit.

Finally, the indicated power will exceed the delivered power by the amount of power lost in the engine and in the transmission system (shafting and gearing losses).

5.3.1.1 Estimation of Thrust Power and Force

The following equation defines the thrust power:

$$P_T = T \times V_A \tag{5.5}$$

P_T Thrust power (*W*)
T Propeller thrust force (*N*)
V_A Speed of water passing propeller (*m/s*)

The following equations are used to estimate the thrust force.

$$P_D = 0.97 * P_B \quad (5.6)$$

$$Q = P_D / 2 \pi n \quad (5.7)$$

$$K_Q = Q / \rho n^2 D^5 \quad (5.8)$$

Using propeller design charts e.g. Wageningen propeller series (Kuiper, 1992) and using the K_Q value to get K_T and J. Finally, the thrust force would be estimated (Carlton, 1994) as the following equation:

$$T = K_T \rho n^2 D^4 \quad (5.9)$$

Where:

P_D Delivered power at propeller (W)
Q Torque (Nm)
n Rotational speed (rps)
K_Q Torque coefficient
ρ Density of the fluid (kg/m^3)
D Propeller diameter (m)
K_T Thrust coefficient
T Thrust force (N)

5.4 Rudder Lift Forces

The rudders used in the two containerships and the VLCC are balanced semi-spade rudders but the bulk carrier is a spade rudder. They are placed at the ship's stern behind the propeller and on a vertical or nearly vertical axis producing a transverse force and a steering moment. The forces are created by deflecting the water flow to a direction of the foil plane during the motion to create transverse force in opposite direction of the foil (Munson, *et. al*., 1988). The rudders lifting coefficients at different angels are calculated as follows (Brix, 1993):

$$J = V_A / nD \quad (5.10)$$

Where:

J Propeller advance coefficient
V_A Speed of advance (velocity behind ship)

$$C_{Th} = T / (\frac{\rho}{2} V_A^2 A_p) = \frac{8}{\pi} . \frac{K_T}{J^2} \quad (5.11)$$

$$V_\infty = V_A \sqrt{1 + C_{Th}} \quad (5.12)$$

C_{Th} Thrust loading coefficient

V_A Mean axial speed of inflow to the propeller (*m/s*)

A_p Propeller area (m^2)

V_∞ Mean axial speed of the ship stream far behind the propeller (*m/s*)

$$r_\infty = r_o \sqrt{\frac{1}{2}\left(1 + \frac{V_A}{A_\infty}\right)} \quad (5.13)$$

r_∞ Theoretical slipstream radius far behind the propeller (*m*)
(that follows from the law of continuity, assuming that the mean axial speed at the propeller is the average between V_A and V_∞)

r_o Half of the propeller diameter (*m*)

$$r = r_o . \frac{0.14(r_\infty / r_o)^3 + r_\infty / r_o . (X / r_o)^{1.5}}{0.14(r_\infty / r_o)^3 + (X / r_o)^{1.5}} \quad (5.14)$$

r Propeller slipstream radius in rudder position (*m*)

X distance of the respective position behind the propeller plane (*m*)
(To determine rudder force and moment, it is recommended to use the Position to the centre of gravity of the rudder area within the propeller slipstream)

$$V_x = V_\infty . (r_\infty / r)^2 \quad (5.15)$$

V_x Mean axial speed of the ship stream at rudder position (*m/s*)

$$\Delta r = 0.15 X . \frac{V_X - V_A}{V_X + V_A} \quad (5.16)$$

Δr Added value to potential slipstream radius because of the increasing in the slipstream diameter with increasing X due to turbulent mixing with the surrounding fluid (m/s)

$$V_{corr} = (V_X - V_A) \left(\frac{r}{r + \Delta r} \right)^2 + V_A \tag{5.17}$$

V_{corr} Mean value of the axial speed component over the slipstream cross section (m/s). V_{corr} is corrected according to the momentum theorem

$$\Lambda = \frac{b}{main\ (c)} \quad (6.20) \quad \& \quad \Lambda = \frac{2\ b}{main\ (c)} \tag{5.18}$$

Where:

Λ Rudder aspect ratio

b Rudder height (span), (m). Span is multiplied by 2 if the rudder angle does not exceed 5 degrees and there is no space between the rudder top when it is at midship and ship's hull

c Chord length (m)

$$C_L = \frac{2\pi.\Lambda.(\Lambda+1)}{(\Lambda+2)^2} . \sin\alpha + C_q . \sin\alpha . \mid \sin\alpha \mid . \cos\alpha \tag{5.19}$$

Where:

C_L Lift force coefficient

α Angle of attack

C_q Resistance coefficient ≈ 1

$$L_1 = \frac{1}{2} \rho V_{corr}^2 A_1 C_L \tag{5.20}$$

$$L_2 = \frac{1}{2} \rho V_A^2 A_2 C_L \tag{5.21}$$

$$L = L_1 + L_2 \tag{5.22}$$

Where:

A_1 Rudder area that faces propeller slipstream (m^2)

A_2 Rudder area that faces speed of advance at ship's stern (m^2)

L_1 Rudder lift force at A_1 (N)
L_2 Rudder lift force at A_2 (N)
L Total rudder lift forces (N)

Rudder forces are made dimensionless by the stagnation pressure $\frac{1}{2}\rho\ V_{corr}^2$ and the projected rudder area. Calculating rudder lift forces of the different ship types at any angles and the thrust forces with different speeds are essential to build up the main inputs to the force model. In the force models, the rudder forces that cause the yaw moment are about the ships' pivot point (Rowe, 1996).

5.5 ANN Force Model Prediction Systems

5.5.1 Data Generation

In addition to the data files generated for the direct model, the navigation simulator was used to generate the rest of the required data for the training and validation of the force model prediction system. The study was carried out for the same ships used in chapter four. One of the advantages of using the same ships is to compare the two different models as direct model and force model.

The data files of the initial brake powers that matched the investigated speeds in the previous experimental manoeuvre's data files were measured and documented. The ships run in straight course for a long time until the engine power was adjusted as constant values. The initial lift forces were calculated under the condition of the initial constant heading run thrust.

The data files of thrust forces and rudder lift forces replaced the data files of ships' speeds and rudder angles. Both Table 5.1 and Table 5.2 include four different cases as regards rudder angles and ship's speeds, thrust and lift forces. The first table represents containership 1 and the second table represents the VLCC. The system is developed and trained only in similar procedures as in the direct model. The predicted different transient phases are similar to those in the previous chapter.

Table 5.1: Thrust forces and rudder lift forces replaced (δ_r) and (U_G) for containership (1)

Recorded Data	Unit	Investigated ship Containership 1			
		Case 1	Case 2	Case 3	Case 4
δ_r	*degree*	35	35	20	25
U_G	*knot*	24.7	18.5	24.7	24.7
Calculated Data	Unit				
T	*kN*	2699	1273	2699	2699
L	*kN*	4564	2281	2553	3241

Table 5.2: Thrust forces and rudder lift forces replaced (δ_r) and (U_G) for the VLCC

Recorded Data	Unit	Investigated ship VLCC			
		Case 1	Case 2	Case 3	Case 4
δ_r	*degree*	35	15	35	35
U_G	*knot*	14.7	14.7	10.0	12.5
Calculated Data	Unit				
T	*kN*	2374	2374	1242	1691
L	*kN*	1642	673	667	1206

As is well known, the behaviour of the ship with a single propeller, when turning to starboard side, is different from her behaviour when turning to port side, even if the ship is considered a stable ship in her motion ahead (Journee, 2002). Her maximum advance and total diameter will differ when she turns to starboard side from turning to port side with the same rudder angle. The direct model in chapter four succeeded in predicting the motion to both sides with high accuracy. Even when the ship turns to both sides with the same rudder angle, the outcome results of the direct model have sufficient accuracies (see the results in Chapter 6). Logically, as regards interruption, if we use only the initial situation of equal forces

to both sides to feed into the system, the trajectory to starboard side is identical to port side

From this point of view, it is preferred to solve only the problem of prediction to one side as the starboard side. Data files of more than hundred experimental manoeuvres were recorded and documented. The recording of the data files was documented as fifty-nine of such data files to the starboard data file and a second set of more than fifty files representing the port side data files. The data files of the starboard side as experimental manoeuvres, power and forces calculations were divided into two sets. The first set is about two thirds of such data files for training and was provided to the system. A second set of the rest of the data files that represented blind manoeuvres was used for validation. The first training set of the data files comprised forty-two files and the second set of blind manoeuvres comprised seventeen files to starboard. The problems of solving the port side prediction are clarified in the force model predictor in (5.6).

5.5.2 Data Formation and Structure

Formatting and structuring the data inputs of the force models were not an easy task of networks simulation. These processes were more complicated than the direct model built in chapter four. Firstly, the force model inputs were built as in the direct model. Then, the outcome prediction results were poor relative to those results of the direct model in chapter four. The results of testing blind manoeuvres could not validate the system prediction of the force model. Therefore, the formatting and structuring strategy in the force model must be different from the direct model.

Describing and learning ships' parameters and controllability actions to the networks system in chapter four depends on figuring out visual description to physical meaning. In the direct model the small rudder angles or big rudder angles are well known to the networks. Different ships' speeds will not affect the rudder angles definition to the networks.

The force model is completely different in this area from the direct model. The thrust is one of the main factors that have strong influence to estimate the lift force

of the investigated ship. While in the direct model the definition of the rudder angles will remain as it is in the networks.

The parameters of each investigated ship such as machinery, shaft, propeller and rudder and are used to calculate rudder lift forces and thrust forces. The thrust forces of each ship depend on the load condition of the engine. Consequently, the same rudder angle will have different lift forces with each thrust force. In the force model, the superior rudder lift force is not always the bigger rudder angle.

The applied network technique has a static structure (has no feedback or delays). In this case, it is essential to define well the initial situation to the networks system. It is possible to treat the inputs as concurrent. A matrix of concurrent vectors is inserted in the network taking into consideration the rudder lift forces and no data inputs about the rudder angles are fed to the system. The lift forces are considered as dimensionless values without figuring out this angle physically. It is essential here to get the system to realize the actual rudder lift and the maximum force in each training pattern and the range of the rudder lift force that could be achieved with this specific ship in the training patterns. It is necessary to implement the batch mode as a batch steepest descent training function.

Describing and learning the previous concepts to the networks system will enable the system to have reasonable meaning of the controllability action that affects the different transient phases of a ship motion. It is not enough to learn the system the actual lift forces that come out with the specific thrust forces with limited numbers of patterns. Thus, it is essential that the system can realize the range of the rudder lift force in the patterns fed to the system.

The developed structure of the integrated inputs gave the system the ability to realise the importance of each input and the impact of those inputs on the output variables taking into consideration the ambiguity that could arise from the hydrodynamic forces. A matrix of concurrent vectors is presented to the network to define the initial manoeuvring situation and the controllability action. The network produces a matrix of concurrent vectors as output. The same concept was built with many networks operating in parallel and each network received the input vectors and produced the decision outputs.

The ordering of the input vectors is not important as they do not interact with one other but they must integrate with each other to represent and realise the ships' main parameters and the controllability forces from the engines and rudders. Although the inputs do not interact with one other, they have impact on each other in terms of weights and biases in addition to the suitable applied functions.

The success of the system prediction depends on the inputs to the neurons in the first layer realizing the real factors that affect the ship motion with its different transient phases' characteristics.

5.5.3 Force Model Architecture

The structures built in chapter four cannot give the same performance in the force model. As mentioned before, the best architecture to use depends on the type of problem to be represented by the network. However, the force model needs to have powerful structures. Several neurons reach double the inputs in the first layer and combined into multiple layers that have in some cases one hidden layer more than the direct model. Multiple feed-forward layers with this construction in the force model give a network greater freedom especially in the training of the trajectory. The more neurons in a hidden layer, the more powerful the networks are. In the force model, the neuron numbers were higher in the first layer and falling down largely from the first layer to the last hidden layer. The model's architecture is built and constructed only in the same procedures of the direct model. Similarly, the training and testing processes were the main pedestal to build the predictor. See the block diagram in Figure 5.1 that demonstrates the force model prediction.

The above mentioned difficulties arose because some of the inputs into the systems such as thrust and rudder lift forces were not accurate enough due to the neglecting of the influence of the direction of rotation of the propeller on calculating rudder forces in addition to hull and stern form.

From this point of view, it is found that the training process in the ANN of the force models requires a different strategy to realise these margins of tolerance and to solve the prediction problem. Multiple feed-forward network needs greater

freedom and power to solve such a problem. Consequently, more computational effort was required.

Feed-forward networks cannot perform temporal computation. More complex networks with internal feedback paths are required for temporal behaviour. In case of Feed-forward networks, if several types of input vectors as mentioned above are to be presented to a network, they may be presented sequentially or concurrently. The matrix notation used in MATLAB enhanced batching operation. Batching of concurrent inputs is computationally more efficient and desired in the force model of this chapter. The new objects concerning the predictor and accuracies will be discussed later in this chapter.

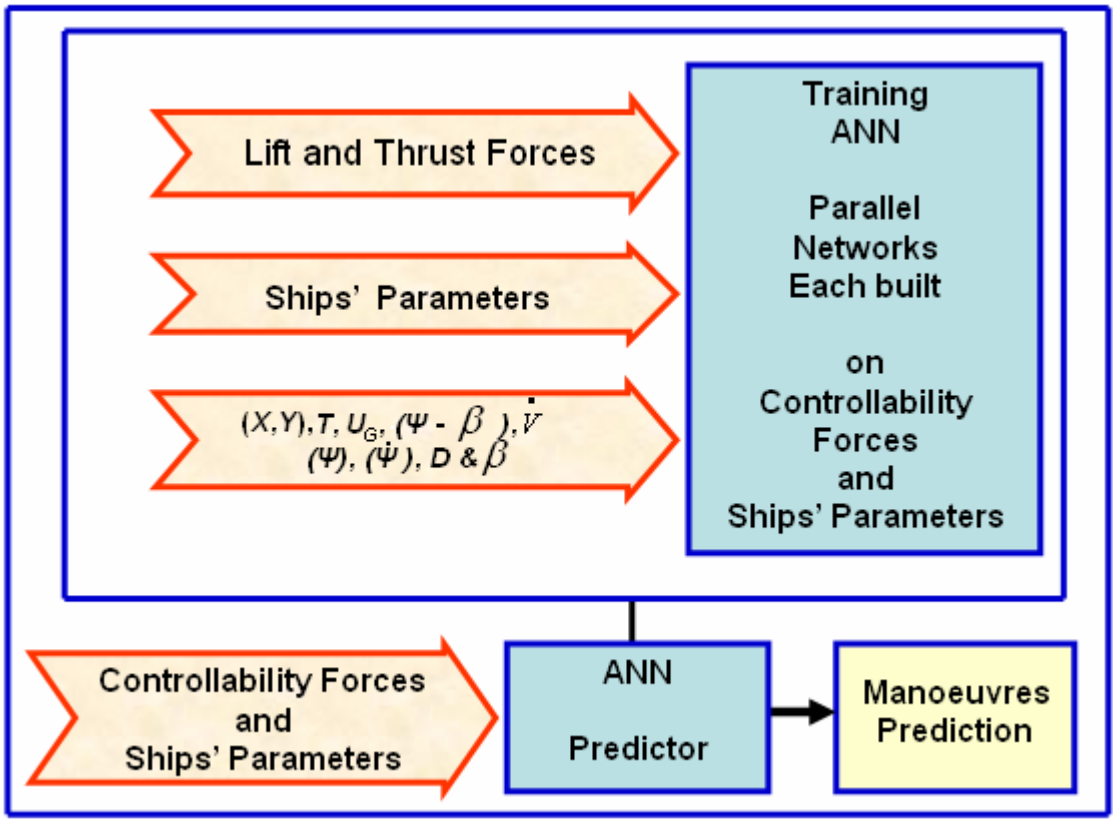

Figure 5.1: Block diagram of the force model prediction

5.5.4 System Validation

The same strategy of the training, testing procedure and testing of the random choice has been done only with the starboard turn and the results are discussed in chapter four for the validation of the system prediction.

In this chapter the study of the ANN application went further than testing the blind manoeuvres. It extends the test to the training process for deeper recognition of the system ability of evidential response, contextual information and fault tolerance. As is well known, the good performance of the neural network predictor can give prediction output close to the measured data with high accuracy for the unknown patterns. This property can be used to validate the system. The results with sufficient accuracies from such a complicated problem of ship manoeuvring motion for different types of ships motivated this study to go deeper for more verification of the features and benefits of the ANN.

Containership (1) has a single right-handed propeller and semi-spade rudder. Turning to port side has smaller maximum advance and total diameter than to turn to starboard side. Forty-two experimental data files for the starboard side turn as a set were provided to the system for training. Only one file of the containership (1) from the forty-two files was replaced with a port side turn file in the training process. The replaced file has a lift force of rudder angle of 35 degrees and speed of 22.1 *knots*. If the Trajectory defined as (*x* and *y*), then for port side the signal of (*y*) could be converted and structured to be plus (+) sign in the file of training process.

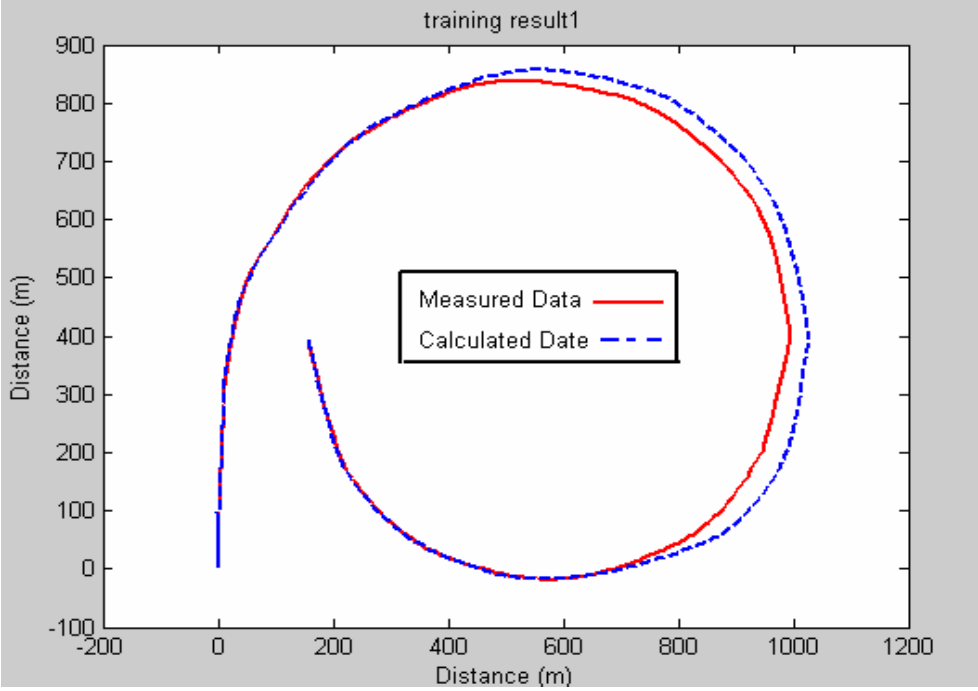

Figure 5.2: Training result using one only of the port side data of Containership 1 as turning to starboard side, rudder 35 degrees and speed 22.1 *knots*

The main point in this operation is that the system will train to a file with trajectory smaller in its advance and diameter than the real trajectory of this containership that has different behaviour for each side. The result is depicted in Figure 5.2: The system actually was trained on trajectory bigger than the trained file trajectory which has the error when inserted into the system.

Then, the investigation was extended to do the second operation by replacing this one file with a correct file of the turning to starboard side. Afterwards, the training process was repeated again. The outcome result is depicted in Figure 5.3: The trained trajectory was identical to the correct trajectory.

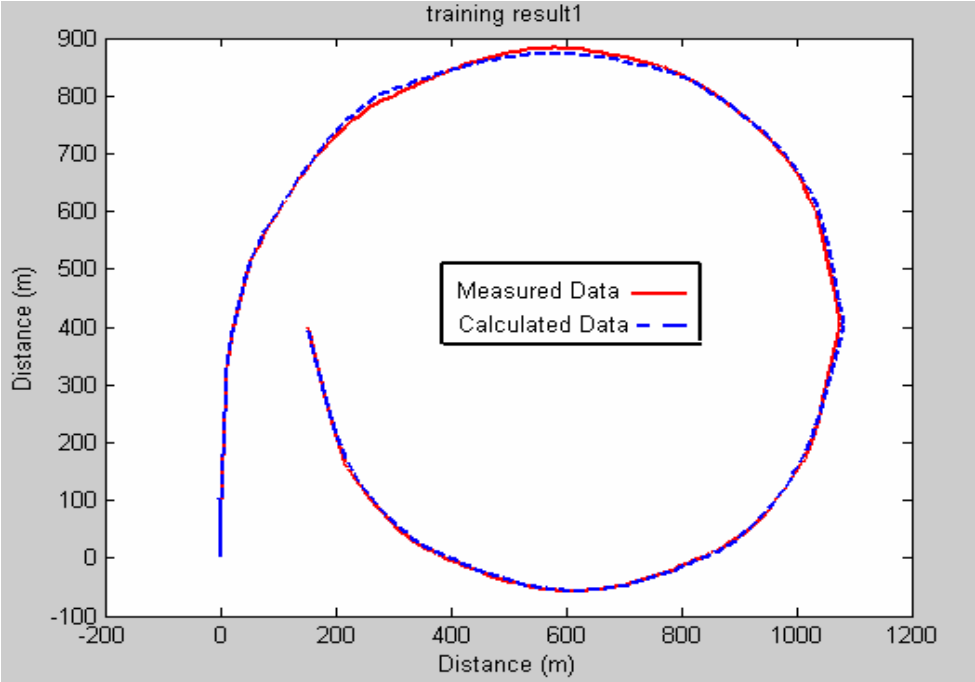

Figure 5.3: Training result using the right data of Containership (1) of turning to starboard side, rudder 35 degrees and speed 22.1 *knots*

These supplementary steps in system validation led to give ANN the confidence in the decision made especially with this ability to reject ambiguous patterns and to have acceptable mathematic fault tolerance within the range of contextual information.

Finally, due to neglecting the influence of the direction of rotation of the propeller on the lift forces in addition to the interaction of hull, propeller and rudder, the results of the general direct model in the previous chapter have higher accuracies

than the results that evolved from the general force model (refer to Table 4.4 in Chapter 4 and Table 5.2 in Chapter 5). These results were investigated and analyzed to find out that the different types of the inputs in the force model; especially the estimated inputs have different accuracies compared with the other real and measured inputs. Therefore, the trustful prediction needs more tolerance to solve the problems of the force model. However, the direct model depends on more accuracy in data inputs and this means the range of errors in the inputs data is smaller compared to the force model inputs. Therefore, the results of the direct model will have better accuracies than the results of the force model.

5.6 Estimation of the Differences in the Initial Side Forces between Port and Starboard Turns

As mentioned earlier in this chapter in the data generation (5.5.1), the data files were divided into two sets, port and starboard files. The work here is directed to solve only prediction problems of one side. The starboard side was selected to illustrate the different side forces and hence the associated turning moments. The stern flow, rudder lift force, propeller transverse force and the interaction among these components are responsible for the resulting transverse forces; the following paragraphs use this designation.

Logically, the set representing the port side turn data file must have transverse forces causing different turning moments from the starboard side, whenever a ship has different behaviour and trajectory for each side. Currently, the role of the predictor came to estimate the different transverse forces between port and starboard sides whenever the predictor fulfilled the prediction task with enough accuracy. If the trajectory defined as (x and y) then, for port side the signal of (y) could be converted and structured to be plus (+) or minus (-) sign in the NN force model predictor to convenient the plotting process.

The differences between the measured data trajectories of port side and starboard side at same rudder angle are corresponding to the differences in the turning moment between both sides. The next step is to predict these differences in the transverse forces when the moment arm is the same for both sides.

For the simplification of this approach, instead of applying the transverse forces, the starboard side rudder lift forces were used as a reference to estimate lift forces.

Then, it is required to estimate the initial rudder lift forces of the port side with different rudder angles and speeds. The ANN system prediction is modified to be able to estimate the lift forces of the rudder angles to the port side. The result of this operation is shown in Table 5.3 where the predicted forces' differences are recorded.

Table 5.3: Differences in the initial side force of same rudder angles to both sides port and starboard (Bulk Carrier's sp.=13.1 *knots* and VLCC 's sp.=14.7 *knots*)

Bulk Carrier's δ_r	Predicted Forces' Differences	Percentage of Forces' Differences	**VLCC 's** δ_r	Predicted Forces' Differences	Percentage of Forces' Differences
12	- 10.3 *kN*	1.87614 %	10	25.0 *kN*	5.74713 %
15	-16.3 *kN*	2.63328 %	15	49.7 *kN*	7.38484 %
20	- 20.3 *kN*	2.41093 %	20	64.3 *kN*	7.02732 %
25	- 36.3 *kN*	3.40525 %	25	113.6 *kN*	9.74271 %
30	- 41.9 *kN*	3.25817 %	30	129.1 *kN*	9.16253 %
35	- 35.3 *kN*	2.35963 %	35	158.0 *kN*	9.62241 %

The first column on the left records different rudder angles to port side of the bulk carrier and the second column presents the initial differences in the lift forces of the same rudder angles between port side and starboard side. The minus signs (-) mean that the starboard forces turning the bulk carrier to port side is smaller than the port forces turning the bulk carrier to starboard side (refer to Fig. 6.12 and 6.13 in Appendix C.3 on p.183). The fourth column presents the rudder angle of the VLCC that has the plus (+) sign in the fourth column which means the opposite of the clarification of the bulk carrier. Then the force model predictor can apply the modified rudder lift forces to turn the ship to port side in order to predict ship trajectories. Figure 5.4 depicts the starboard trajectory of the VLCC.

The rudder lift force of 1166 Newton (at 25 degrees) and the thrust force of 1642 Newton (at a speed of 14.7 *knots*) are replaced with rudder lift force equal to 1280 Newton (include the added force from Table 5.3) while the thrust force remains the same. The results based on this approach are shown in Figure 5.5.

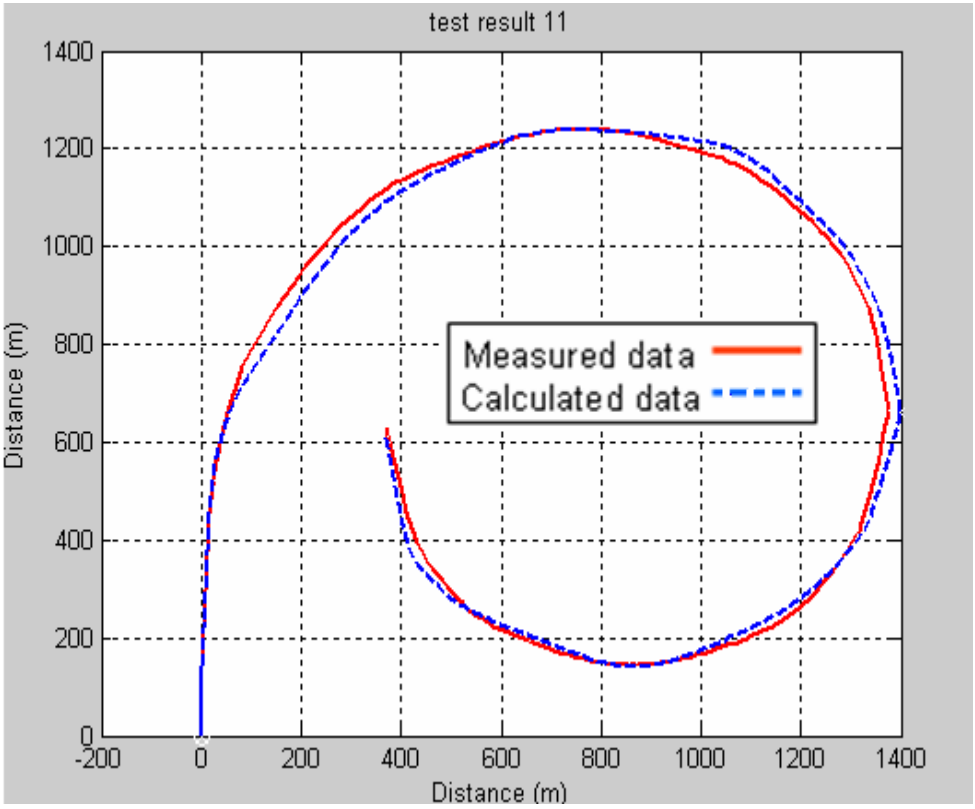

Figure 5.4: Turning manoeuvre tracks test to starboard side of VLLC, approach thrust = 1642 *kN* (speed = 14.7 *knots*) and the initial rudder lift force = 1166 *kN* ($\delta_{r=}$ 25°)-(Force Model)

The second approach is to tune the starboard rudder lift force till the maximum advance is equal to the measured maximum advance of port side. In this case, the rudder lift force increased more than the applied force in Figure 5.5. Consequently, the turning circle will be smaller than the measured turning circle as shown in Figure 5.6.

The results of applying both approaches gave acceptable accuracies for port side predictions. The starboard side predictions seem to be more accurate. Table 5.4 is in good agreement with this result.

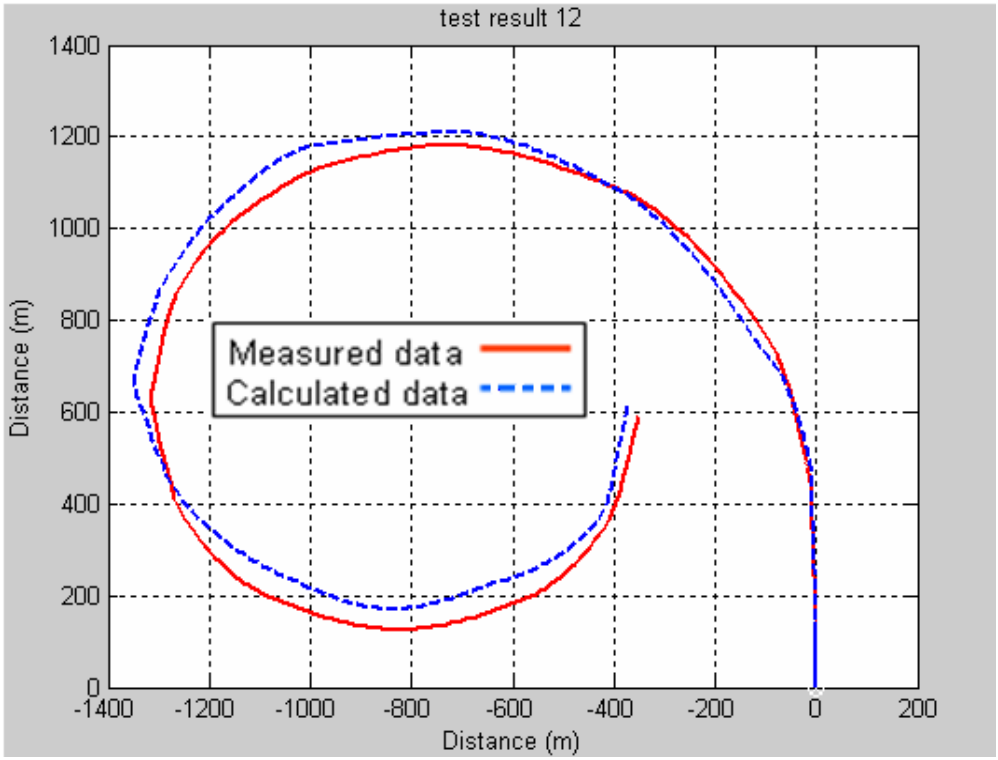

Figure 5.5: Turning manoeuvre tracks test to port side of VLLC, approach thrust = 1642 *kN* (speed = 14.7 *knots*) and the initial rudder lift force = 1280 *kN* ($\delta_{r=}$ 25°)-(Force Model)

Table 5.4: Different accuracies between starboard and port turn
applying the predictor estimation of the differences in the initial side forces between both sides

	Measured Data	Calculated Data
Starboard Turn		
Max. Advance	1240 m	1238 m
Total Diameter	1400 m	1377 m
Port Turn		
Max. Advance	1181 m	1208 m
Total Diameter	1317 m	1352 m

To train the system prediction to measured data files of both port and starboard sides is more trustful than depending on one side to train the system. Moreover, the prediction of the different transient phases' characteristics would have better accuracies. Even though, these estimation procedures would dramatically decrease the computational effort and time as important issues. The increase in every sample will increase the computational efforts and time. Consequently, this issue would

rely on the type of the applications and the needs of the advantages and disadvantages of both approaches.

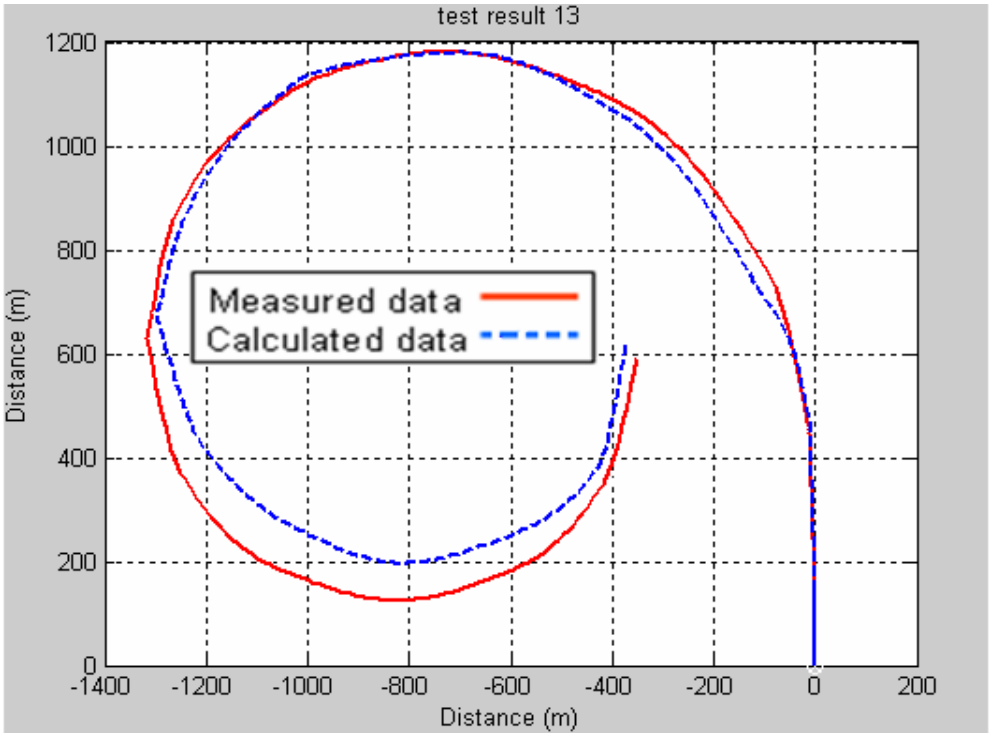

Figure 5.6: Turning manoeuvre tracks to port side of tuned initial lift force of VLLC, approach thrust = 1642 *kN* (speed = 14.7 *knots*) and the initial tuned rudder lift force = 1395 *kN* (δ_r= 25°) (Force Model)

5.7 Improving the Performance through Optimizing the Data among Model Series

The accuracy of the mathematical model based-ANN as a direct model and force model could be improved through optimizing the data among models series. In addition, models series could obtain better performance. Thus, it could have one model as a general ANN mathematical model prediction and many series of models prediction.

The data describe a specific type of ships having - so called - family types of behaviours which differ from the other families or ships' types. The different transient phases' characteristics of ship motion demonstrate ship behaviours. In other words, they describe the time dependency of the different types of variables. Specific variables of each ship's type, when summed up and delivered to one of the

model series as grouped data will have better accuracy in the training and test processes.

Data of the different transient phases were grouped in the most meaningful way. Two of the containerships (Containership 1 and Containership 2) were grouped together as one series called series (1). The VLCC and the bulk carrier were grouped together as series (2). The outcome of each of these two series was connected together through the PNN model prediction to have the optimum training performance ended with better result accuracies for the testing blind manoeuvres and the unknown patterns (see figure 5.7 which shows block diagram of two series of force model prediction).

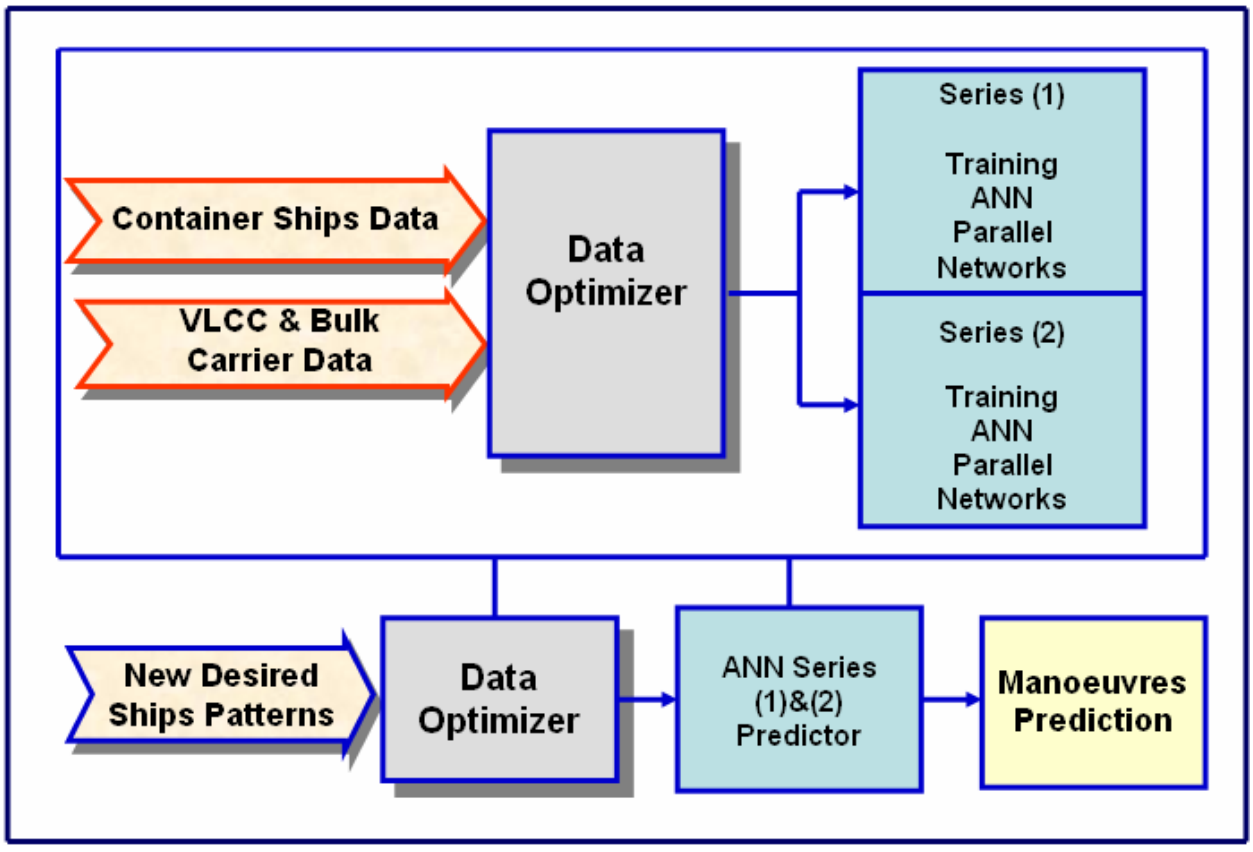

Figure 5.7: Block diagram of the force model prediction through optimizing the data between two models series

The measured data errors of the general model and series models were estimated according to the traditional methods as in chapter four. The errors that were estimated for the data groups of one series type and delivered to the system as

intended goals are more precise for each group. In other words, the intended goals are different from series to series and they are even different in the general model.

Moreover, in chapter four, a method is developed to check the given data accuracies through the training and testing random processes and finding out the values of accuracy ranges of the data files or to estimate the errors as closer to the realistic errors. These procedures are applied in this chapter with the force models. The same results of different intended goals among different models were found as in the traditional methods but with better accuracies.

The further important step is to evaluate the general force model and the series force models accuracies. Thus, it is necessary to summarize all data of the different models prediction for the measured and calculated data. Subsequently, the essential step is to estimate the standard deviation. The measured variability is for all the different phases' characteristics in the general and series models predictions to detect the standard deviation of the main variables that govern the ship motion.

Table 5.5: Main transient phases' standard deviations of the NN general force model predictor for one of the random test selection

Variable	Standard deviation	Unit		Variable	Standard deviation	Unit
U_G	0.50	*knot*		ψ	3.17	*degree*
R.P.M	2.21	*1/min*		$\psi - \beta$	3.07	*degree*
$\dot{\psi}$	1.26	*1/min*		β	0.48	*degree*
$\dot{u}$	0.17	*knot/min*		(x, y)	0.19 *L.O.A.* 52.42	*m*

The results are shown that the series models neural network predictors have higher accuracy prediction for the testing blind manoeuvres than the general force model (see Tables 5.5-5.7). The tables show one of the standard deviation results of the random test selection to predict the main variables that describe ship motion for the general force model and the force models series.

Table 5.6: Main transient phases' standard deviations of the force model (series 1) predictor for one of the random test selection

Variable	Standard deviation	Unit		Variable	Standard deviation	Unit
U_G	0.71	*knot*		ψ	2.92	*degree*
R.P.M	2.3931	*1/min*		$\psi - \beta$	3.01	*degree*
$\dot{\psi}$	1.50	*1/min*		β	0.38	*degree*
$\dot{u}$	0.21	*knot/min*		*(x, y)*	0.17 *L.O.A.* 45.54	*m*

Table 5.7: Main transient phases' standard deviations of the force model (series 2) predictor for one of the random test selection

Variable	Standard deviation	Unit		Variable	Standard deviation	Unit
U_G	0.21	*knot*		ψ	1.95	*degree*
R.P.M	2.26	*1/min*		$\psi - \beta$	2.28	*degree*
$\dot{\psi}$	0.55	*1/min*		β	0.44	*degree*
$\dot{u}$	0.06	*knot/min*		*(x, y)*	0.166 *L.O.A.* 46.09	*m*

The main variables that demonstrate ship motion are depicted in the three tables, the length overall (*L.O.A*) mentioned in standard deviation tables is presented as the main *L.O.A* for the number investigated ships. All variables in the series models show higher accuracies than the general model except for three variables in force model series (1) which are U_G, *R.P.M* and $\dot{u}$. This observation is investigated and analyzed in the following paragraph.

These three variables in force model series (1) were predicted with sufficient accuracies although they have less accuracy than the similar variables in the general model. The main reason of this result is not the ability of the series model

to predict. As long as the accuracy results of the corresponding variables and all the other variables of the all random test selected prediction were better for the series models than in the general model. The reason of this result is the data file contains engine and shaft powers available to calculate the thrust forces and rudder lift forces (see ship propulsion and rudder lift forces in (5.3 and 5.4) in this chapter), but some of the brake power data in the files of containership (2) were missed. Brake power is one of the main items to estimate the thrust force. It was required to determine some of the brake powers in the missing files to complete the data files of containership (2). Good evidence that the estimation was good enough is the prediction of motion which had sufficient accuracy; but the measured data files as in the reality of the rest of these commercial ships related to the brake power were more accurate than the estimation methods. Consequently, this accuracy affects the standard deviations of those mentioned variables in series (1) that contain only two containerships.

Moreover, force model (series 1) contains thirty-one data files. A set of twenty two of these data files has been trained for the system and 50% of these trained file were for container (2). The rest of nine blind manoeuvres were used for validation. At the same time, the other general model contained fifty-nine data files. Forty-two of these files were for training and the rest were for validation. Container (2) trained files were only about one quarter of the trained files that contained less accuracy compared to the rest of files in the general model. The benefits of ANN as evidential response, contextual information and fault tolerance could improve the result accuracies of one quarter trained data than 50% trained data files that both have less accuracy compared to the rest.

The procedures of grouping the data files in a meaningful way of series models decreased dramatically the computational efforts (see Figure 5.8 and 5.9 where the trained epochs about 50000 and a similar case in the general model could pass hundred thousand epochs).

Furthermore, the computations time for the same number of epochs is achieved faster and easier in case of the force model series. The prediction results of the force model as ship’s trajectory plotting and ship motion simulation are described and figured in chapter six.

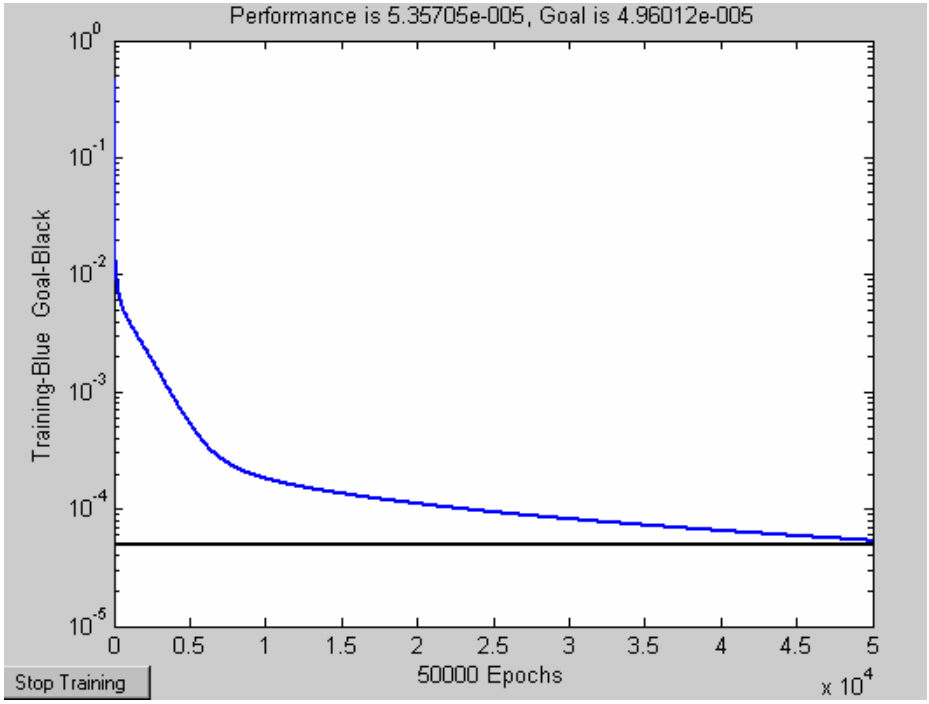

Figure 5.8: Performance and goal of one case of PNN for force model (Bulk carrier and VLCC) series (2) at 50000 epochs

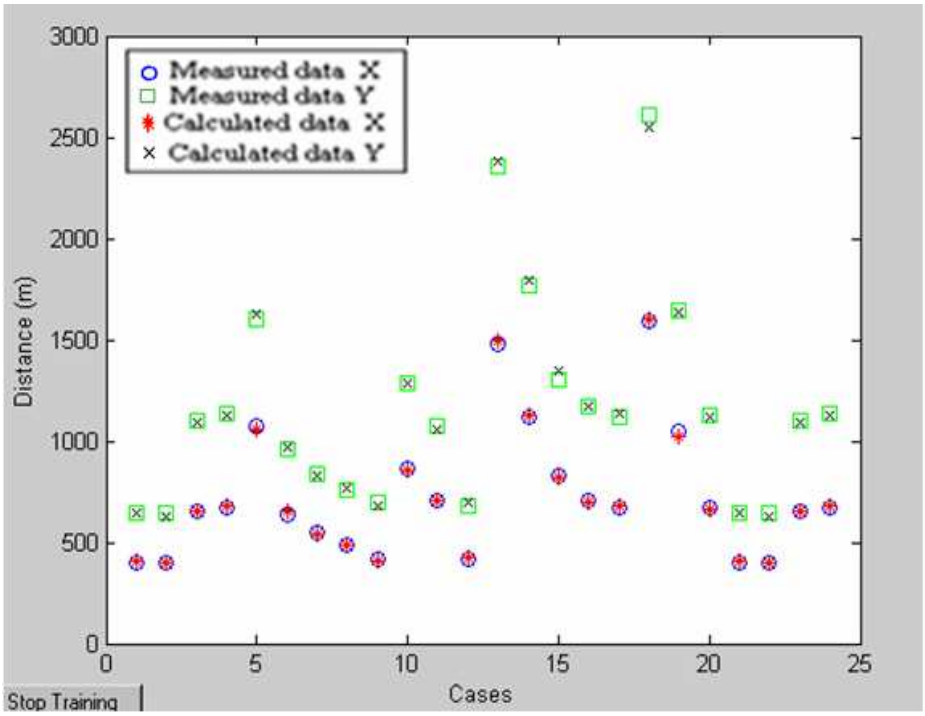

Figure 5.9: Results of training goal of 50000 epochs for the outcome case of figure 5.3

5.8 Conclusion

Artificial neural networks mathematical force models have been developed by means of describing the main forces which affect ship motions in addition to ship's main parameters as inputs into the system to predict the turning manoeuvres.

It was expected during the work development that the force mathematical model would achieve better performance and accuracies than the direct model developed in chapter four. The results were opposite to this expectation due to neglecting the affect of the direction of rotation of the propeller and the interaction among hull, propeller and rudder. This fact was found clearly from the results after applying the different models prediction. It proved the ability and validity of the ANN as a prediction tool and the coherence of the structure and the methods applied to build the system prediction.

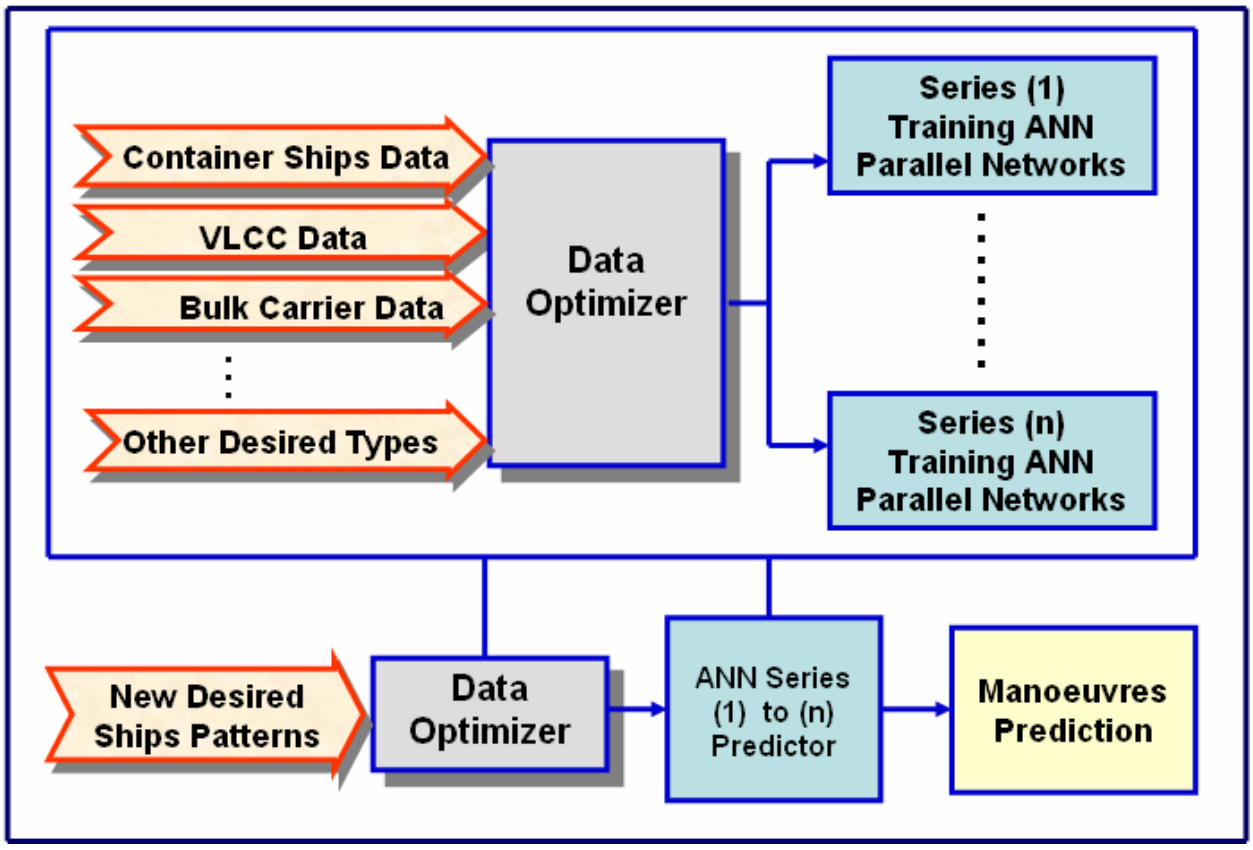

Figure 5.10 : Future block diagram demonstrates the force model prediction through optimizing the data among models series

Within the context of this chapter, neural network can be designed to provide information not only about which particular pattern to select, but also about the confidence in the decision made. This latter information may be used to reject ambiguous patterns and thereby improve the classification performance of the network; an example can be found in (5.5.4 System validation). The forces of the contextual information are that every neuron in the network is potentially affected by the global activity of all other neurons in the network and ANN performs gracefully with the patterns that have adverse operating conditions.

The system model prediction structure in this chapter is different from the system in chapter four and the training processes depend only on the starboard data files and this decreased dramatically the computational time. But on the other hand, the level of the prediction accuracies of turning the ship to port side was less than of turning the ship to starboard side. Therefore, the choice depended on the purposes of the applications and the desired requirements.

The main future contribution of the chapter results is that it could improve the models prediction through optimizing the data among models series for each type of ship or in the same family parameters; the block diagram in Figure 5.10 demonstrates the force model prediction through optimizing the data among models series. Many stored exemplars-based learning algorithms which are not related to the specific task during generalization could lead to an oversensitivity and noise. The problem of deciding which instances or other exemplars-based learning algorithms to store for use during generalization are solved by series model prediction.

The generalization in the domains of series model has many advantages that can obtain reasonable storage data, fast execution time, very low sensitivity to noise and high ability to have right decision boundaries for the different domains of the application areas.

Chapter 6

Results and Analyses

6.1 Introduction

The different approaches for the ANN mathematical models have been verified in the previous chapters: Four and five. The different approaches for NN direct models were described in chapter four and NN force models in addition to NN series models were described in chapter five.

The predictive systems validation was applied to different application issues for three types of ships presented by four different ships (two containerships, a bulk carrier and a VLCC). The obtained accuracies were verified for the following issues: The first issue is the trajectory as well as the predicted limits of turning manoeuvres with small and maximum angles of rudder tested. The second issue is the motion simulation taking into consideration the required space for the manoeuvring. The third and last issue is the variables' characteristics at the transient phases of the manoeuvre turns.

Other factors that might have an influence on the model were dealt with as follows: The size of the ship is scaled corresponding to the scale factor. The measured and calculated ships' contours were plotted during the manoeuvring motion as in real time. The prediction process has been done with different random selections of the test patterns to prove sufficient accuracy of the applied prediction method. All results' figures, tables and investigated ships figures of this chapter are given in appendices (A-I).

6.2 Turning Circle Limitation

The study was conducted for three different ships; one containership, one bulk carrier and one VLCC (Ebada and Abdel-Maksoud, 2005*a*). In the prediction process the rudder angle was varied from 4 *degrees* till 35 *degrees*. The minimum ship approach commenced speed was 4.5 m/s, the maximum was 13.1 m/s and

speeds during the manoeuvre decreased in some cases to be 1.5 m/s. The highest investigated speeds were for the containerships and the lowest speeds for the bulk carrier.

The training results of the limits of turning manoeuvres for small and maximum rudder angles are shown in Figure 6.1. The plotted circles are for measured data and the plotted stars are for calculated data. The blue circles and red stars are for the maximum advances, where the green circles and stars are for the total diameters. The test manoeuvres were used to verify the accuracy of the applied method by predicting the limits of turning manoeuvres at small and maximum rudder angles of some of the random blind manoeuvres were depicted in Figure 6.2. The containership was tested at a starting speed of 24.8 *knots* and rudder angles of 10, 15, 30 and 35 *degrees*. The starting speed of the bulk carriers was 13.1 *knots*. The tests were carried out at rudder angles of 10 and 20 *degrees* for the bulk carrier. The red lines are used for the measured data where, the blue lines are used for the calculated data. The vertical lines are presented the x-axis of the maximum advances and the horizontal lines are presented the y-axis of the total diameters. A comparison between measured and calculated values is shown in Figure 6.3 and its subfigures. The calculated results agree well with the data of the blind manoeuvres.

The developed method was applied to estimate the differences in the limits of turning manoeuvres when the tanker turns to port or to starboard. The tests were carried out for a rudder angle of 25 *degrees* to both side port and starboard (see Figure 6.4). The calculated results clarify that the developed method is able to estimate accurately the limits of the two turning manoeuvres.

6.3 Manoeuvre Tracks

The study was conducted for four different ships, two containerships, one bulk carrier and one VLCC (Ebada and Abdel-Maksoud, 2005*b*). One case of the training process is shown in Figure 6.5. All the manoeuvring files were delivered to the built system and the blind manoeuvres graded to validate the applied methods. The prediction for the training manoeuvres were not graded with the set of blind manoeuvres but kept as a separated set. In the process to predict ship

track, the only information provided to the blind manoeuvres for testing was the initial condition and ship parameters. Figure 6.6 contains twelve subfigures to depict some of the predicted manoeuvres. The rudder angles were varied from 5 *degrees* to 35 *degrees* to port and to starboard side. Four of the training tests are shown in subfigures (6.6.1-6.6.4) while the rest are presented in the testing results for the blind manoeuvres, see subfigures (6.6.5-6.6.12). The red turning circles are used for the measured manoeuvres, where the blue dot circles are used for the predicted manoeuvres.

The applied method is able to predict the different tracks behaviour of the turning manoeuvres of the investigated ship. Figure 6.7 depicts the behaviour of the tanker ship when it turns to port and to starboard with the same rudder angle. The test conditions were 269 869 tones of displacement weight, starting speed of 14.7 *knots* and rudder angle of 25 *degrees*.

It is clear to observe from the results that the applied method accuracy shows that the behaviour of the turning track manoeuvres from ship to ship is completely different not only in the advance distance and diameter but also in positions of the complete turn which mainly depend on the displacement and the ship's geometry.

6.4 Simulation Results

6.4.1 NN Direct Model Results

For the simulation of the turning manoeuvre, it is not only important to calculate the trajectory with high accuracy, but it is also necessary to have a precise prediction of the main parameters describing the turning manoeuvre such as acceleration, speed, heading and drift angles, angular velocity, distance run, revolution per minute of the propeller *(R.P.M),* etc. with respect to the time (Ebada and Abdel-Maksoud, 2006).

The results of the goal, performance and trajectory of turning manoeuvres with small and maximum angles of rudder are shown in Figures 6.8 – 6.13 (refer to C.1-C.3). The plotted circles and squares are used for the measured data, where the

stars are used for calculated data. The training results for trajectories of turning manoeuvre of the containership 1 are presented in Figures 6.9.1 - 6.9.2 for two different rudder angles to port side. The red ships for all the simulation are used for measured manoeuvres and the blue ships are used for the predicted manoeuvres. The comparison between the calculated and the measured results shows a good agreement except the region of heading angle equals –180 *degrees* in Figure 6.9.2. The trajectory for rudder angle 5 *degrees* to starboard side is presented in Figure 6.9.3. The results of the simulations included in Figure 6.9.1-6.9.3 are for the same ship speed. Therefore the comparison between the three figures gives an indication of the influence of the rudder angle on the tactical diameter and maximum advance. With the increase of the rudder angle, the limits of the turning manoeuvre are reduced. Figures 6.9.4-6.9.6 include similar results for the other three investigated ships. As seen, a good agreement between the results of the training and the measured results has been achieved.

Some representative results of the trajectory of blind turning manoeuvres of the VLCC and a comparison with measured data are shown in Figures 6.10.1 - 6.10.3. Figure 6.10.4 includes the corresponding results for containership 2. The results in Figures 6.10.1 - 6.10.4 confirm that the applied ANN is able to recognize the difference in ship behaviour when the ship turns to port or starboard side and to predict the trajectory for both sides with high accuracy.

The interaction between the propeller and the rudder has a noticeable influence on the maximum advance and the tactical diameter. For a right handed propeller, the force induced from the propeller flow on the rudder part above the rotation axis of the propeller is directed to starboard and below this axis directed to the port side. The direction of resultant force depends on the circumferential thrust distribution of the propeller and the shape of the rudder. For a spade shape rudder, the area of the rudder above the propeller axis is lager than below it. This means that the resultant force will be directed to the starboard side. Consequently, the ship will have a smaller maximum advance and tactical diameter by turning to the port side in comparison to the starboard one. When the rudder has a different shape, for example a constant chord length, the resultant force will be directed to the port side. In this case, a ship arranged with a constant chord length rudder may then have the opposite behaviour of a ship arranged with a spade rudder.

Many turning manoeuvres were carried out to investigate the capability of the developed PANN to distinguish between the different behaviours of ships by turning to starboard and port side. For these simulations, the containership 2 and the bulk carrier were selected. The containership 2 has a spade rudder and the bulk carrier has a rudder with a constant chord length. Figure 6.11 depicts a comparison between the calculated and the measured trajectory of blind turning to starboard and port side. The corresponding results for the bulk carrier can be seen in Figures 6.12 and 6.13. For all six manoeuvres, good agreement has been achieved between the calculated and the measured results. The comparison between the trajectory for turning manoeuvres to starboard and to port side shows that for containership 2, the turning manoeuvres to the port side have smaller maximum advance and tactical diameter than to the starboard side. The bulk carrier shows the tendency vice versa. Figures 6.12 and 6.13 include the results for the same ship velocity at two different rudder angles of 30 *degrees* and 10 *degrees* respectively. The comparison between both figures shows that the effect of the interaction between the propeller and the rudder on the maximum advance and the tactical diameter is reduced by decreasing the rudder angle. This effect is also correctly predicted by the developed PANN structure.

The curves of the different transient phases' characteristics demonstrate ship turning manoeuvre simulation. The main parameters describing the turning manoeuvre are in Figures 6.14 and 6.15. They show a comparison between the calculated time dependency of main parameters by turn to port and to starboard side. The written number and name on each curve are the rudder angle and the ship investigated respectively. The red curves are used for the measured data, where the blue dot curves are used for the predicted curves of the different transient phases' characteristics. Figures 6.14 and 6.15 have each 14 subfigures, the odd numbers present the test results while the even numbers include the training results.

Figures 6.14.1, 6.14.2, 6.15.1 and 6.15.2 depict the change of the acceleration during the manoeuvre. All curves start at zero acceleration because the manoeuvre begins from constant velocity condition. After that a strong negative acceleration takes place. The peak of the negative acceleration increases with increasing the rudder angle. The sharp reduction of the acceleration is gradually diminished. The end value of the acceleration is zero, which means a steady turn condition.

The change of the ship velocity during the turning manoeuvre is shown in Figures 6.14.3, 6.14.4, 6.15.3 and 6.15.4. By increasing the rudder angle the final velocity of the ship during the steady turn is reduced. The same can also be seen for the number of revolutions of the propeller (see Figures 6.14.5, 6.14.6, 6.15.5 and 6.15.6). When the ship has a non-zero drift angle, the resistance of the ship and the required torque of the propeller will be increased.

The turning velocity rises dramatically with altering ship's course (see Figures 6.14.6, 6.14.8, 6.15.7 and 6.15.8). At low rudder angle, the increase of the turning velocity takes place until a maximum value is reached and this value will be the end value. At higher rudder angle, the maximum value of the turning velocity will be much higher than the end value. According to the applied definition, turning angle is positive to starboard and negative to the port side. Figures 6.14.7 and 6.14.8 show the same tendency as in Figures 6.15.7 and 6.15.8 but with different direction of rotation. The same is valid also for the drift and heading angles. All the heading angle curves for a turn to the starboard side begin at 0° and end at 360°. The corresponding curves by a turn to the port side begin at 360° and end at 0°. After changing the rudder angle from zero, the heading angle will remain unchanged for a short period, after that it increases nearly linear. The slope of the curve increases with increase of the rudder angle (see Figures 6.14.11, 6.14.12, 6.15.11 and 6.15.12).

The length of the trajectory against the time factor during the turning manoeuvre for a certain ship depends on the approach speed and the rudder angle. Figures 6.14.13, 6.14.14, 6.15.13 and 6.15.14 depict the length of the trajectory in nautical miles.

The results in Figures 6.14 and 6.15 confirm that applied PANN is able not only to predict the coordinates of a complete turn with its advance distance and turning diameter, but also able to simulate the turning motion in real time. Therefore, the developed method is suitable to be applied in navigation simulators.

6.4.2 NN General Force Model

The general force model has sufficient accuracies prediction but less than the direct model due to neglecting the influence of the direction of rotation of the propeller on the lift forces in addition to the interaction of hull, propeller and rudder. This fact could be observed in the standard deviation tables as presented in chapter four (4.4) and chapter five (5.5). As mentioned in chapter five, the unexpected results were that the direct model has higher accuracies than the force model. This result describes the strong ability of the ANN in ship motion prediction application (see the analysis and discussion in Chapter 5).

The test blind results of the simulation of turning manoeuvres with small and maximum rudder angles and different approach speeds are shown in Figure 6.16. The test blind results are depicted and the training results of the three ship types were similar to the results presented above. A part of test manoeuvring simulation plotting of containership 1 and 2 are presented in Figures 6.16.1 - 6.16.4, while the bulk carrier and VLCC are presented in Figures 6.16.5 - 6.16.6. The test manoeuvring simulations have different approach speeds for each ship in addition to different rudder angles.

Some of random test blind results of the different transient phases' characteristics of the turning motion are represented in Figure 6.17 and its eight subfigures. The next paragraph analyses the prediction of significant ship motion behaviour.

If the ship approaches the manoeuvre with a speed less than full ahead speed, like half speed and then, the controllability action of the rudder takes place even with hard rudder angle, the number of *RPM* will be nearly constant during the manoeuvring motion but all the other different transient phases' characteristics of the turning motion will be changed. When the ship has a non-zero drift angle, the resistance of the ship and the required torque of the propeller will be increased. Increased resistance will have an impact on the speed, acceleration, rate of turn, ship's heading and etc. The ship's ability to maintain the number of *RPM* will increase the power to the required torque. But when the ship is running with maximum speed, the number of *RPM* will not be maintained as it is because the machine will not be able to deliver the required high torque. Figure 6.17.3

demonstrates these two cases. Figures 6.17.1, 6.17.2 and 6.17.4 - 6.17.8 show the impact of a non-zero drift angle and the outcome curves that demonstrate ship motion with different approach speeds.

6.4.3 NN Series Force Models

The further development of force model, it was found that the series force models obtain higher accuracies than the general force model (see standard deviation tables 5.5 - 5.7 presented in Chapter 5 and the analysis of these results).

As in the general force model, only some of the test blind results are represented without the training results to avoid repeating main principles. Some of the random test blind results simulations of turning manoeuvres of force model series (1) are shown in Figure 6.18 and its four subfigures 6.18.1 - 6.18.4 for both containerships. While Figure 6.19 and its four subfigures 6.19.1 - 6.19.4 depict some of the test blind results simulation of turning manoeuvres of series (2) for the bulk carrier and the VLCC, the test manoeuvring simulations of the series models have different approach speeds and rudder angles for each ship.

Some of random test blind results of the different transient phases' characteristics of the turning motion are represented in Figure 6.20 and its eight subfigures (6.20.1-6.20.8): The four odd numbers for series (1) and the four even numbers for series (2).

The comments on the previous paragraphs concerning manoeuvring simulations prediction and the curves that demonstrate the different transient phases' characteristics are similar in their discussion and analysis as the results of the direct model and general force model. The next paragraph analyses some important feature observations with regards to ship trajectory characteristics and curves demonstrating the motion in case of different speeds at same rudder angle.

The first issue was the prediction results of the turning manoeuvre trajectories of different approach speeds, e.g., the containership (2) manoeuvres. The speeds of the approach are 25.5 *knots* and 15.5 *knots*; the difference between these speeds is about 5m/sec in the approach speeds. The two manoeuvres have the same rudder

angle (δ_r = 35°). Figure 6.21 depicts the trajectories resulting from the two manoeuvres. The trajectories are nearly similar in the predicted track although the difference in the containership's approach speeds was 10 *knots*.

The second issue was the predicted results of the different transient phases' characteristics that are shown in the demonstrated curves in Figure 6.22 with its eight subfigures. Seven subfigures (6.22.1-6.22.6 & 6.22.8) out of the eight sight subfigures have tremendous differences in curves characteristics between the two manoeuvres that are U ,$\dot{U}$, *RPM*, r , ψ, (ψ - β) and distance travel. The curves in Figure 6.22.7 obviously show a slight difference in ship drift angle but the drift angle curve of the speed 25.5 *knots* was ended at the time of about 502 seconds from the beginning of the manoeuvre till the track completed 360 *degrees* with a value of 17.2 *degrees* (see Figure 6.21.1). While the drift angle of the curve of the speed 15.5 *knots* was ended at the time of about 720 seconds with a value of 17.9 *degrees* (see Figure 6.21.2).

The two manoeuvres took place under the same conditions except for one factor which is the ship's initial speed. The passes of the resultant forces that direct the containership in the two manoeuvres have the same trajectories at the same projected ship position but at different times.

Figure 6.22.1 shows that the approach speed with 25.5 *knots* causes tremendous changes in the acceleration in comparison to the approach speed of 15.5 *knots*. Consequently, the momentum changing rate in the first case is much bigger than in the second case. At the same time higher speed will cause higher hydrodynamic forces towards the centre of turn. In addition, the centrifugal forces direct the ship away from the centre of turn. The resultant value of these forces in the first manoeuvre is bigger than in the second manoeuvre. But the ratios among these forces in the two manoeuvres are nearly same and independent of the ship's speeds. Thus, at the higher approach speed the time required for the turning manoeuvre is shorter but the distances travelled are nearly same in the both manoeuvres. Therefore, the first manoeuvre was ended in 502 sec. instead of 720 sec. in the second manoeuvre.

The drift angle (β) is the main factor causing the resultant of the side forces as hydrodynamic forces to the centre of turn. It is a resultant of different several forces. The balance among the moment caused by hydrodynamic forces, tangential forces and centrifugal forces lead to the same (β). The ship has at equal projected positions of the track the same (β) but at different time. It will change with the time factor till reaching the steady turn at the third stage (refer to Chapter 3), and then the ship has single resultant value to the centre of turn. Therefore, the track will be the same for both manoeuvres.

The drift angle (β) has a strong influence on ship's speed since it is proportional with the loss of speed. As regards to initial speed, the percentage of reduction of forward speed in a turn is nearly constant for all initial speeds when the engine is able to maintain the *RPM*. At the same time, ship's rate of turn is proportional to initial speed (see Figure 6.22.4). Thus, ship turn track and diameter are independent of ship's speed but dependant on rudder angle. Moreover, all the other different transient phases' characteristics depend on ships' speed and rudder angle.

6.5 Prediction Results of using Ship Analytics Ship Simulators Data as another Source of Verification

"Norcontrol simulators" and "Ship Analytics Ship Simulators" were integrated together in the NN direct model predications. The results of the blind manoeuvres of "Norcontrol simulators" data files had accuracies similar to the accuracies that obtained from the direct model before. The experimental data files were only for starboard side manoeuvres. Fifty two manoeuvres for training process contained only ten data files of Ship Analytics Ship Simulators; twenty three blind manoeuvres for system validation contained six blind manoeuvres of four different ships (two containerships, one bulk carrier and on VLCC) of Ship Analytics Ship Simulators which are different in sizes, lengths and the other parameters from the four ships of "Norcotrol simulators". The simulation period for each of the sixteen manoeuvres in the "Ship Analytics Ship Simulators" were compressed between two to four times the real periods of the manoeuvres to reduce the simulations' costs. In this case, ship's tracks will be same except to the recording time must be multiplied as it is compressed.

The results of the blind manoeuvres of both simulators show sufficient accuracies in ships' turning manoeuvres limitations and ships' tracks. Refer to Figure 6.27 "Ship Analytics Ship Simulators" for the results of the turning manoeuvres limitations and Figure 6.28 for the results of the ships' tracks. The results of the ship motion simulations had high accuracies for Norcontrol Simulators data files but the results of the ship motion simulations of "Ship Analytics Ship simulators" have less accuracy (refer to Fig. 6.29 to see the fair accuracies). One reason is the error value of time could be increase to be four times because of using the property of "compressed the simulations period".

In addition to ship motion simulations have different variables and needs more experimental data files to train the system for different nonlinear characteristics' variables of motion but the generation of training and testing data is costly in simulation. Therefore, results could have better accuracies if the data files were increased in the system.

The limitations of turning manoeuvres and the turning manoeuvre tracks are easier to predict since they need fewer patterns than motion simulations. In addition, ship's tracks remain without any changing although the simulation times were compressed. Appendix F shows the prediction results applied on Ship Analytics Ship Simulators as another source of verification.

Several comparisons showed the numerical results of the NN models prediction to be in good agreement with the experimental data. Finally, the processes to build NN mathematical models showed the complexity to solve the multi-problems of different characteristics among the different phases in ship motion running at the same time. The results show the ability of the system to simulate the manoeuvring motion for different types of ships which have different nonlinearity behaviours.

Chapter 7

Summary and Conclusions

7.1 Summary

Artificial neural networks-based mathematical models have been developed by means of describing the ship and the operational data as inputs into the system to predict the turning manoeuvres and altering courses. The application of Parallel Neural Networks (PNN) in this work is based on the Back Propagation Feed Forward Neural Network (BPFFNN). The system was trained and tested for different ship types in addition to the random repetition selection of the test patterns to verify the ability of the system to predict the manoeuvring motions. The results obtained from the training process and the testing of blind manoeuvres proved an acceptable accuracy level of the proposed technique. In addition, the applied methods have the capability to solve the problems of different displacements, speeds and ship types which have completely different nonlinearity characteristics.

Artificial Neural Networks Direct Model depends on figuring out visual descriptions to physical meaning for learning and testing processes. Ships' parameters and controllability actions are inserted into the system as inputs for manoeuvring predictions.

Hydrodynamic Mathematical Model (Force Model) has also been developed by describing the initial forces and moments acting on the predicted ship as inputs into the system. Both of the NN direct model and NN force model reveal good accuracies despite the higher accuracies of the direct model.

Analysis and discussions concerning the decreasing limitation of the system predictability for new unknown ships call for introducing additional meaningful patterns. In addition, the analysis led to expert selection of the variables' range that

governs the ships motion behaviours to cover the different ships' sizes, parameters and conditions to be inserted into the learning process.

An additional improvement has been established through optimizing the data among series models prediction. The performance and accuracies of ANN-based mathematical model have been improved through these series models prediction, which also facilitate the ability of system to predict the manoeuvring behaviours of other unknown ships.

7.2 Conclusions and Implications

The main utility of the new applied models is to be applied on-line. Consequently, it is necessary to provide an adequate level of redundancy with built-in backup prediction system for occasions when the running system is unreliable or unavailable. At least two independent prediction systems will be on board the ship for backup. Operation criteria for the two systems will be defined to contain some form of backup system to enable one of the system or both to continue operating to meet the required accuracy levels.

The new applied models also offer an opportunity to analyze the motion and to compare among different ships' parameters to achieve the best performance and to choose the most suitable ship for its purposes. It is considered as an expert tool which gives the users -in advance- the characteristics of transient phases. This is demonstrated by curves which describe the real motions of ship as a time dependent problem before any on-line training.

The developed system will reduce the distance travelled and ship resistance by selecting the optimum mode of navigation in cases of multi-courses alterations.

Further, in terms of engine power, the hydrodynamic artificial neural networks-based mathematical models could optimize the best mode of navigation regarding delivered power, thrust power and propeller efficiency.

Another benefit of the proposed technique appears in the design stage. PANN-based mathematical model helps to realize the safe margin according to IMO manoeuvring requirements of different ship types in the design stage in order to improve the performance.

Moreover, the application of ANN could be used to enhance the empirical traditional methods such as the method based on predicting the ship motion from model tests results of the towing tanks, lacks, etc. (see Chapter 3). Free-running model test, captive model test and force modes can be integrated with ANN to predict ship motion for higher accuracy, wider applications, better management of the time factor and lower costs.

Likewise, the ANN is able to create prediction tools that accurately recover measured data (forces, thrust, etc.) for those propellers, rudders, etc. for whose measured data are available. Similarly, a method was developed in chapter five to check out the given data accuracies, whenever the inputs and the outputs data are available. The method can also find out the correct values of the data files or to detect the error corrections as closely to the realism rational to the measured data and the inputs, through random training and testing processes. Additionally, it can predict the missing data for which no measured data are available such as powers, forces and…..etc. (see Chapter 5). In case of on-line training and prediction, if the data source such as *RPM* source fails to feed the system, the intelligent technique can predict the missing data in order to fulfil the prediction requirement task.

Collision and grounding are the most common accidents in ship operations. Despite the advances in navigational aids and aids to navigation for ships which are improving on an ongoing basis, every year risks of collision and grounding are still possible and relatively high. Some accidents are attributed to human failures and several research projects have shown that a high percentage of these accidents could have been avoided if the ship's Master had had better manoeuvrability prediction. Realising the limitation track of the emergency manoeuvre with different rudder angles and speeds is required for the ship's Master for decision making to avoid collision and grounding. Such type of predictions is not easy to find out on

board but through the application of such NN mathematical models part of the problem can be solved.

The skill of users could be improved dramatically in the area of manoeuvrability prediction. The user can gain many benefits by simulating the ship turning motion time as it occurs in the real manoeuvre time in order to have the same body clock time prediction. Moreover, the user can accelerate the manoeuvre speed in the system prediction according to any desirable needs to save time and to generalize the understanding of the behaviour of the predicted units within a limited time. In this case, the characteristics of transient phases of all turns will be the same as the real ship to the degree that even the plotted time will be the same as the real ship. Only the simulation period will be compressed according to the desired period.

In addition to the above, the dynamic characteristics of new ships are rapidly changing and the impact of new technology on ship manoeuvrability has tremendous effects on the ship Master and crew on board in order to judge the consequences of these developments. It becomes increasingly difficult in such case to correctly identify the dangerous risk of collision combinations. Ships' Masters face all these challenges. This fact makes it necessary to realize how essential it is to have an intelligent technique on board for each individual ship that can enable ship Master to solve these ambiguities.

Avoidance of dangerous situations through observation and alertness to navigational warnings and regional stations advice is not enough to avoid casualties. Applying A.I. system in the ship operations will enhance ship Master, crew, pilots and shore advice such as Vessel Traffic Services (VTS) to have safer voyages and to guide arrival and departure ships.

Furthermore, the navigational areas and time factor are very important aspect in deciding which performance is needed and in case of severe risks, the ship Master is not able to take the right decision within a short time to solve the problem. Therefore, many accidents happen because of the short time needed to make a decision as well as lack of hydrodynamic knowledge. ANN-based mathematical model is thus a powerful tool to enable the ship Master to take the right decision within a short time.

Further innovations could be added to the Automatic Radar Plotting Aid (ARPA), through the uses of numerical methods to solve collision avoidance problems to improve its function and performance. Intelligent techniques such as those introduced in this research could be integrated with ARPA to plot on its monitor -in advance- the predicted track related to the controllability actions. This application will add more benefits to ARPA predictions and enhance its safety and validity collision avoidance.

It should be noted that the existing IMO regulations, operation guidance of ship manoeuvring and handling and also the guidance of emergency procedures are important safety tools. However, these regulations provide only some phases of general unified boundary of safe and unsafe combinations of the operational parameters for limited conditions. But the actual motion with different displacements, drafts, rudder angles, speeds, stability and dynamic characteristics of individual ships are left to the ship Master's prediction and decision. There is a great demand for more reliable and up-to-date computerized system guidance than the current general ones applied.

Finally, in order to have an intelligent system which is practical, friendly and simple application, the above mentioned intelligent system-based models must have the ability to integrate with other navigation systems in the context of bridge intergraded system to widen their application range. Consequently, the users will be able to choose the best emergency procedures; otherwise the system will react if they have a robust system of prediction.

7.3 Future Directions

PANN mathematical models to simulate the manoeuvring motion at three degrees of freedoms (surge, sway and yaw) applied in this research can be extended to have the capability to solve the problem of environmental sea conditions such as wind, waves and current. In addition, the development can be wider for different ship forms, sizes and advanced controllability devices with the increasing of the required data for such applications. Prediction of other unknown different ship types and sizes needs to train the NN system models through applying some

selected different variables such as ships' sizes, forms, etc. Thus, it is necessary to compactly summarize the necessary meaningful patterns of the different ships' parameters, variables of transient phases of ship motion and environmental conditions to avoid unnecessary patterns ensuing huge computational efforts. One of the main advantages of series models prediction is to facilitate the training process to accommodate the essential variables in the architecture system which is needed to accomplish a system prediction. Thus, the future work in this area can be directed to develop a single general ANN mathematical model in addition to many series of prediction models capable of predicting other different ships' types and sizes or other marine units.

Effort has been exerted to categorize the strengths and weaknesses of the presented approach with the intent of guiding future research efforts to investigate more variables. One of the main aims of the future research is to provide guidance for the ships' Masters, through allowing the auto control system to operatively estimate the safe modes of navigation more accurately at any loaded draft, trim and real environmental conditions.

A new system must be established to support the ship's Master decision making using computer-based system not only for manoeuvres but also for the other three degrees of freedom of stability and sea keeping. The optimum system should be able to predict and optimize the best mode of operation (manoeuvre and sea keeping). In addition to that, there is a need for a comprehensive manual on operational guide and prediction of ship performance navigating in different circumstances to be available on the bridge.

One of the most important goals of the future research is to design a fuzzy-logic controller or to develop a neural-network controller to optimize the three main topics of ship controllability, power consumption and safe and optimum manoeuvring.

References

[1] Abdel-Maksoud, M., Rieck, K., and Hellwig, K., "*Numerical Calculation of Induced Velocities of a Self Propulsed Inland*", The Resistance Committee, November 1998, Madrid, Spain, Final Report and Recommendations to the 22nd ITTC, 1998.

[2] Abe, S. and Inoue, T., "*Fuzzy Support Vector Machines for Multiclass Problems*" European Symposium on Artificial Neural Networks, Bruges (Belgium), d-side publi., PP. 113-118, 24-26 April 2002.

[3] Alello, L. C. and Massacci, F., "*Verifying Security Protocols as Planning in Logic Programming*", ACM Transactions on Computational Logic, Vol. 2, No.4, PP., 542-580, 2001.

[4] Bender and Edward A., "*Mathematical Methods in Artificial Intelligence*", IEEE Computer Society Press, Los Alamitos, CA, chapter 1, pp. 26, 1996.

[5] Brix, J., "*Manoeuvring Technical Manual"*, Seehafen Verlag GmbH, Hamburg, 1993.

[6] Buchanan, B.G., "*A (Very) Brief History of Artificial Intelligence*", American Association for Artificial Intelligence, AI Magazine, 25th Anniversary Issue, 2005.

[7] Cao, Y., Zhou, Z. and Vorus, W., S., "*Application of Neural Network Predictor/Controller to Dynamic Positioning of Offshore Structures*", Dynamic Positioning Conference October 17-18, 2000.

[8] Carlton, J. S., "*Marine Propellers and propulsion"*, Senior Principal Surveyor Technical investigation, Propulsion and Environmental Engineering Department, Lloyd's Resister, Butterworth-Heinemann Ltd 1994.

[9] Charytoniuk, W., Chen, M. S., "*Very short-term load forecasting using artificial neural network*", IEEE transactions on Power Systems, Vol. 15, No.1., February 2000.

[10] Chauvin, Y. and Rumelhart D. E., "*Back propagation: Theory, Architectures and Applications"*, pp. 1-34, Lawrence Erlbaum, Hillsdale, NJ, 1995.

[11] Cockcroft, A., N. and Lameijer J., N., F., "*A Guide to the Collision Avoidance Rules*", International regulations for Preventing Collisions at sea, MPG Books Ltd, Great Britain, Bodmin, Cornwall, 1999.

[12] Demuth H. and Beale M., "*Neural Network Toolbox, for use with matlab*", version 3 ed., Mathworks Inc., January 1998.

[13] Deng and Visonneau. "*Flow and Resistance Prediction for a Container Ship*", The Resistance Committee, November 1998, Madrid, Spain, Final Report and Recommendations to the 22nd ITTC, 1998.

[14] Ebada, A., Abdel-Maksoud, M., "*Applying Artificial Intelligence (A.I) to Predict the Limits of Ship Turning Manoeuvres*", STG meeting, News from Hydrodynamics and Manoeuvring, Hamburg, September 2005*a*.

[15] Ebada, A., Abdel-Maksoud, M., "*Applying Neural Networks to Predict Ship turning track manoeuvring*" , 8th Numerical Towing Tank Symposium, Varna, Bulgaria, October 2005*b*.

[16] Ebada, A., Abdel-Maksoud, M., "*Prediction of ship turning manoeuvre using Artificial Neural Networks (ANN)*" , 5th International Conference on Computer and IT Application in the Maritime Industries, Delft, Netherlands, May 2006.

[17] Elliott, T. and Shadbolt, N. R., "*Multiplicative Synaptic Normalization and a Nonlinear Hebb Rule Underlie a Neurotrophic Model of Competitive Synaptic Plasticity*", ECS EPrints Service, neural Computation 14 (6) pp. 1311-1322, 2002.

[18] El-Sharkawi M.A., "*Neural network and its ancillary techniques as applied to power systems*", IEE Colloquium on Artificial Intelligence Applications in Power Systems, Page(s): 3/1-3/6, 1995.

[19] El-Tahan, H., "*Development and Field Testing of a Neural Network, Ship predictor System (SPS)*", Transportation Development Centre, Transport Canada (TDC), Coretec Incorporated, 1999.

[20] Faller, W.E., Smith, W.E., and Huang, T.T. "*Applied Dynamic System Modelling: Six Degree-Of-Freedom Simulation Of Forced Unsteady Manoeuvres Using Recursive Neural Networks"*, 35th AIAA Aerospace Sciences Meeting, Paper 97-0336, pp. 1-46, 1997.

[21] Faller, W.E., Hess, D.E., Smith, W.E. and Huang, T.T., "*Full-Scale Submarine Manoeuvre Simulation,*" 1st Symposium on Marine Applications of Computational Fluid Dynamics, U.S. Navy Hydrodynamic / Hydro acoustic Technology Centre, McLean, Va., May 1998*a*.

[22] Faller, W. E., Hess, D. E., Smith, W.E., and Huang, T.T. "*Applications of Recursive Neural Network Technologies to Hydrodynamics"*, Proceedings of the Twenty-Second Symposium on Naval Hydrodynamics, Washington, D.C., Vol. 3, pp. 1-15, August 1998*b*.

[23] Fukuda, T., Shibata, T., "*Theory and applications of Neural Network for industrial control systems"*, IEEE Trans. on Industrial Electronics, vol. 39, No. 6, pp. 472-489, 1992.

[24] Hagan, Demuth H.B. and Beale M.H., "*Neural Network Design"*, Chapters 11 and 12 of M.T, PWS Publishing Company, Boston, 1996.

[25] Haugeland, J., Ed., "*Artificial Intelligence: The Very Idea*", MIT Press, Cambridge, 1985.

[26] Hearn, G. E., Zhang, Y. and Sen P., "*Comparison of SISO and SIMO neural control strategies for ship track keeping*", IEE Proceedings, 1997.

[27] Hess, D.E., Faller, W.E., Smith, W.E., and Huang, T.T., "*Simulation of Ship Tactical Circle Maneuvers Using Recursive Networks*", Proceedings of the Workshop on Artificial Intelligence and Optimisation for Marine Applications, Hamburg, Germany, pp. 19-22, September 1998.

[28] Hess, D.E., Faller, W.E., Smith, W.E., and Huang, T.T., "*Neural Networks As Virtual Sensors*", 37th AIAA Aerospace Sciences Meeting, Paper 99-0259, pp. 1-10, 1999.

[29] Hess, D. E., Faller, W. E., "*Simulation of Ship Maneuvers Using Recursive Neural Networks*", Proceedings of the Twenty-Third Symposium on Naval Hydrodynamics, Val de Reuil, France, September, 2000.

[30] Hess, D. E., Faller, W. E., "*Using Recursive Neural Networks for Blind Predictions of Submarine Manoeuvres*". 24th Symposium on Naval Hydrodynamics Fukuoka, Japan, 13 July 2002.

[31] Hess, D. E., Robert, F. R. and Faller W. E., "*Uncertainty Analysis Applied to Feed forward Neural Networks*", 5th International Conference on Computer and IT Application in the Maritime Industries, Delft, Netherlands, May 2006.

[32] Hirose, A., "*Complex-Valued Neural Networks, Theories and Applications*", World Scientific Publishing Co. Pte. Ltd, 2003.

[33] Hodju, P. and Halme, J., "*Neural Networks Information Homepage*", [cited 29 June 2005], Available from the Internet, <koti.mbnet.fi/~phodju/nenet/index.html>

[34] Hopfield, J.J., "*Neural networks and physical systems with emergent collective computational abilities*". Proceedings of the National Academy of Sciences USA, **79** (April): p. 2554-2558, 1982.

[35] International Maritime Organization, "*Code of Intact Stability for all types of ships covered by IMO Instruments*", London: Author, 1995.

[36] International Maritime Organization, MSC/Circ.1053, "*Explanatory notes to the standards for ship manoeuvrability*", IMO Instruments, London-IMO, 16 December 2002.

[37] International Maritime Organization, "*Guidance to master for avoiding dangerous situations in following and quartering seas*", (MSC/circ.707 IMO), Author, London, 1995.

[38] International Safety Management Code (ISM Code), Guidelines on the Implementation of the ISM Code, IMO, London, 1997.

[39] Journee, J. M. J., "*Introduction in Ship Hydromechanics*", Lecture MT516, Delft University of Technology, April 2002.

[40] Karayiannis, N. B. and Xiong, Y., "*Training Reformulated Radial Basis Function Neural Networks Capable of Identifying Uncertainty in Data Classification"*, Neural Networks, IEEE Transactions on, Volume 17, Issue 5, Page(s):1222 – 1234, Sept. 2006.

[42] Kolen, J., F. and Kremer, S., C., "*A Field Guide to Dynamical Recurrent Networks*", Wiley, IEEE Press, 2001

[41] Konar A., "*Uncertainty Management in Expert Systems using Fuzzy Petri Nets*", Ph.D. thesis, Jadavpur University, Calcutta, 1994.

[43] Koushan, K., and Mesbahi, E. "*Empirical Prediction Methods for Rudder Forces of a Novel Integrated Propeller-Rudder system*", Ocean'1998 Nice, France, 1998.

[44] Koushan, K., "*Environmental and interaction effects on propulsion systems used in dynamic positioning, an overview*", 9th Symposium on Practical Design of Ships and Other Floating Structures, Luebeck-Travemuende, Germany, 2004.

[45] Kuiper, G. "*The Wagneningen Propeller series*". Marin publication 92-001, published on the occasion of its 60th anniversary, May 1992.

[46] Kurzweil, R., "*The Age of Intelligent Machines*", MIT Press, Cambridge, 1990.

[47] Le Callet, P., Viard-Gaudin, C. and Barba D., "*A Convolutional Neural Network Approach for Objective Video Quality Assessment*", Neural Networks, IEEE Transactions on, Volume 17, Issue 5, Sept. 2006 Page(s):1316 – 1327.

[48] Lee, T., Cao, T. and Lin, Y., "*Application of an On-Line Training Predictor/Controller to Dynamic Positioning of Floating Structures*", Tamkang Journal of Science and Engineering, Vol. 4 No. 3, pp. 141-154, 2001.

[49] Lewis, E. V., "*Principles of Naval Architecture*", Volume II, Resistance, Propulsion, and Vibration, Chapters 5 & 6, SNAME, USA, Jersey City, NJ, 1988.

[50] Lewis, E. V., "*Principles of Naval Architecture*", Volume III, Motions in Waves and Controllability, SNAME, USA, Jersey City, NJ, 1989.

[51] Ling, C. X., "*Artificial Intelligence for Improving Children's thinking*", Second International Conference on Cognitive Science. Japan, July 27-30, 1999.

[52] Luger, G. F. and Stubblefield, W. A., "*Artificial Intelligence: Structures and Strategies for Complex Problem Solving*", Benjamin/Cummings Publishing, Redwood City, CA, 1993.

[53] Mark, S. "*Introduction to Knowledge Systems*", Morgan Kaufmann, San Mateo, CA, Chapter 5, pp. 433-458, 1995.

[54] Masuko, A., "*Numerical Simulation of the viscous Flow for Complex Geometries Using Overset Method*" ", The Resistance Committee, November 1998, Madrid, Spain, Final Report and Recommendations to the 22nd ITTC, 1998.

[55] Michalewicz, Z., "*Genetic algorithms + Data Structures = Evolution Programs*", Springer-Verlag, Berlin, 1996.

[56] Minsky, M. and Papert, S., Perceptrons: "*An introduction to Computational Geometry*", MIT Press, Cambridge, Mass., 2 edition, 1988.

[57] Munson, B. R., Young, B. F. and Okiishi, T. H., "*Fundamentals of Fluid Mechanics*", (3rd. edn), John Wiley and Sons, New York, 1998.

[58] Narendra, K. S. and Parthasarathi, K., "*Identification and control of dynamical system using neural networks*", IEEE Trans. on Neural Networks, vol. 1, pp. 4-27, 1990.

[59] Newell, A .and Simon, H.A**.,** "*Human Problem Solving*", Prentice-Hall, Englewood Cliffs, NJ, 1972.

[60] Nilsson, N. J., "*Principles of Artificial Intelligence*", Morgan Kaufmann, San Mateo, CA, pp. 6-7, 1980.

[61] Ogawa, A. and Kasai, H., "*On The Mathematical Model of Maneuvering Motion of Ships*" International Ship Building Progress, 193, Heemrasdssingel, 3023 CB Rotterdam, the Netherlands, 1978.

[62] Olofsson, H., "*Preliminary Model Testing for a 282,000 DWT VLCC Report 1*", SSPA Report 6294-1, Dec. 1991.

[63] Pedrycz, W., "*Fuzzy Sets Engineering*", CRC Press, Boca Raton, FL, 1995.

[64] Proceedings of Fourth Int. Conf. on Control, Automation, Robotics and Computer Vision, Singapore, 1-376, 1996.

[65] Rao D. H. and Gupta. M. M., "*Dynamic neural unit and function approximation*", Neural Networks, IEEE International Conference, pp. 743-748, 1993.

[66] Reed R., and Marks R. J., "*Neural Smithing: SupervisedLearning in Feed forward Artificial Neural Networks*", The MIT Press, Cambridge, Massachusetts, 1999.

[67] Resolution MSC.64(67), "*Adoption of new and amended performance standards*", (adopted on 4 December 1996). Retrieved 25 June 2001, <Web:http://www.Nortek.net/learning_center/comm./imo standards.htm>

[68] Robert, F., Hess, D.E. and Faller, W.E., "*Neural Network Predictions of the 4-FQuadrant Wageningen B-Screw Series*", 5th International Conference on Computer and IT Application in the Maritime Industries, Delft, Netherlands, May 2006.

[69] Rowe, R. W., "*The Shiphandler's Guide for Masters and Navigating Officers, Pilots and Tug Masters*", The Nautical Institute, Southall, Middlesex UB2 5NB, England, 1996.

[70] Sastry, P. S., Santharam, G. and Unnikrishnan, "*Memory neuron network for identification and control of dynamical systems*", Neural Networks, IEEE Transaction on, 1994.

[71] Schneekluth, H. & Bertram, V., "*Ship design for efficiency and economy*", Oxford; Boston: Butterworth-Heinemann, 1998.

[72] Söding, H., "*Bewertung der Manövriereigenschaften im Entwurfsstadium*", Jahrbuch der Schiffbautechnischen Gesellschaft, Springer Verlag 1984.

[73] Stankovic, A. M., Saric, A. T. and Milosevic, M. "*Identification of nonparametric dynamic power system equivalents with artificial neural network*", Power Systems, IEEE Transactions on, Volume: 18, Issue: 4, Page(s): 1478-1486, Nov. 2003.

[74] Tanaka, K., **"***Stability and Stabilizability of Fuzzy-Neural-Linear Control Systems*", IEEE Trans. on Fuzzy Systems, vol. 3, no. 4, 1995.

[75] Turban, E., "*Decision Support and Expert Systems, Management Support System*", USA, New York, 1993.

[76] Velagica, J., Vukicb, Z., And Omerdicc, E. (November, 2001). "*Adaptive fuzzy ship autopilot for track-keeping Control*"
Engineering Practice", (PERGAMON).
<http://www.elsevier.com/locate/conengprac>

[77] Volker, B., "*Practical Ship Hydrodynamics*", Printed in Great Britain by Biddles Ltd, Butterworth-Heinemann, 2000.

[78] Widrow, B., Winter, R. G. and Baxter R., A., "*Layered neural nets for pattern recognition*", Acoustics, Speech, and Signal Processing, IEEE Transaction on Signal, July 1988.

[79] Wilkins, D., E., "*System for Interactive Planning and Execution*", AI Center, SRI International, USA, 2000.

[80] Wu, W., Black, M. J., Gao, Y., Bienenstock, E., Serruya, M., and Donoghue, J. P., "*Inferring hand motion form multi-cell recordings in motor cortex using a Kalman Filter*", SAB'02-Workship on Motor Control in humans and Robots: On the Interplay of Real Brains and Artificial Devices, Edinburgh, Scotland, 10 Aug. 2002.

[81] Xing-Kaeding Y., "*Unified Approach to Ship Seakeeping and Maneuvering by a RANSE Method*" Tu Hamburg-Harburg Schriftenreihe Shiffbau, March, 2006.

[82] Yu, L., Wang, S. and Lai, K. K., "*An integrated data preparation scheme for neural network data analysis*", Knowledge and Data Engineering, IEEE Transactions on, Volume 18, Issue 2, Page(s):217 – 230, Feb. 2006.

[83] Yusong C., Zhou, Z. and Vorus, W. S., "*Application of a Neural Network Predictor/Controller to dynamic Positioning of Offshor Structures*", Dynamic Positioning Conference, October 17-18, 2000.

Appendices

Appendix A

Figures of the results of Chapter 6:

A.1 Training and testing results of turning circle limitation:

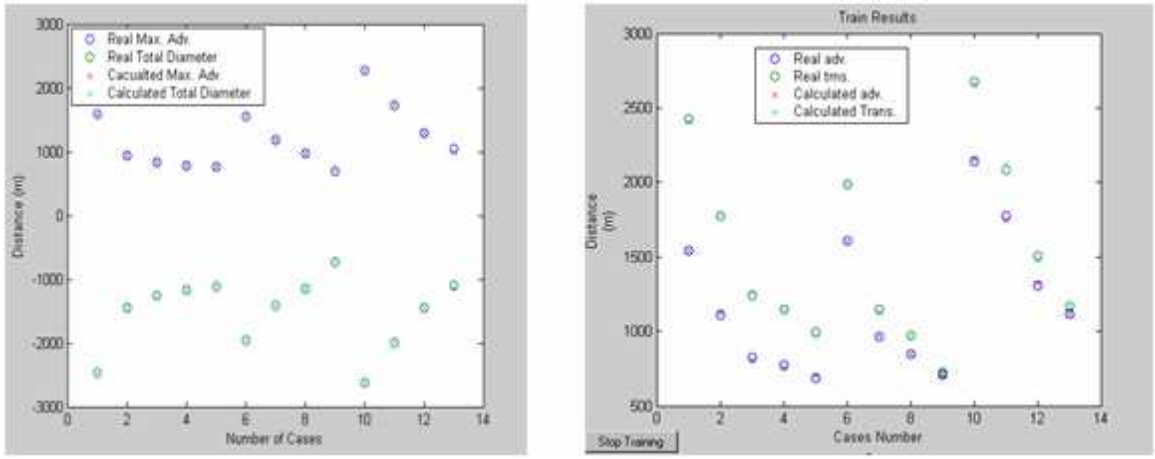

Figure 6.1: Training results of different ships using various rudder angles to port and starboard side (Direct Model)

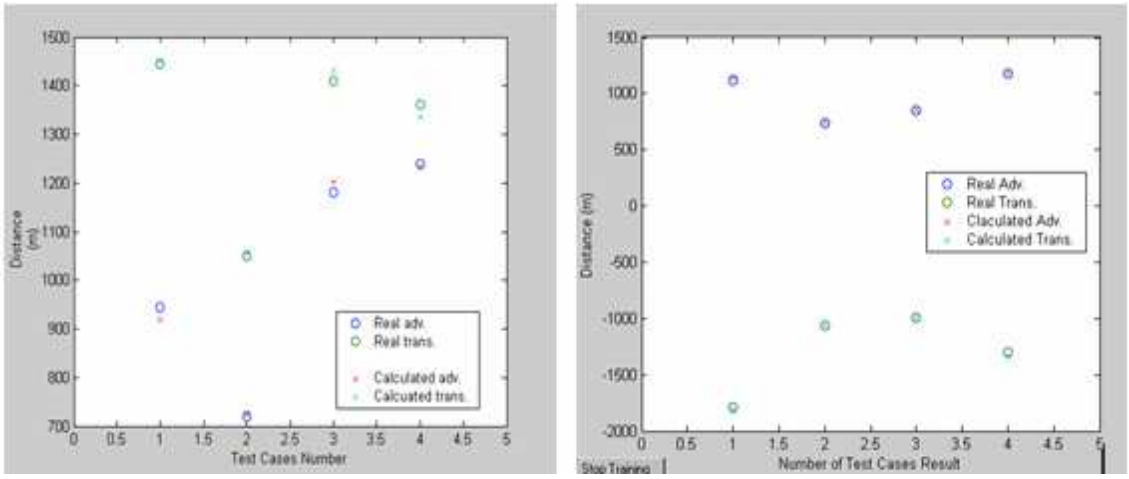

Figure 6.2: Tests results of turning manoeuvre of different ships using various rudder angles to port and starboard side (Direct Model)

A.2

Testing results: Plotting of turning circle limitation:

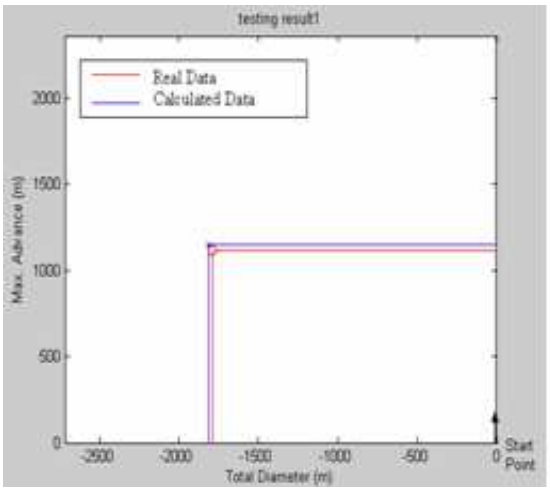

Fig. 6.3.1:
Container, δ_r = 10 degree to port

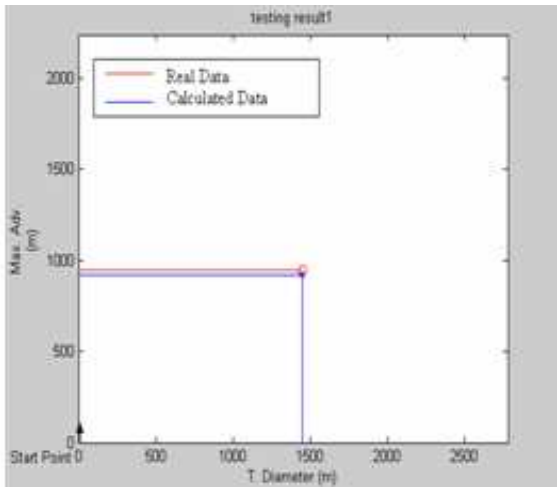

Figure 6.3.2
Container, δ_r = -15 degree to starboard

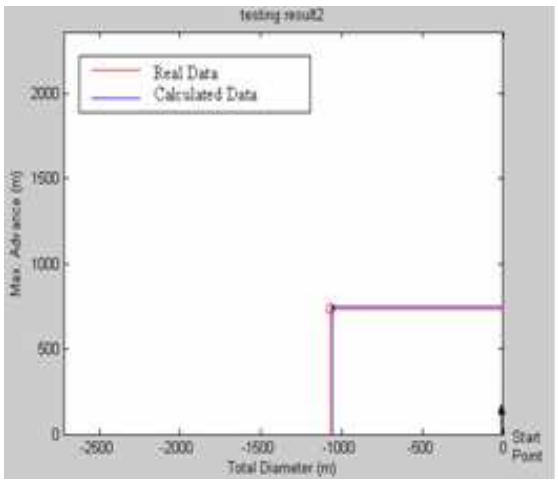

Figure 6.3.3
Container, δ_r =30 degree to port

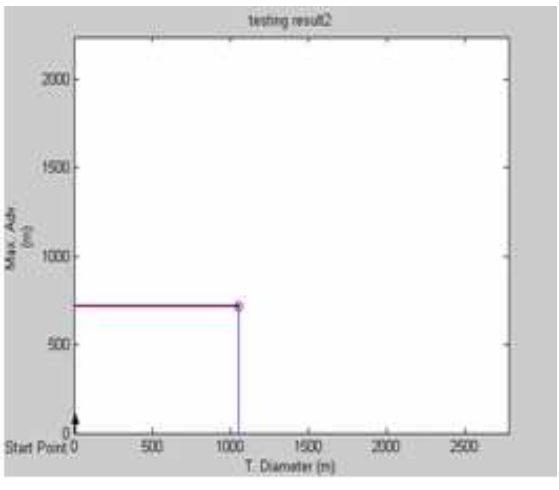

Figure 6.3.4
Container, δ_r = - 35 degree to starboard

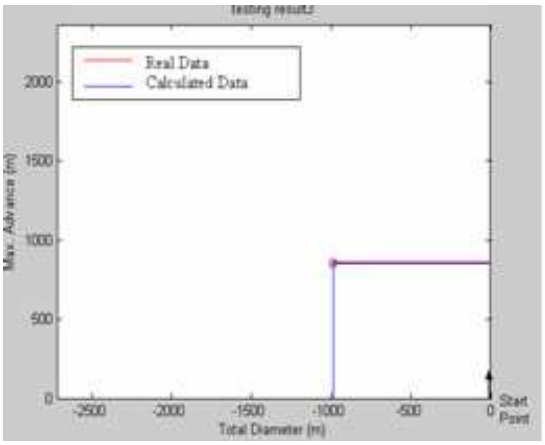

Figure 6.3.5
Bulk carrier, δ_r =20 degree to port

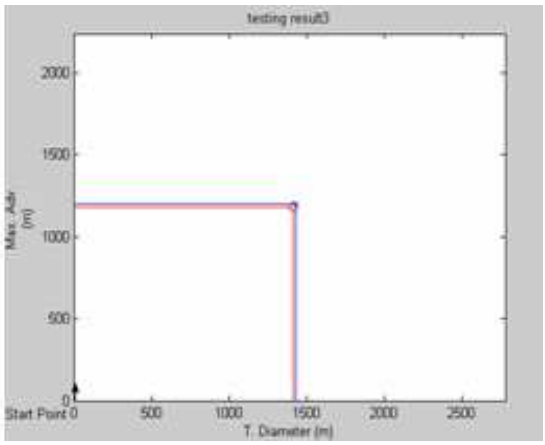

Figure 6.3.6
Bulk carrier, δ_r = - 10 degree to starboard

Figure 6.3: Test results of the maximum advance and total diameter using various rudder angles to port and starboard side (Direct Model)

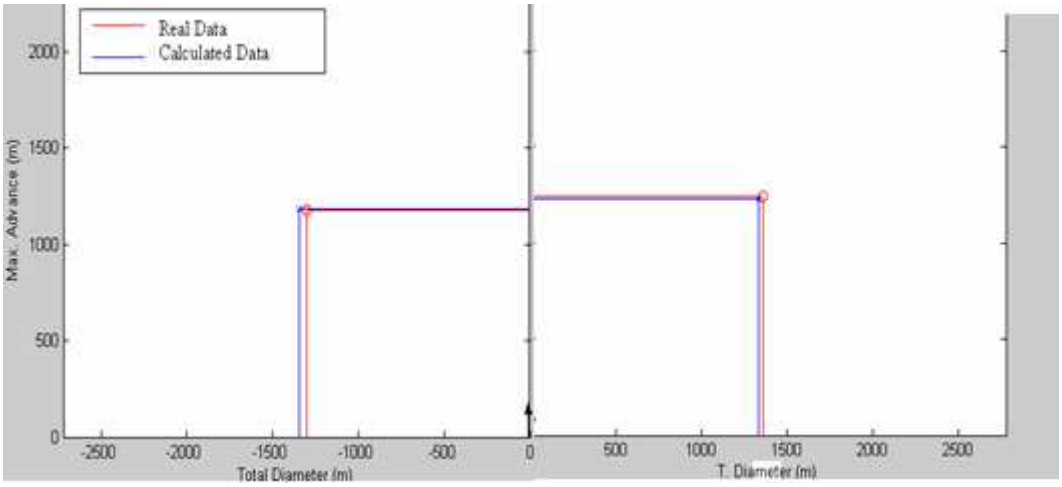

Figure 6.4: Difference in the turning manoeuvres limits of VLCC to port and starboard with same rudder angle (Direct Model)

Appendix B

Figures of the results of Chapter 6: Manoeuvres Track Results

B.1

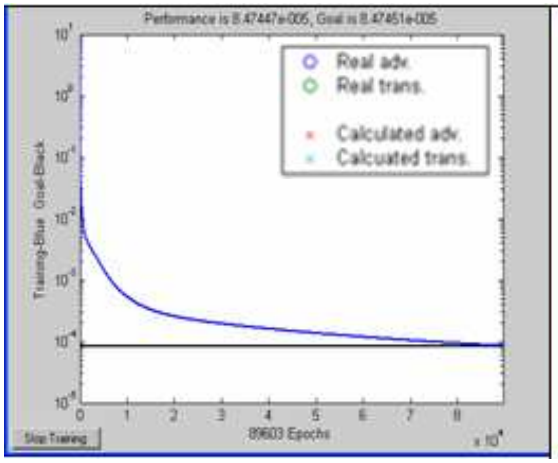

Figure 6.5.1 Epochs and goal of one case of PNN

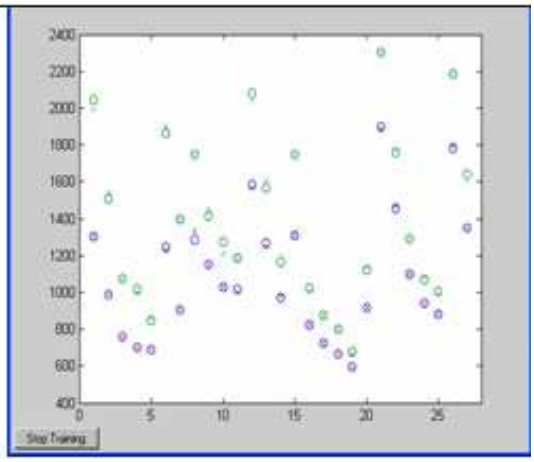

Figure 6.5.2 Results of training goal for one case

Figure 6.5 : One case of PNN, the lift shows performance, goal and epochs and the right: The results of the one case in the lift figure (Direct Model)

B.2

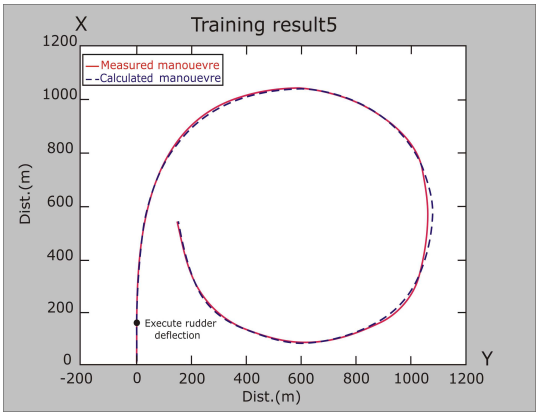

Figure 6.6.1: Containership 1, δ_r= - 35° to starboard

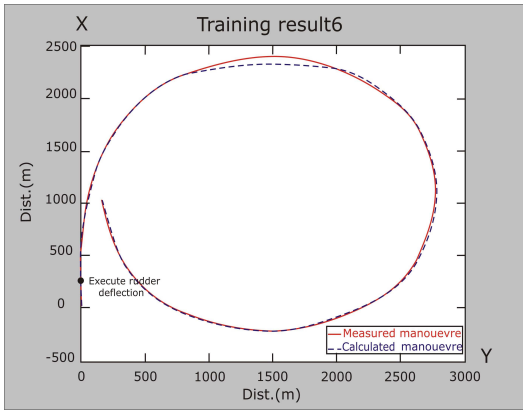

Figure 6.6.2: Containership 2, δ_r= -05° to starboard

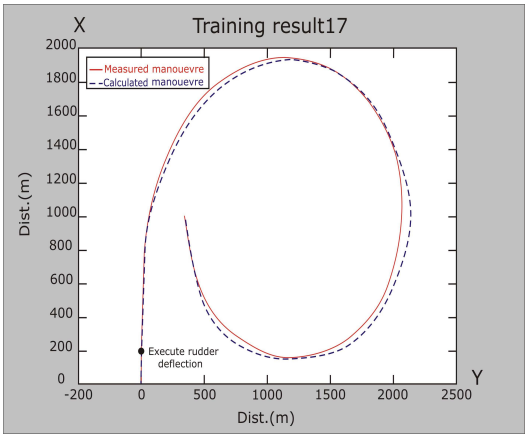

Figure 6.6 4.3: VLCC, δ_r= -10° to starboard

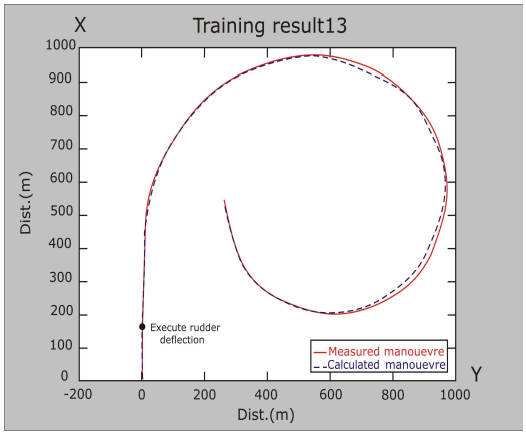

Fig. 6.6.4: Bulk carrier, δ_r= - 20° to starboard

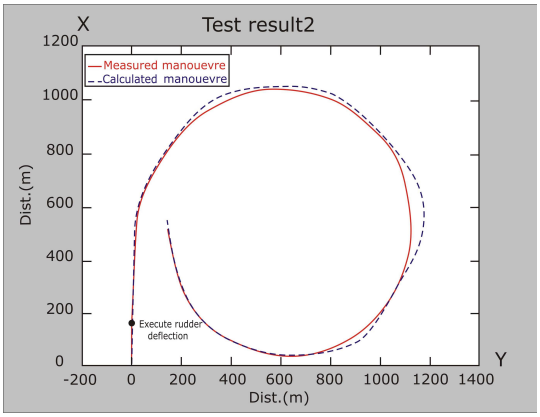

Figure 6.6.5: Containership 1, δ_r = - 30° to starboard

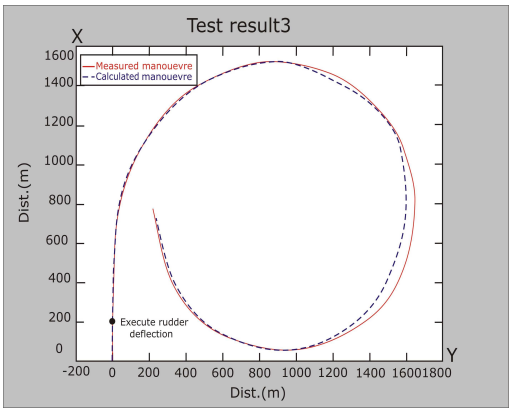

Figure 6.6.6: Containership 2, δ_r= -20° to starboard

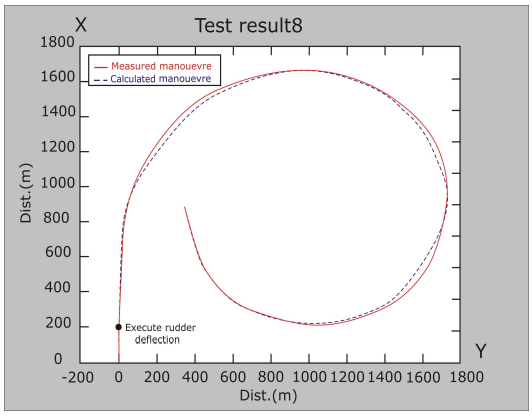

Figure 6.6.7: VLCC, δ_r= -15° to starboard

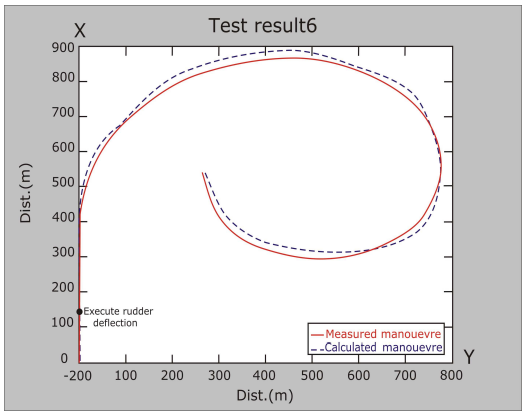

Figure 6.6.8: Bulk carrier, δ_r= -30° to starboard

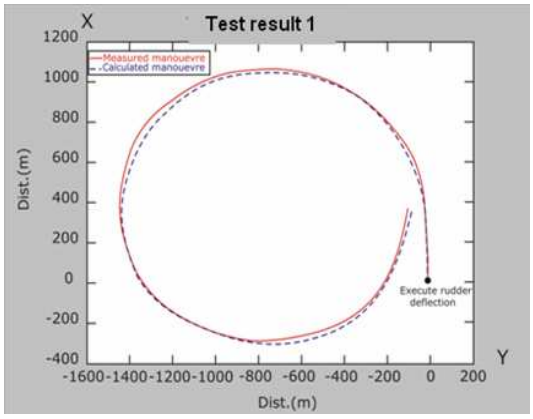

Figure 6.6.9: Containership 1, δ_r= 15° to port side

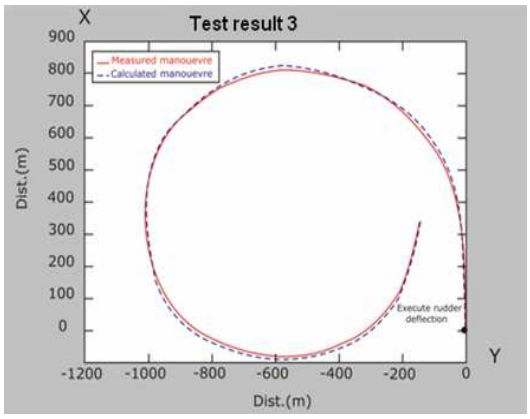

Figure 6.6.10 Containership 1, δ_r= 33° to port side

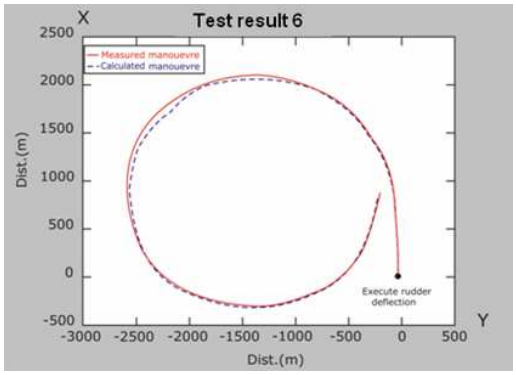

6.6.11 Containership 2, δ_r= 05 ^{o} to port side

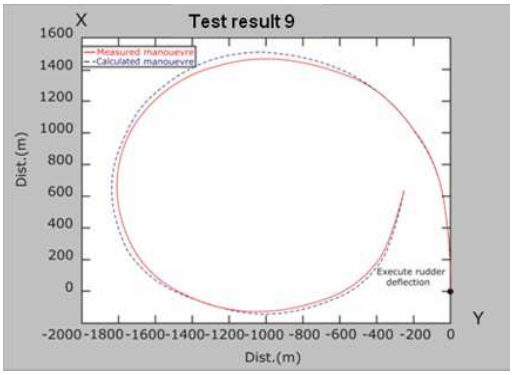

6.6.12 Bulk carrier, δ_r= 06 ^{o} to port side

Figure 6.6 Turning manoeuvre tracks of different ships at various rudder angles (Direct Model)

B.3

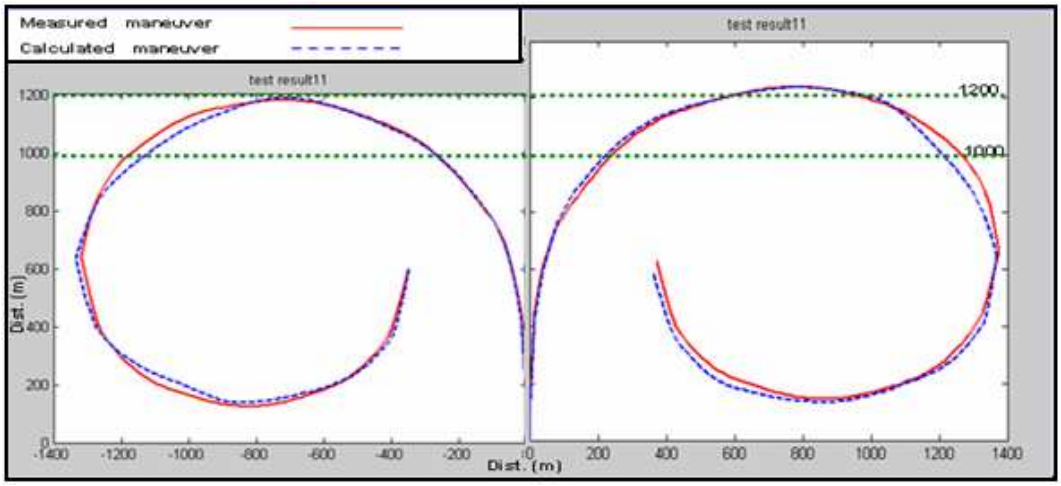

Fig. 6.7: Turning manoeuvre tracks of VLLC, δ_r= 25° degrees to both sides (Direct Model)

Appendix C

Figures of the results of Chapter 6: Simulation Results: NN Direct Mathematical Model Results

C.1

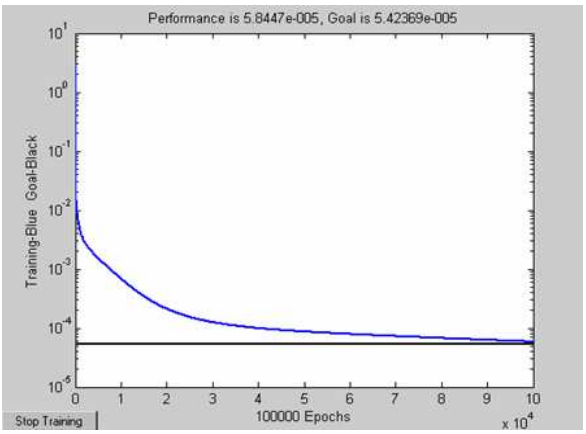

Figure 6.8.1: Epochs and goal of one case of PANN

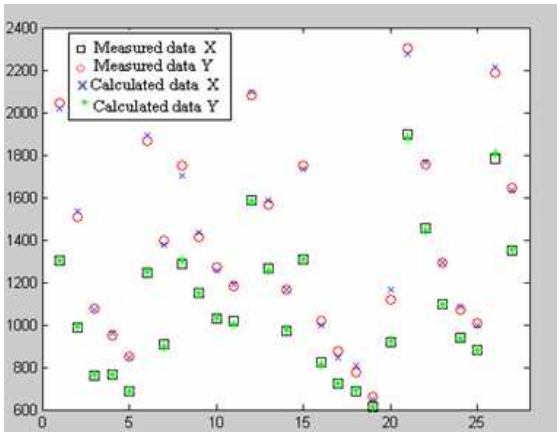

Figure 6.8.2: Results of a training goal

Figure 6.8: One case of PNN of the direct model, the lift side: Performance, goal and epochs and the right side: The results of the one case in the lift figure.

C.2

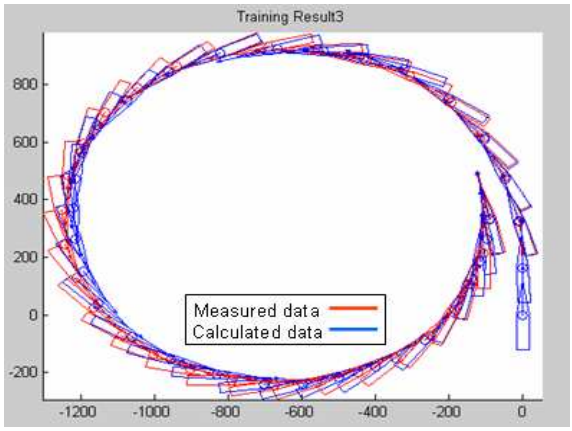

Figure 6.9.1: Containership 1
δ_r = 25°, turn to the port side

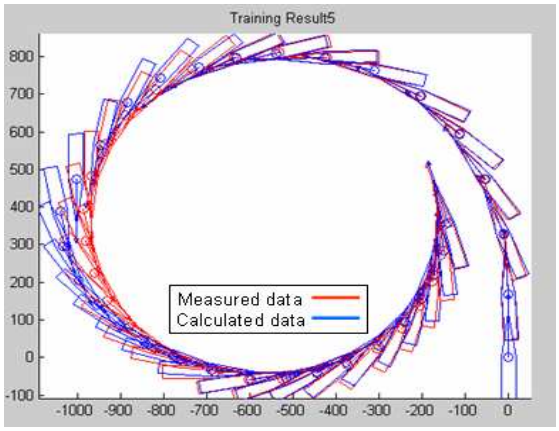

Figure6.9.2: Containership 1
δ_r = 35°, turn to the port side

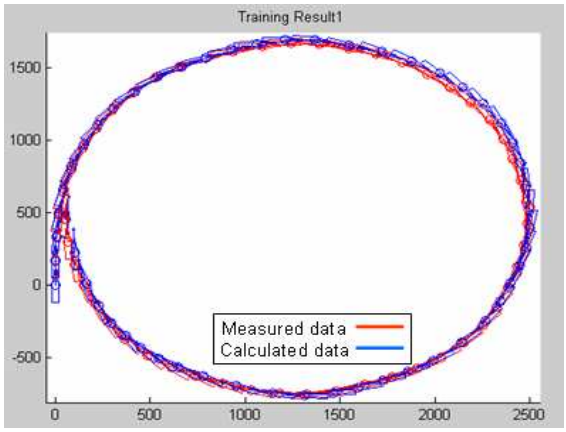

Figure 6.9.3: Containership 1
δ_r = -05°, turn to the starboard side

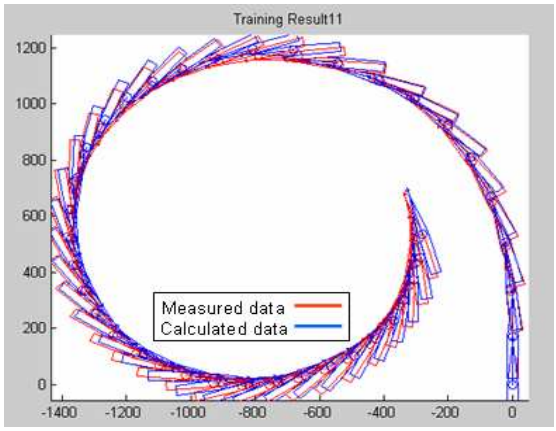

Figure 6.9.4: Containership 2
δ_r = 30°, turn to the port side

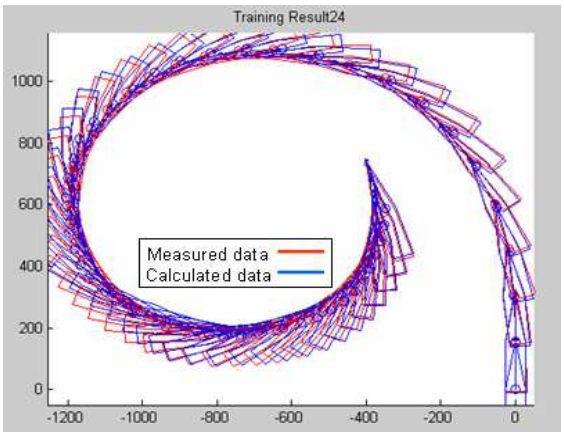

Figure 6.9.5: V.L.C.C.
δ_r = 30°, turn to the port side

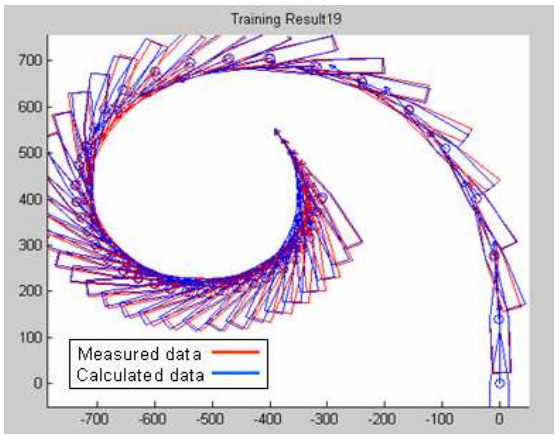

Figure 6.9.6: Bulk carrier
δ_r = 35°, turn to the port side

Figure 6.9: Training results of the direct model, prediction of turning manoeuvre motion of different ships using various rudder angles to port and starboard side

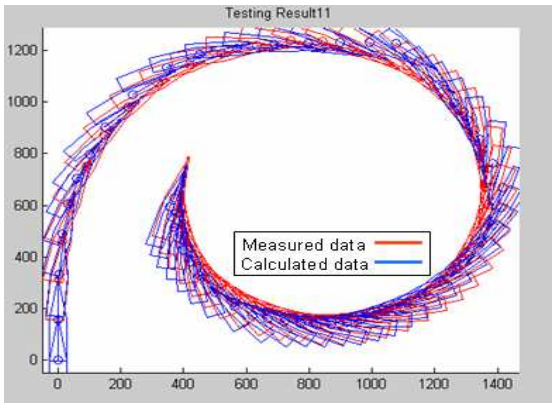

Figure 6.10.1: V.L.C.C.
δ_r = -25 ^{o}, turn to the starboard side

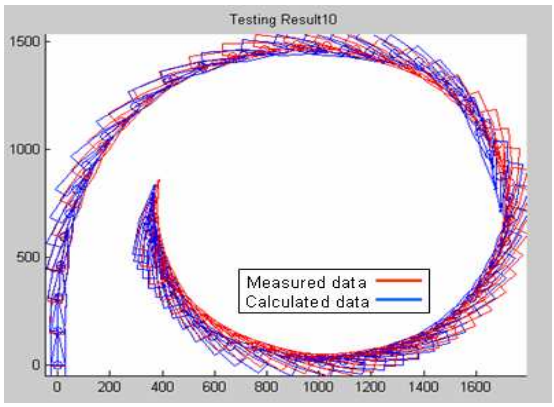

Figure 6.10.2: V.L.C.C.
δ_r = -15^o, turn to the starboard side

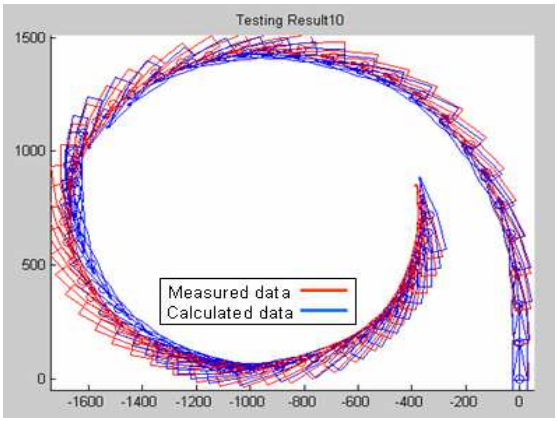

Figure 6.10.3: V.L.C.C.
δ_r = 15^o, turn to the port side

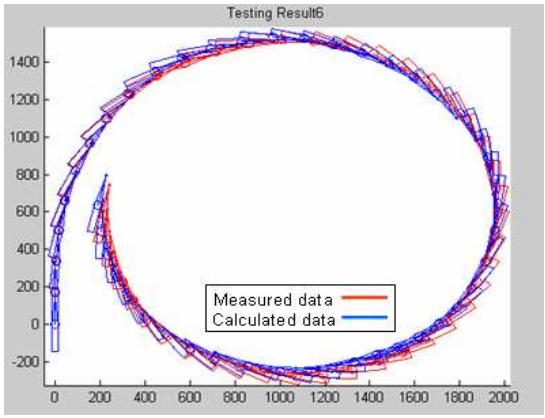

Figure 6.10.4: Containership 2
δ_r = -12^o, turn to the starboard side

Figure 6.10: Test results of the direct model prediction of turning manoeuvre of different ships using various rudder angles to port and starboard side

C.3

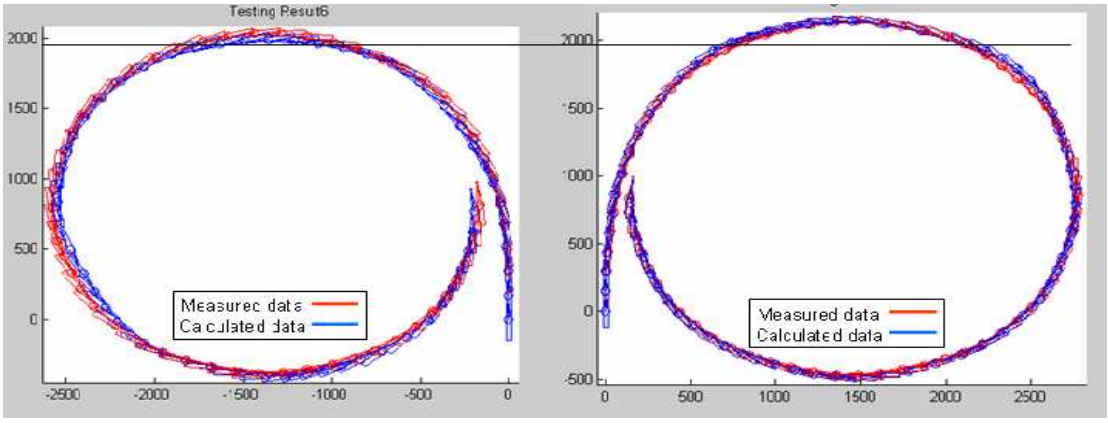

Figure 6.11: Test results of the direct model prediction of turning manoeuvre of Containership 2, δ_r =05^o degrees to both sides

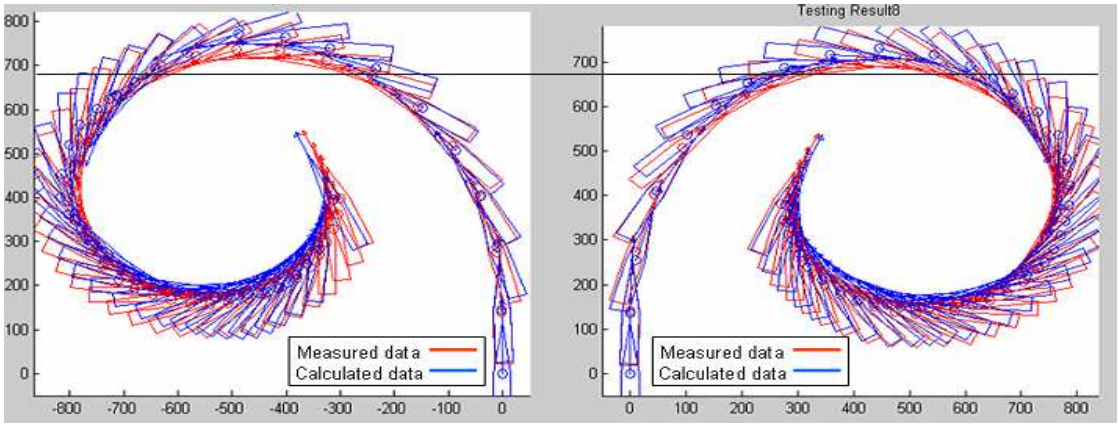

Figure 6.12: Test results of the direct model prediction of turning manoeuvre of Bulk carrier, δ_r = 30 ^{o} degrees to both sides

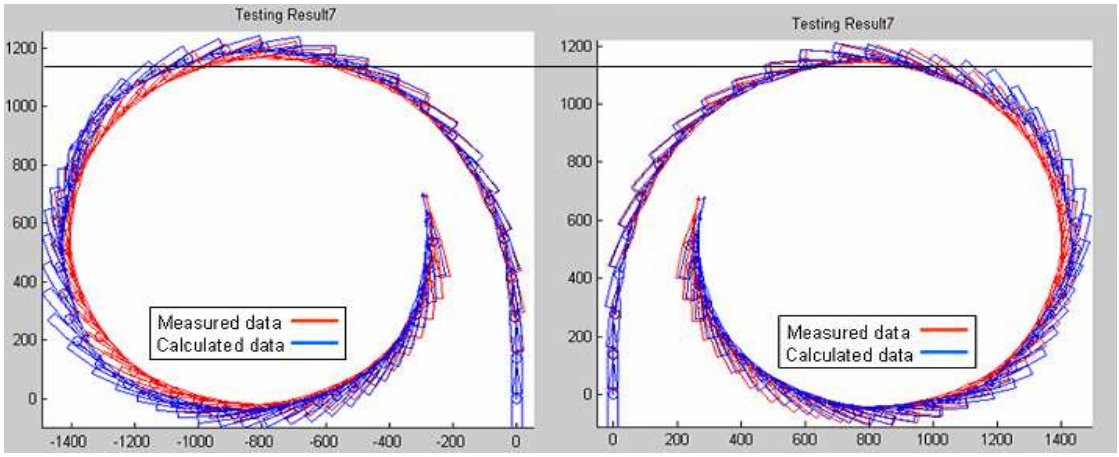

Figure 6.13: Test results of the direct model prediction of turning manoeuvre of Bulk carrier, δ_r = 10 ^{0} degrees to both sides

C.4

Test results

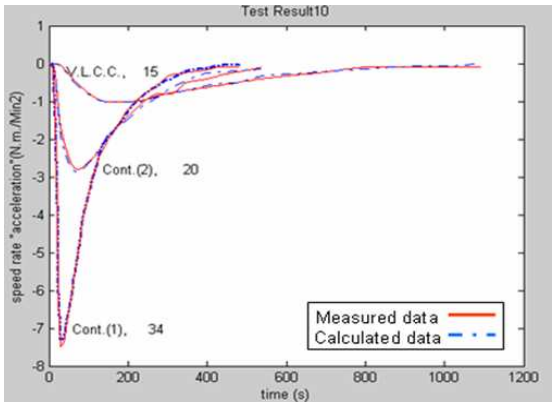

Figure 6.14.1: Acceleration ($\dot{U}$), V.L.C.C., and Containerships 1 & 2

Training results

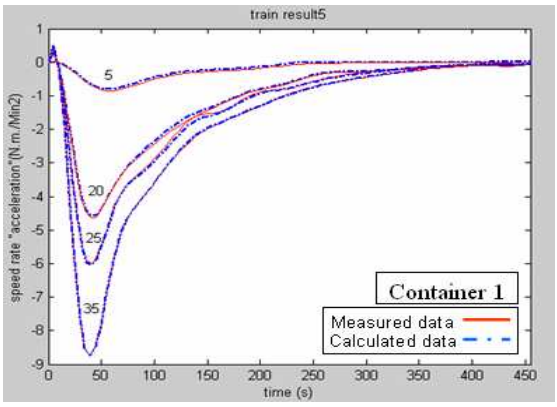

Figure 6.14.2: Acceleration ($\dot{U}$), Containership 1

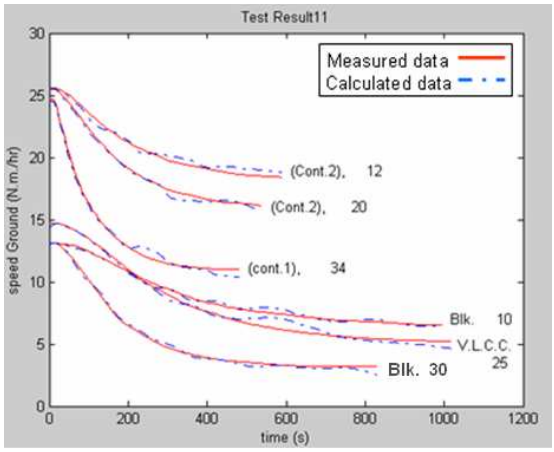

Figure 6.14.3: Speed (U), Containership 1 & 2, Bulk carrier and V.L.C.C.

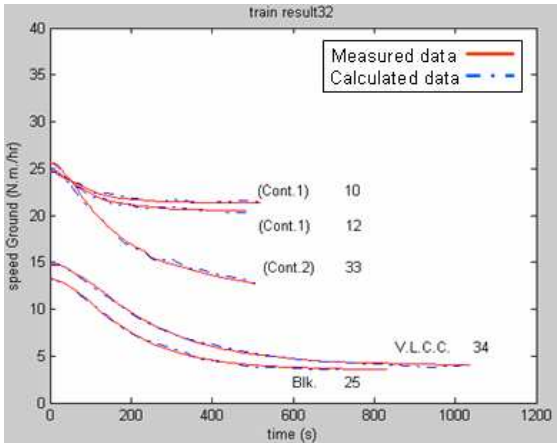

Figure 6.14.4: Speed (U), Containership 1 & 2, Bulk carrier and V.L.C.C.

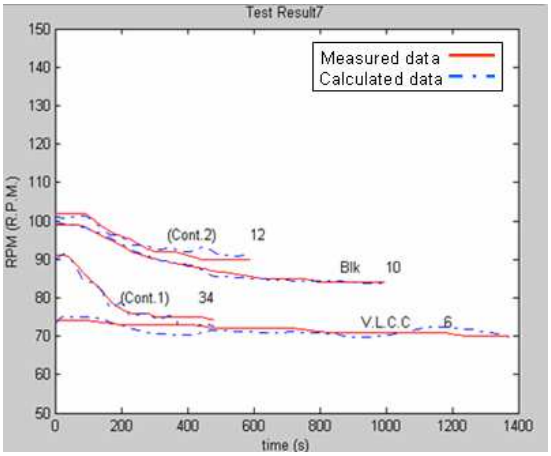

Figure 6.14.5: RPM, Containership 1& 2, Bulk carrier and V.L.C.C.

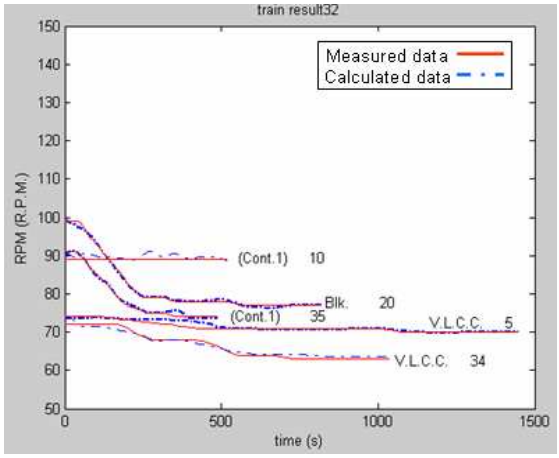

Figure 6.14.6: RPM, Containership 1, Bulk carrier and V.L.C.C.

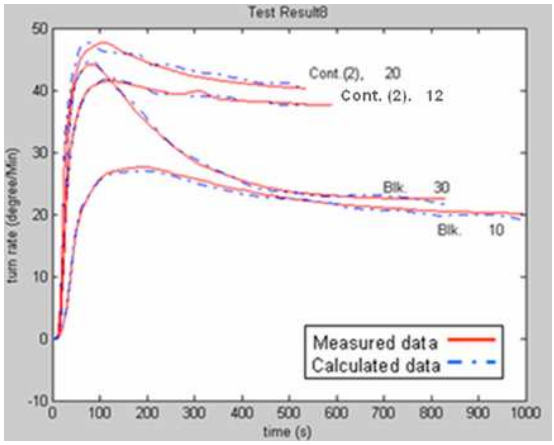

Figure 6.14.6: Angular velocity (r), Containership 2, and Bulk carrier

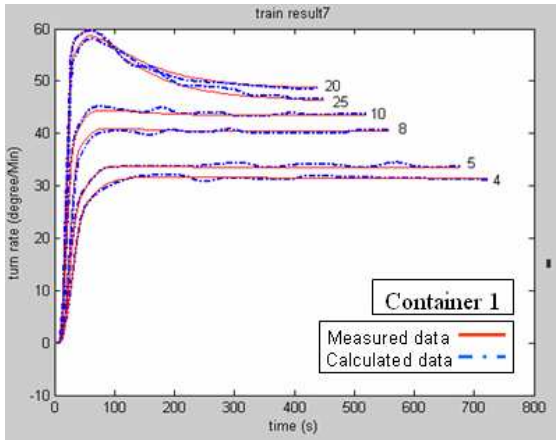

Figure 6.14.8: Angular velocity (r), Containership 1

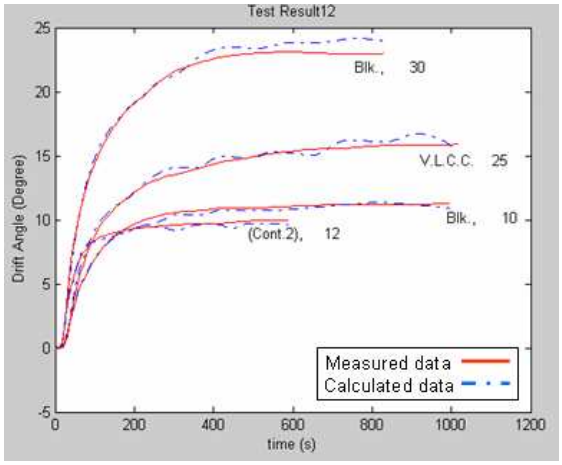

Figure 6.14.9: Drift angle (β), Containership 2, Bulk carrier and V.L.C.C.

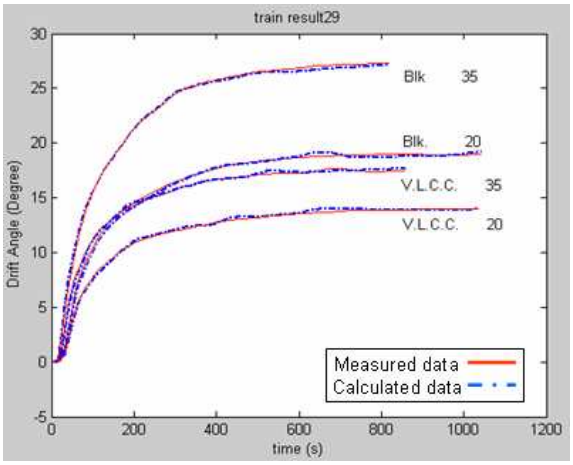

Figure 6.14.10: Drift angle (β), Bulk carrier and V.L.C.C.

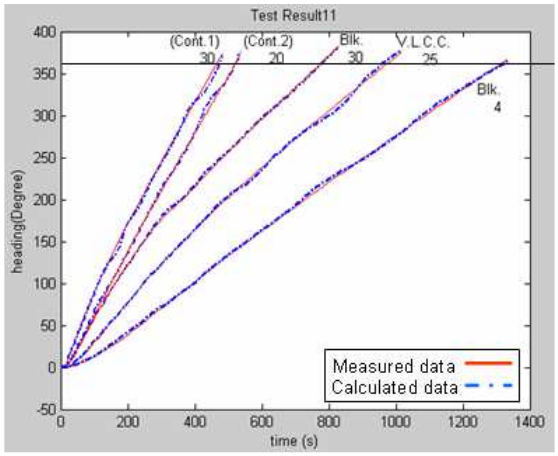

Figure 6.14.11: Heading angle (ψ), Containership 1, Bulk carrier and V.L.C.C.

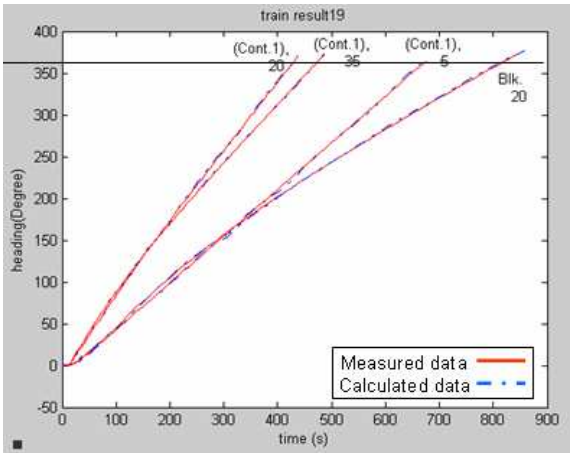

Figure6.14.12: Heading angle (ψ), Containership 1 and Bulk carrier

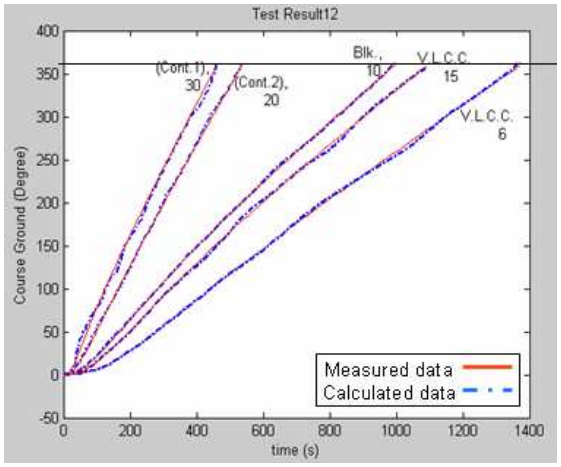

Figure 6.14.13: Test results of the course ground, Cont.1& 2 Bulk carrier & V.L.C.C.

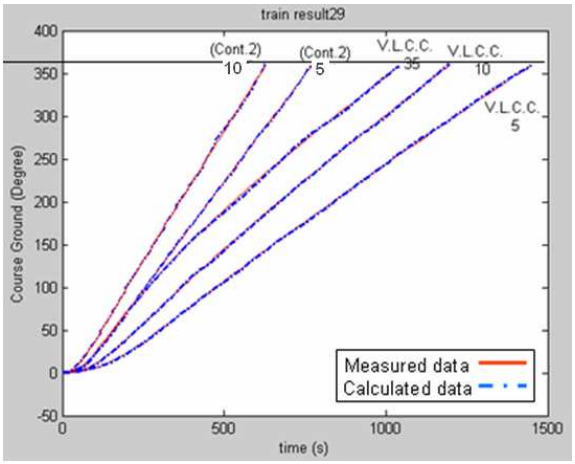

Figure 6.14.14: Train results of the course ground, Container ship 2 and V.L.C.C.

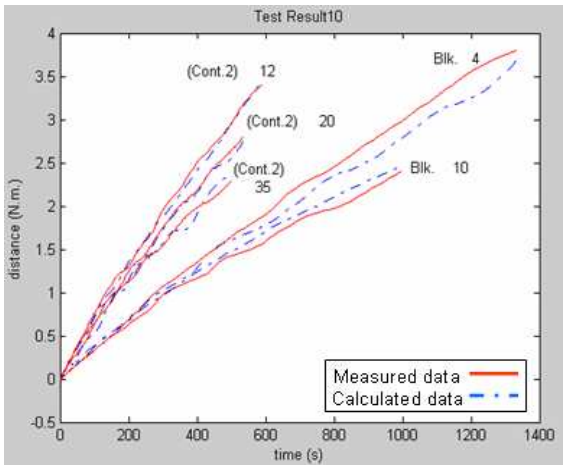

Figure 6.14.15: Travel distance, Containership 2 and Bulk carrier

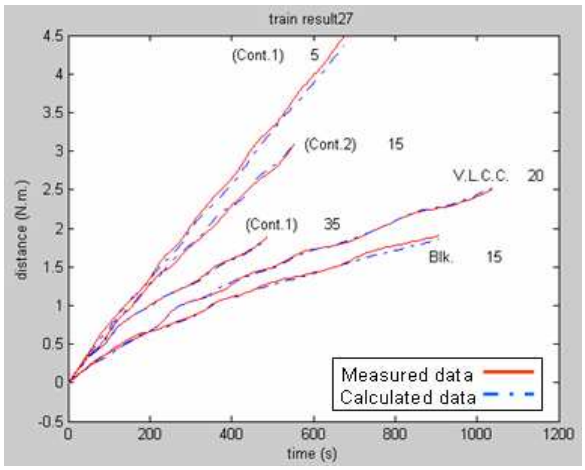

Figure 6.14.16: Travel distance, Containership 1 & 2, Bulk carrier and V.L.C.C.

Figure 6.14: Training and test results of the direct model prediction of the main parameter of turning manoeuvre to the starboard side

Test results

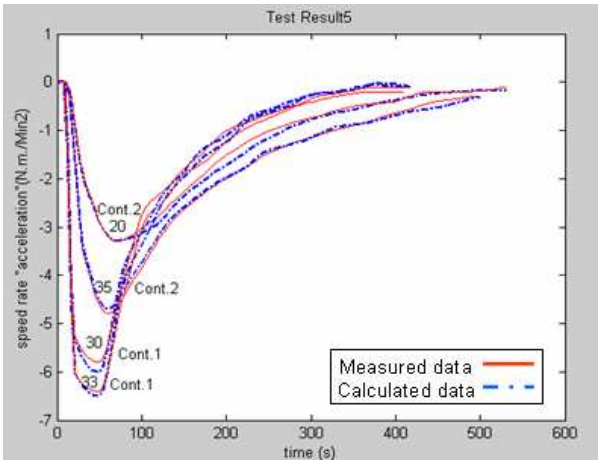

Figure 6.15.1: Acceleration ($\dot{U}$), Containership 1 & 2

Training results

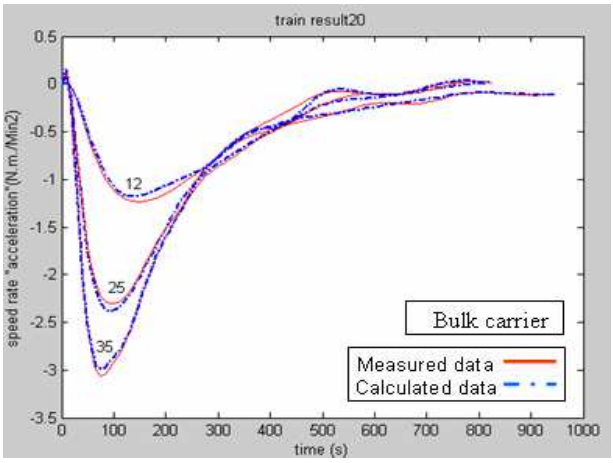

Figure 6.15.2: Acceleration ($\dot{U}$), Bulk carrier

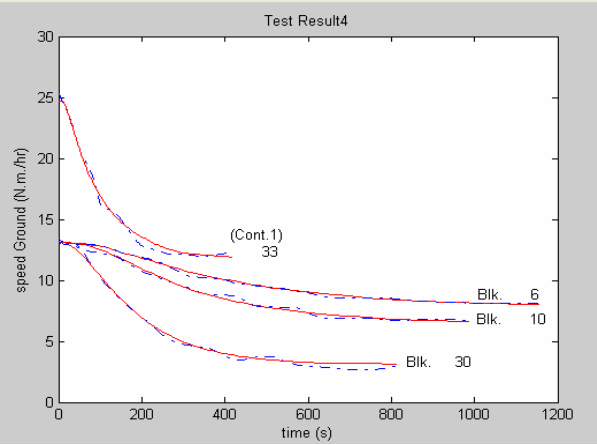

Figure 6.15.3: Speed (U),
Containership 1 and Bulk carrier.

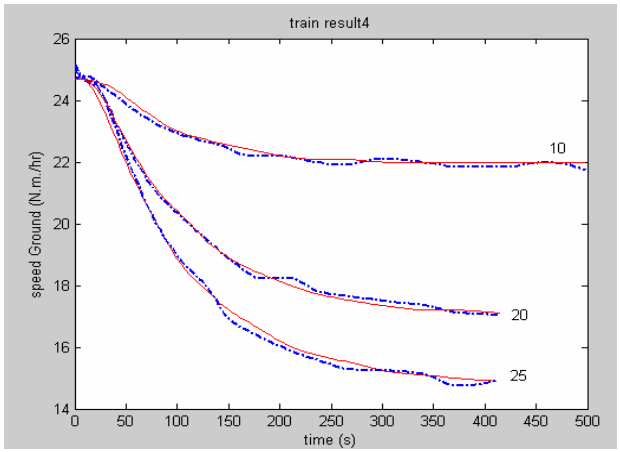

Figure 6.15.4: Speed (U),
Container 1

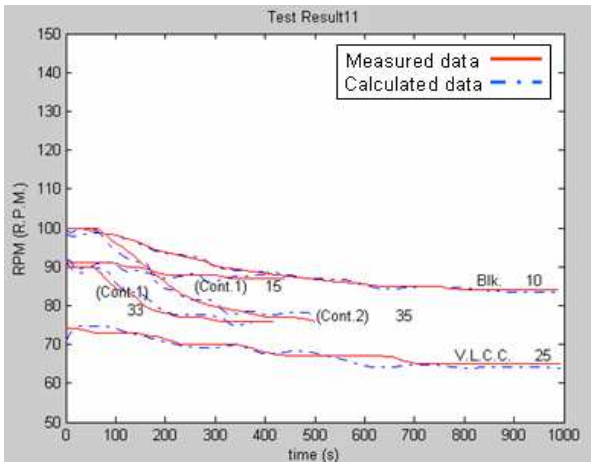

Figure 6.15.5: RPM, Container ship 1 & 2,
Bulk carrier and V.L.C.C.

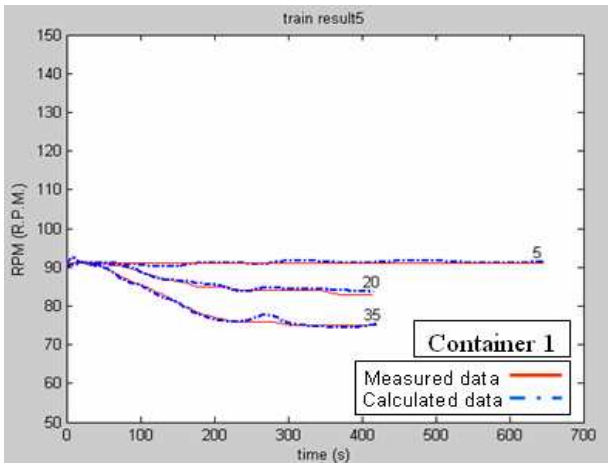

Figure 6.14.7: Angular velocity (r),
Containership 1, and Bulk carrier

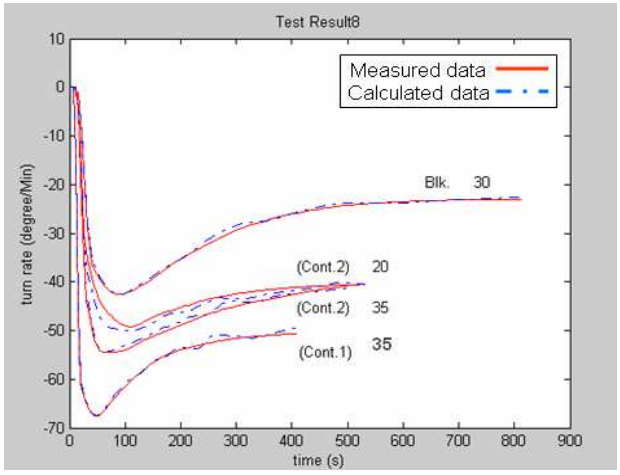

Figure 6.15.7: Angular velocity (r),
Containership 1 & 2 and Bulk carrier

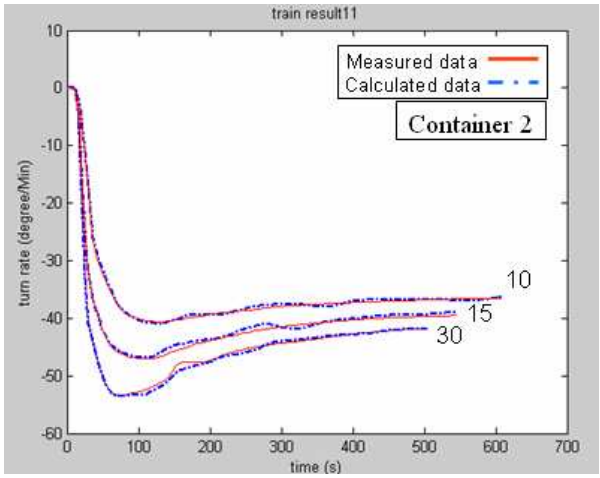

Figure 6.15.8: Angular velocity (r),
Container 2

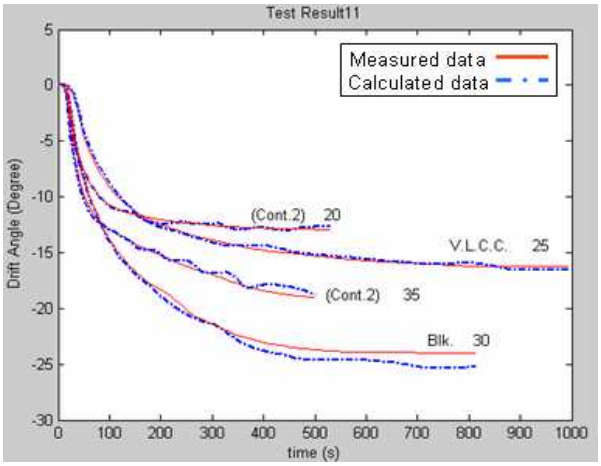

Figure 6.15.9: Drift angle (β), Containership 2, Bulk carrier and V.L.C.C.

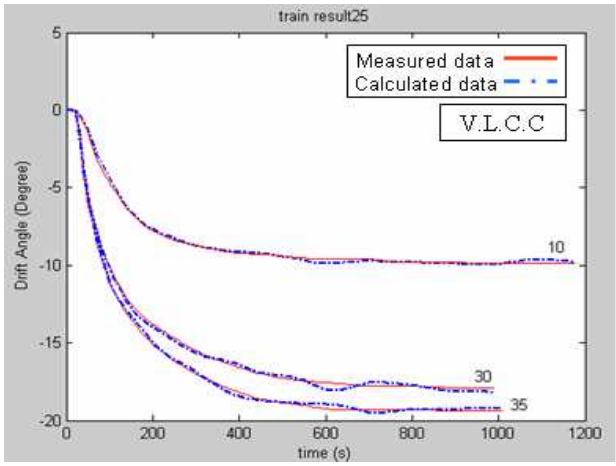

Figure 6.15.10: Drift angle (β), V.L.C.C.

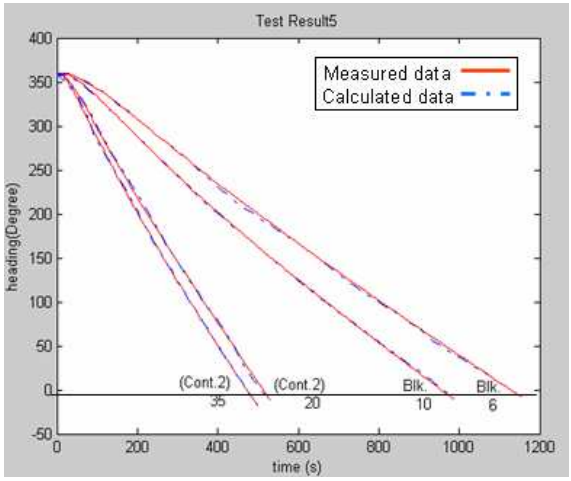

Figure 6.15.11: Heading angle (ψ), Containership 2 and Bulk carrier

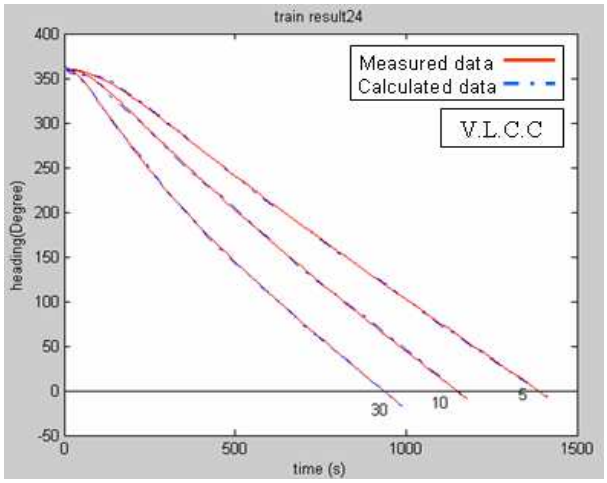

Figure 6.15.12: Heading angle (ψ), V.L.C.C.

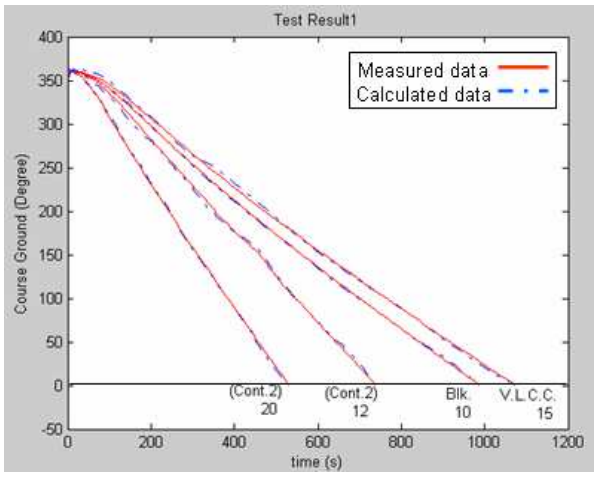

Figure 6.15.13: Test results of course ground, Cont. 2, Bulk carrier and V.L.C.C.

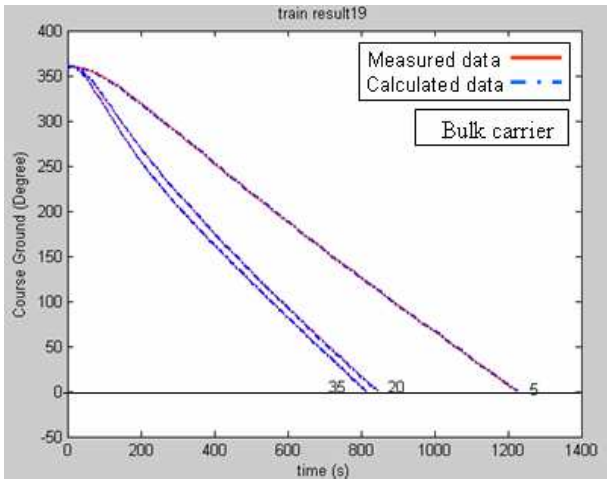

Figure 6.15.14: Train results of course ground, Bulk carrier

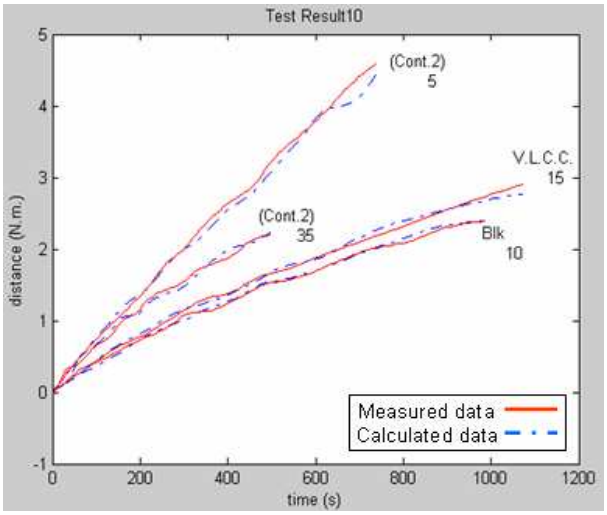

Figure 6.15.15: Travel distance, Containership 2, Bulk carrier and V.L.C.C.

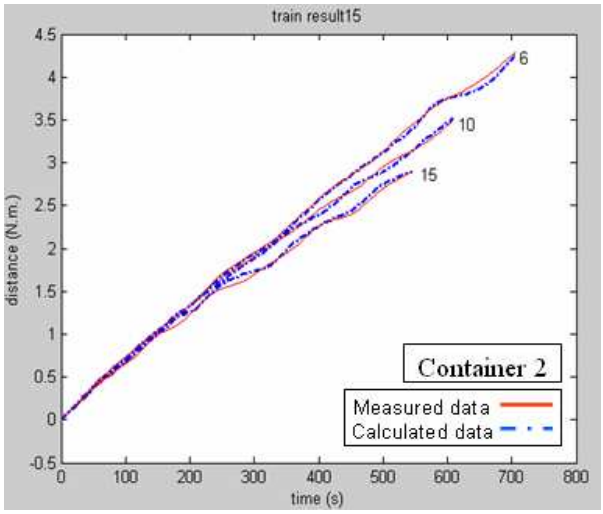

Figure 6.15.16: Travel distance, Container 2

Figure 6.15: Training and test results of the direct model prediction of the main parameter of turning manoeuvre to the port side

Appendix D

Figures of the results of Chapter 6: NN General Mathematical Force Model Results

D.1

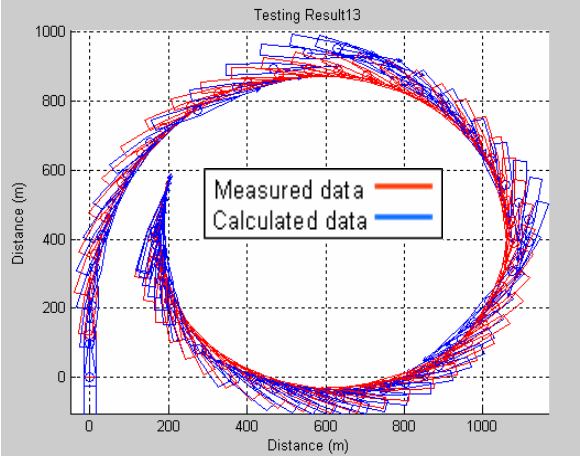

Figure 6.16.1: Containership 1
δ_r = -35°, turn to the starboard side

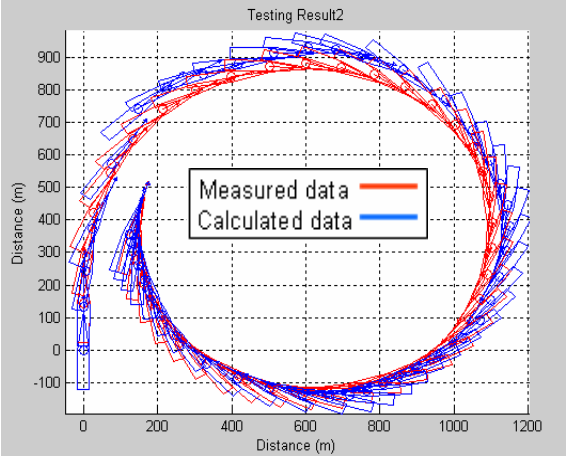

Figure 6.16.2: Containership 1
δ_r = -30°, turn to the starboard side

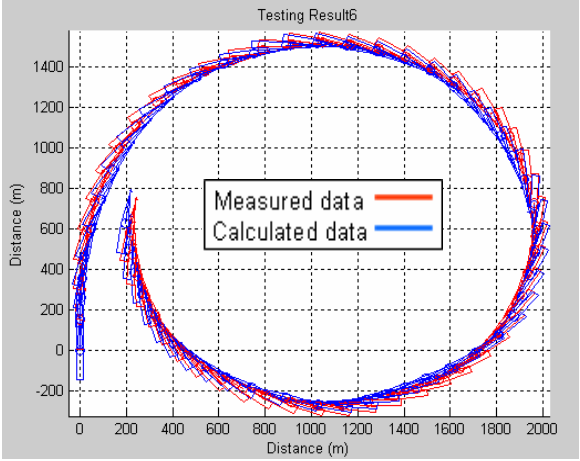

Figure 6.16.3: Containership 2
δ_r = -12°, turn to the starboard side

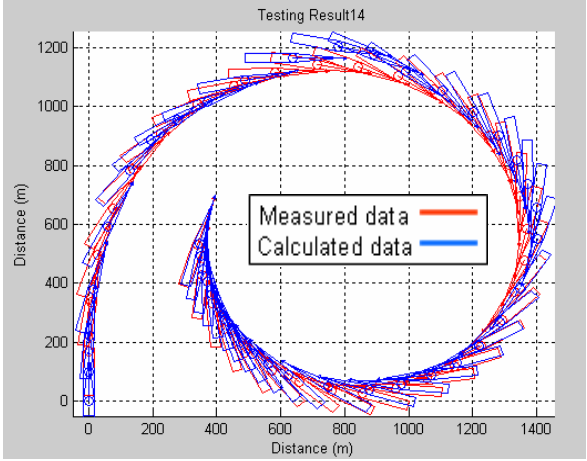

Figure 6.16.4: Containership 2
δ_r = -35°, turn to the starboard side

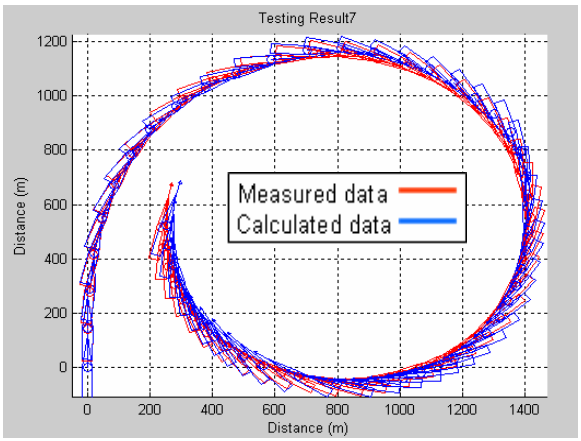

Figure 6.16.5: Bulk carrier
δ_r = -10°, turn to the starboard side

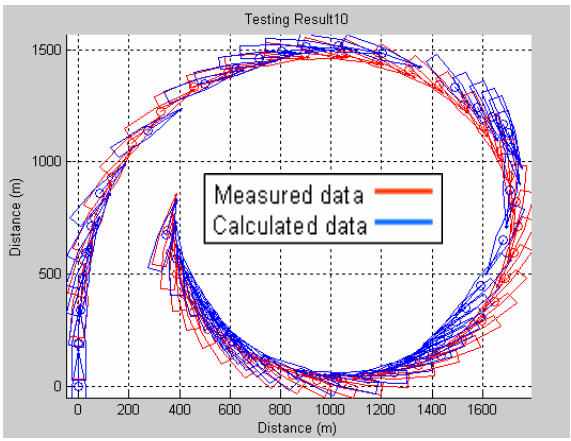

Figure 6.16.6: VLCC
δ_r = -15°, turn to the starboard side

Figure 6.16: Testing results of the general force model, simulation of the turning manoeuvre motion of different ships using various rudder angles and speeds to starboard side

D.2

Test results

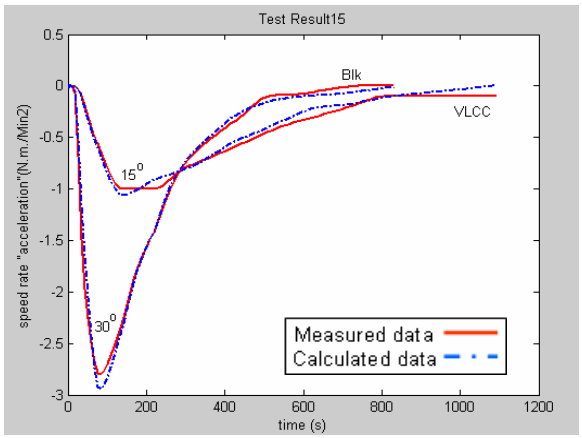

Figure 6.17.1: Acceleration ($\dot{U}$),
Bulk carrier and VLCC

Test results

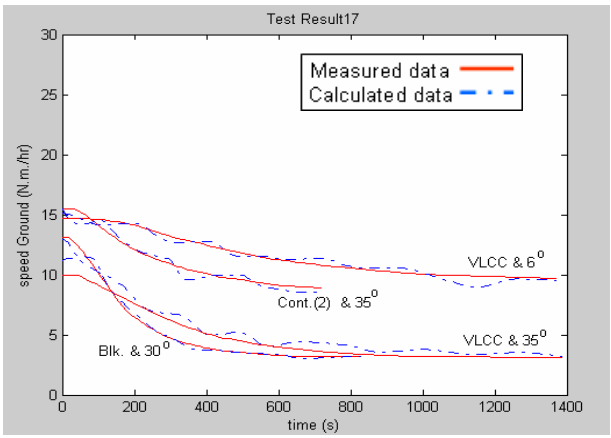

Figure 6.17.2: Speed (U),
Containership 2, VLCC and Bulk carrier.

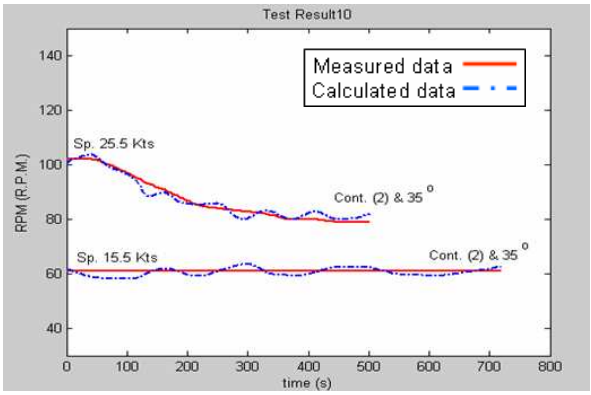

Figure 6.17.3: RPM,
Container ship 2

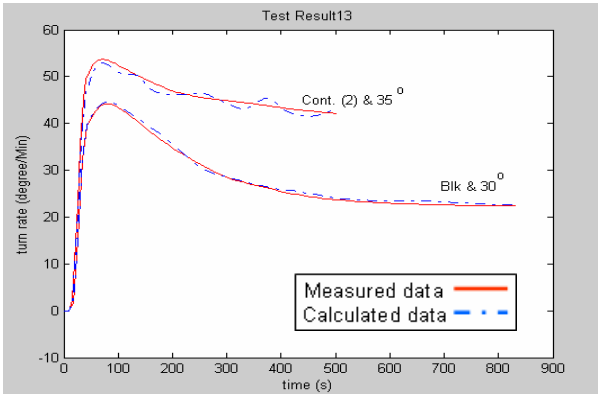

Figure 6.17.4: Angular velocity (r),
Container ship 2 and Bulk carrier

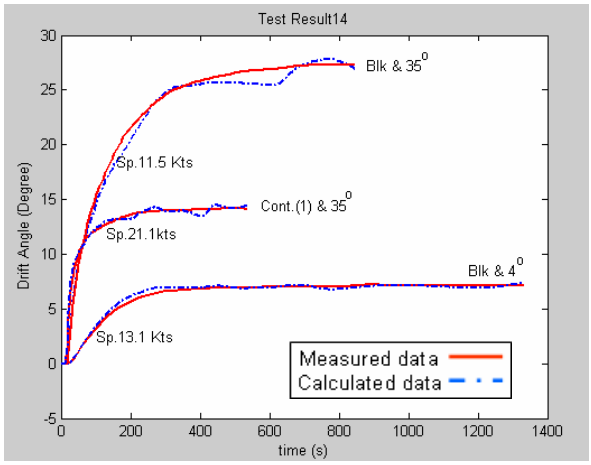

Figure 6.17.5: Drift angle (β), Containership 1 and Bulk carrier

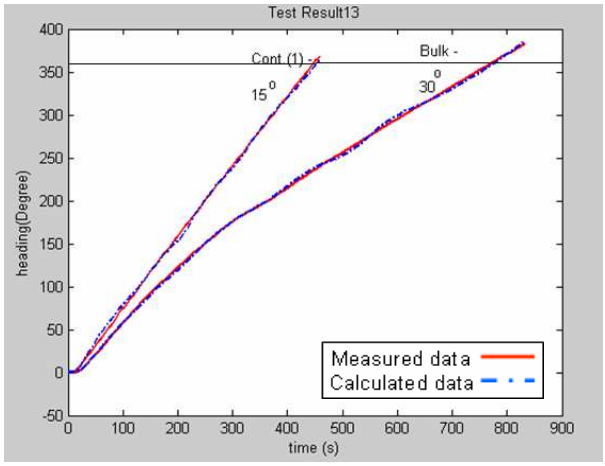

Figure 6.17.6: Heading angle (ψ), Containership 1and Bulk carrier

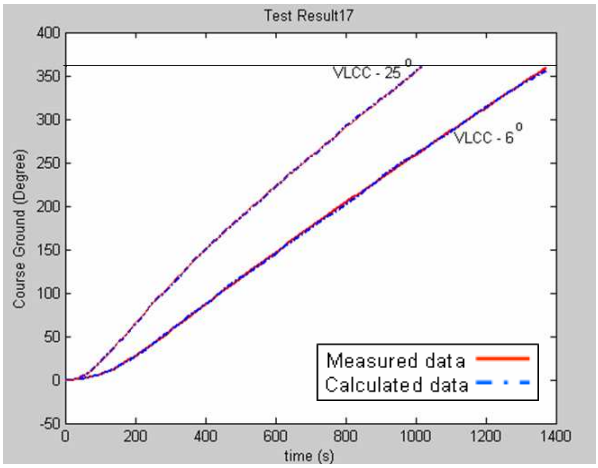

Figure 6.17.7: Test results of course ground, V.L.C.C.

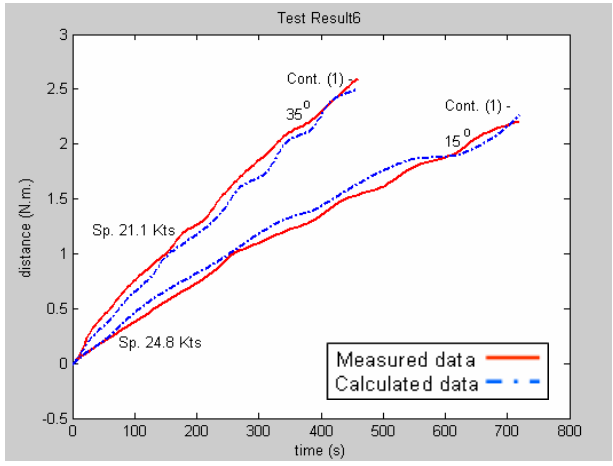

Figure 6.17.8: Travel distance, Container ship 1

Figure 6.17: Test results of the general force model, prediction of the main parameter of turning manoeuvre to the starboard side

Appendix E

Figures of the results of Chapter 6: NN Series Mathematical Force Models Results

E.1

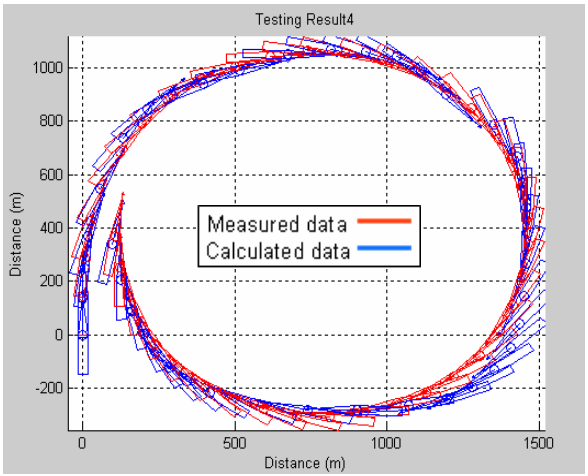

Figure 6.18.1: Containership 1
δ_r = -15°, turn to the starboard side

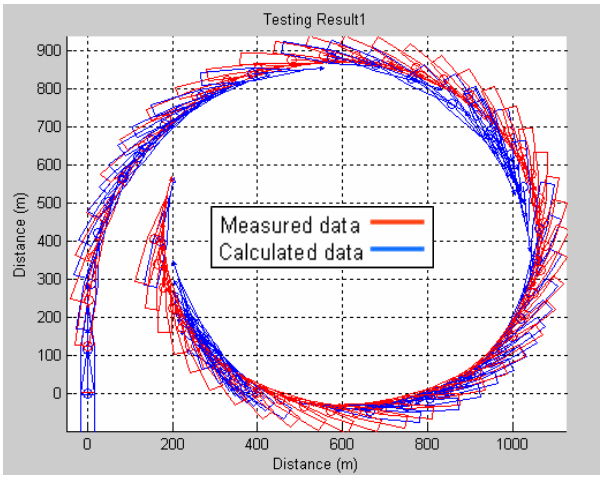

Figure 6.18.2: Containership 1, δ_r = -35°, turn to the starboard side, sp.=21.1 *kts*

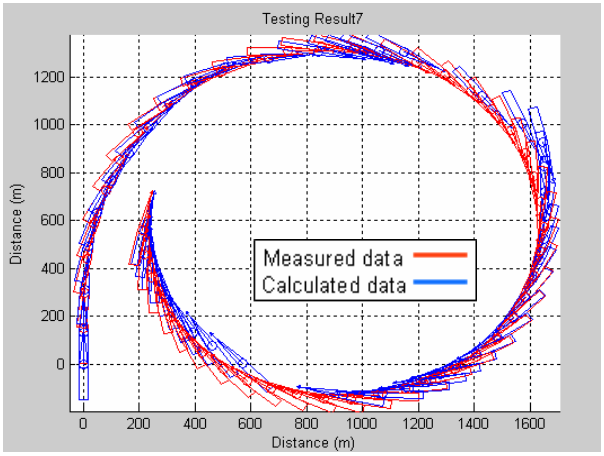

Figure 6.18.3: Containership 2
δ_r = -20°, turn to the starboard side

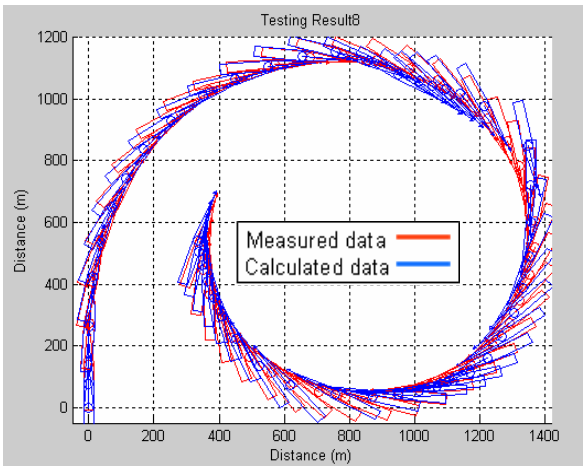

Figure 6.18.4: Containership 2, δ_r = -35°, turn to the starboard side, sp.=15.5 *Kts*

Figure 6.18: Testing results of force model (series 1), simulation of the turning manoeuvre motion of different ships using various rudder angles and speeds to starboard side

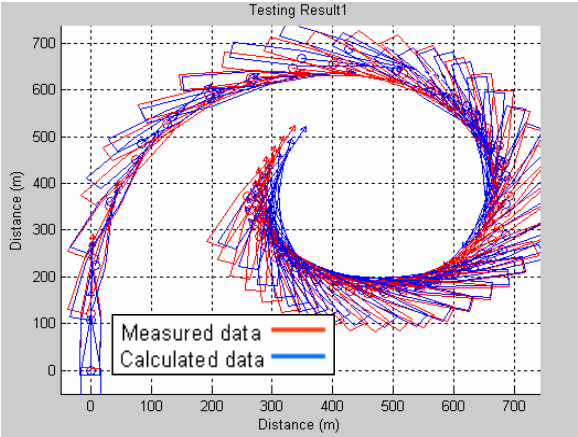

Figure 6.19.1: Bulk carrier, δ_r = -35^o, turn to the starboard side, sp.=11.5 *Kts.*

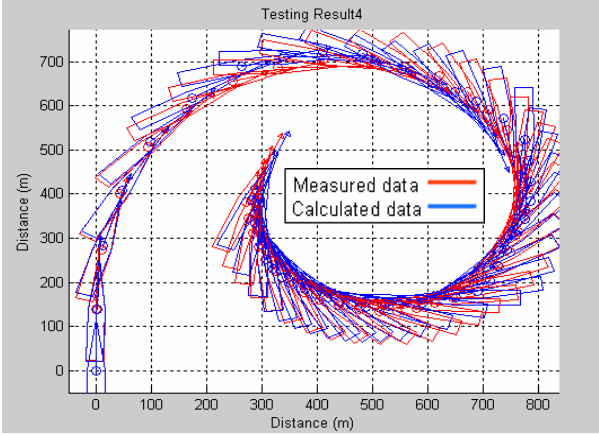

Figure 6.19.2: Bulk carrier, δ_r = -30^o, turn to the starboard side, sp=13.1 *Kts.*

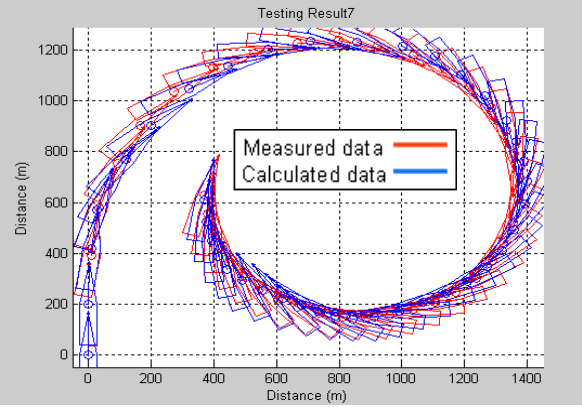

Figure 6.19.3: VLCC, δ_r = -25^o, turn to the starboard side, sp.=14.7 *Kts.*

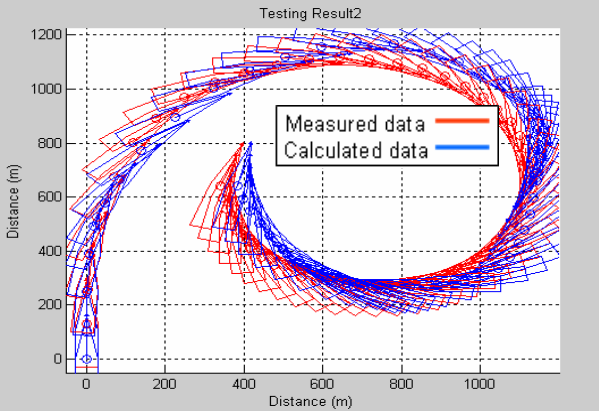

Figure 6.19.4: VLCC, δ_r = -35°, turn to the starboard side, sp.=10.0 *Kts.*

Figure 6.19: Testing results of force model (series 2), simulation of the turning manoeuvre motion of different ships using various rudder angles and speeds to starboard side

E.2

Series (1)

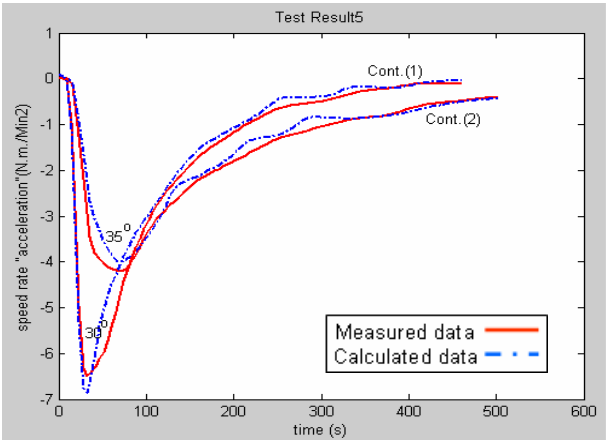

Figure 6.20.1: Acceleration ($\dot{U}$), Containership 1 & 2

Series (2)

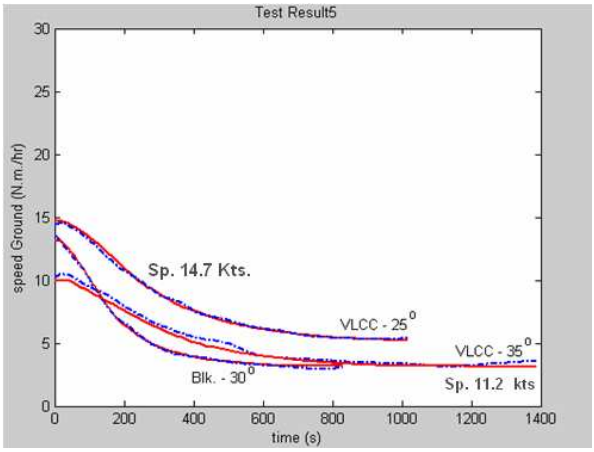

Figure 6.20.2: Speed (U), VLCC and Bulk carrier.

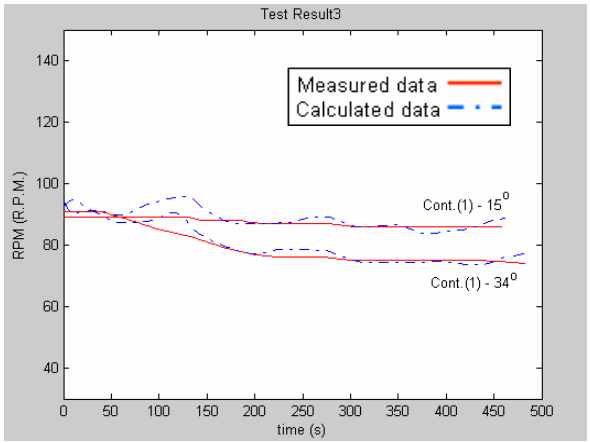

Figure 6.20.3: RPM, Containership 1

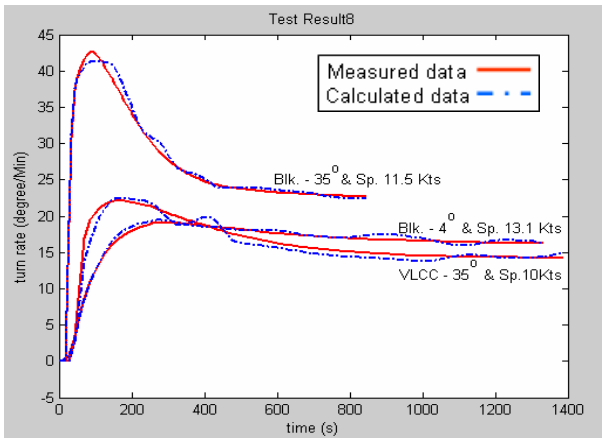

Figure 6.20.4: Angular velocity (r), VLCC and Bulk carrier

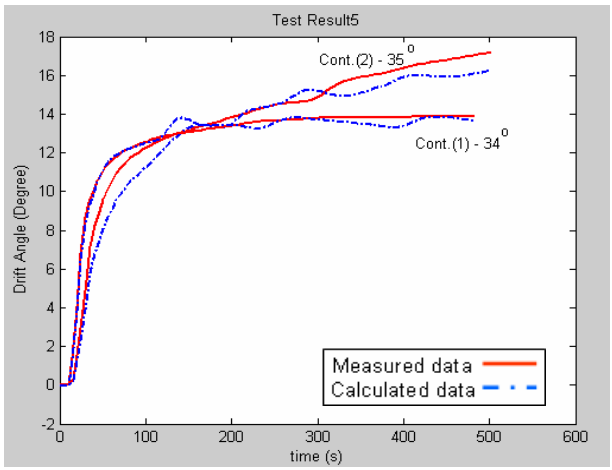

Figure 6.20.5: Drift angle (β), Container ship 1 & 2

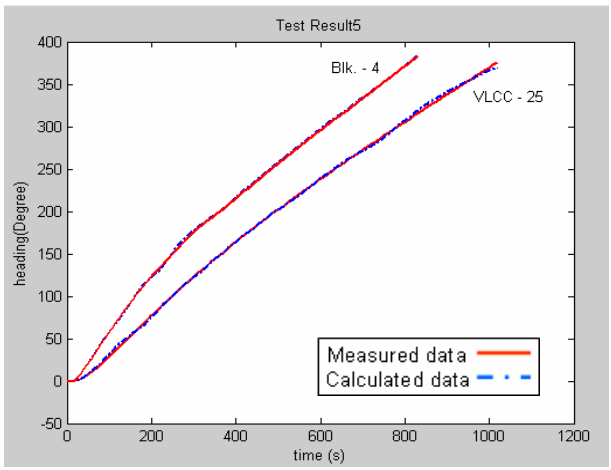

Figure 6.20.6: Heading angle (ψ), VLCC and Bulk carrier

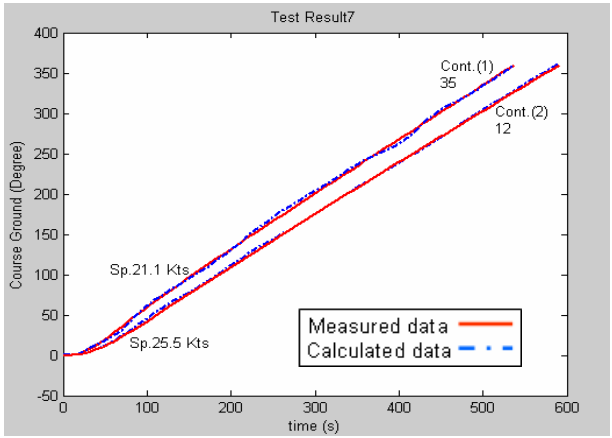

Figure 6.20.7: Test results of the course ground, Containership 1 & 2

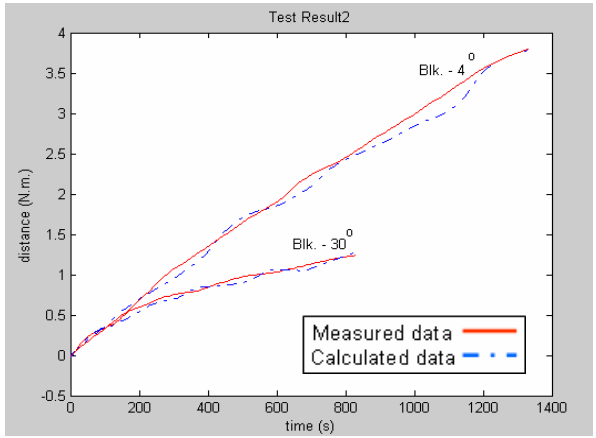

Figure 6.20.8: Travel distance, Bulk carrier

Figure 6.20: Test results of force model series (1&2), prediction of the main parameter of turning manoeuvre to the starboard side

E.3

Simulate ship motion and plot the different transient phases' curves of different speeds and same rudder angle

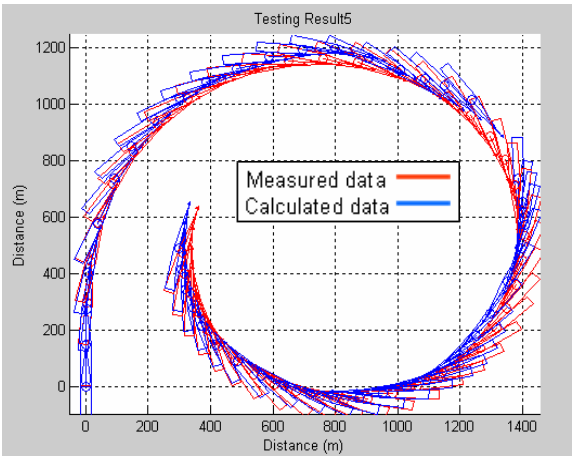

Figure 6.21.1: Containership 2, δ_r = -35°, turn to the starboard side, sp.= 25.5 *kts.*

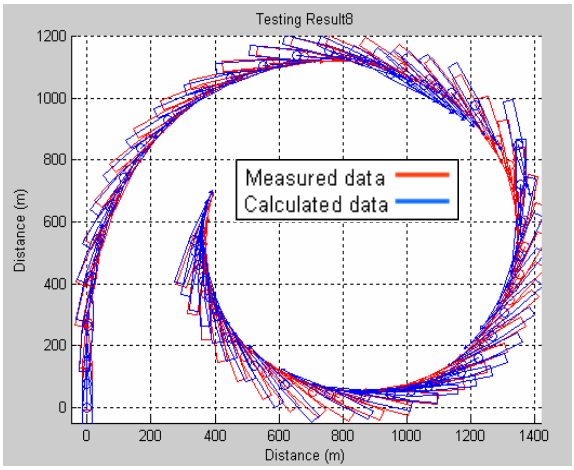

Figure 6.21.2: Containership 2, δ_r = -35°, turn to the starboard side, sp.= 15.5 *kts.*

Figure 6.21: Testing results of force model (series 1), simulation of the turning manoeuvre motion of Container ship 2 using same rudder angle to starboard side but different speeds

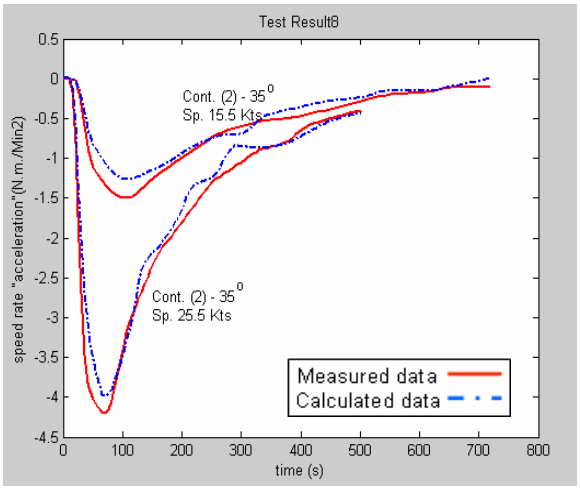

Figure 6.22.1: Acceleration ($\dot{U}$), Containership (2)

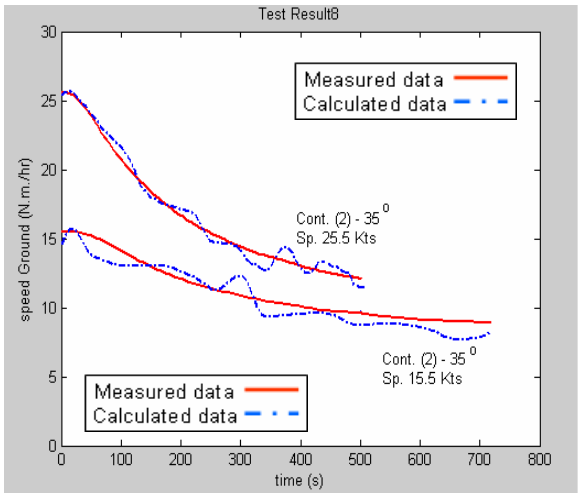

Figure 6.22.2: Speed (U), Containership (2)

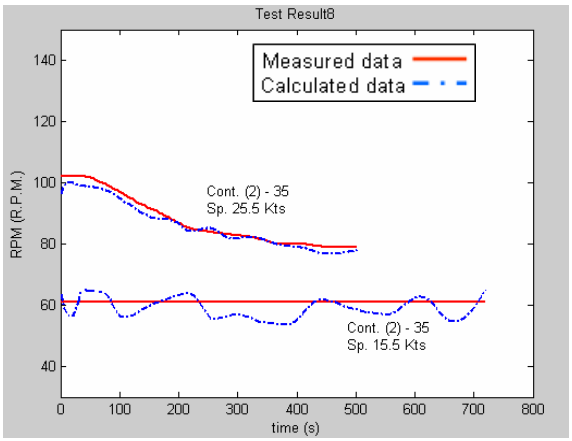

Figure 6.22.3: RPM, Containership (2)

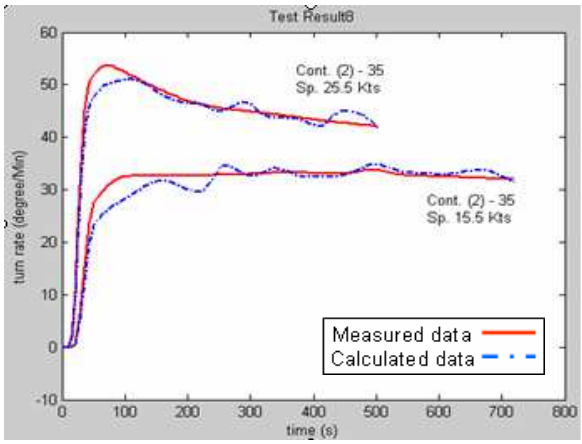

Figure 6.22.4: Angular velocity (r), Containership (2)

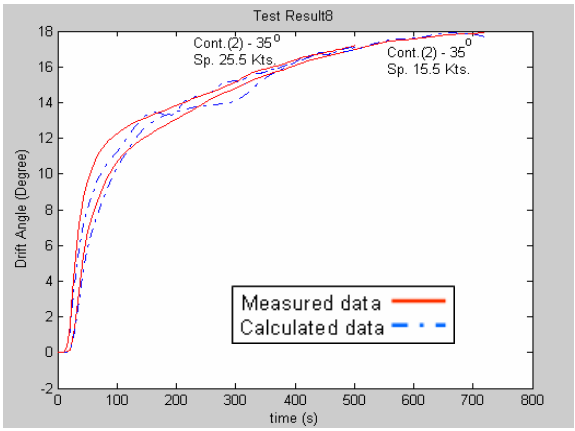

Figure 6.22.5: Drift angle (β), Containership (2)

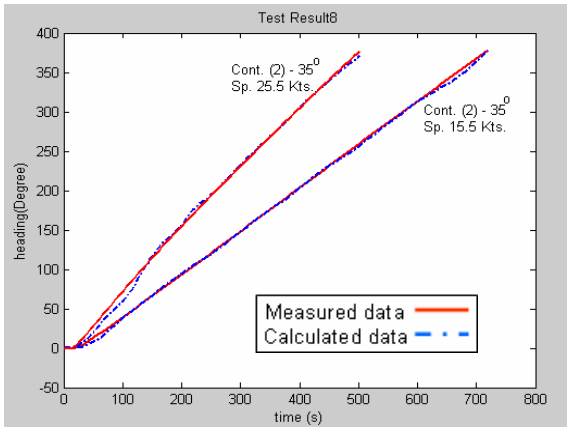

Figure 6.22.6: Heading angle (ψ), Containership (2)

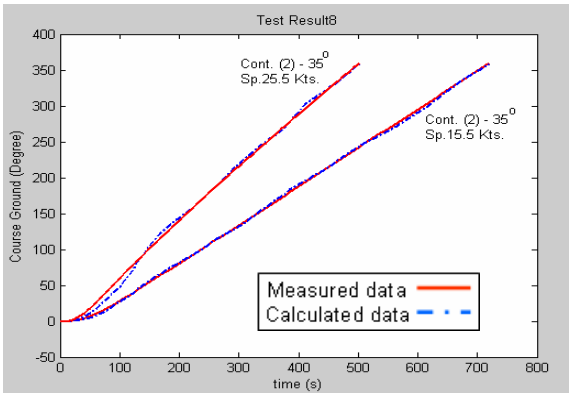

Figure 6.22.7: Test results of the course ground, Containership (2)

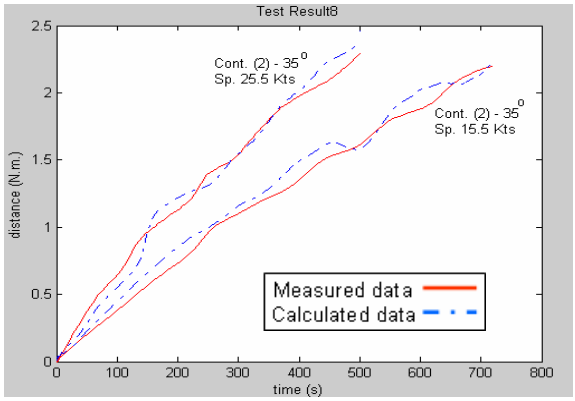

Figure 6.22.8: Travel distance, Containership (2)

Figure 6.22: Testing results of force model (series 1), simulation of the turning manoeuvre motion of Container ship (2) using $\delta_{r=}$ -35° to starboard side but different speeds (15.5 *Kts.* & 25.5*kts*.)

Appendix F

Figures of the training results of Chapter 6: "Ship Analytics Ship simulators":

F. 1

Figures 6.23 and 6.24 show the training, goal and performance of the data files of "Ship Analytics Ship Simulators" with "Norcontrol Simulators" data files. The numbers of epochs and goal results in the two processes indicate that both simulators are accepted to be trained in NNs mathematical model.

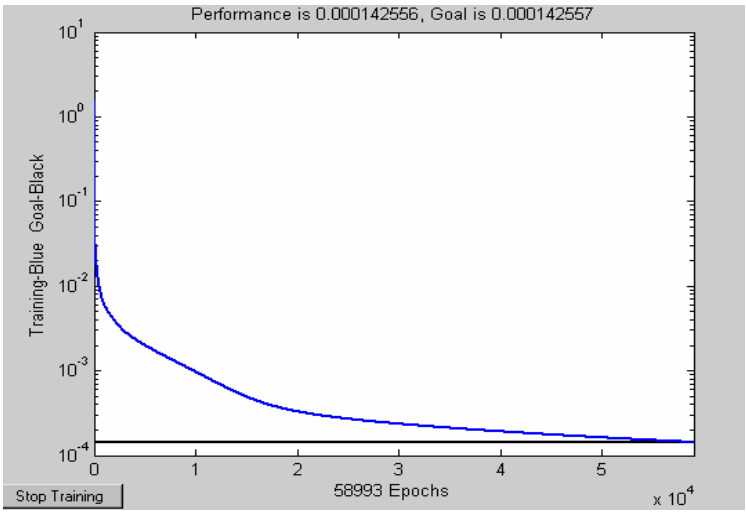

Figure 6.23: Epochs and performance of the training process for both simulators measured data

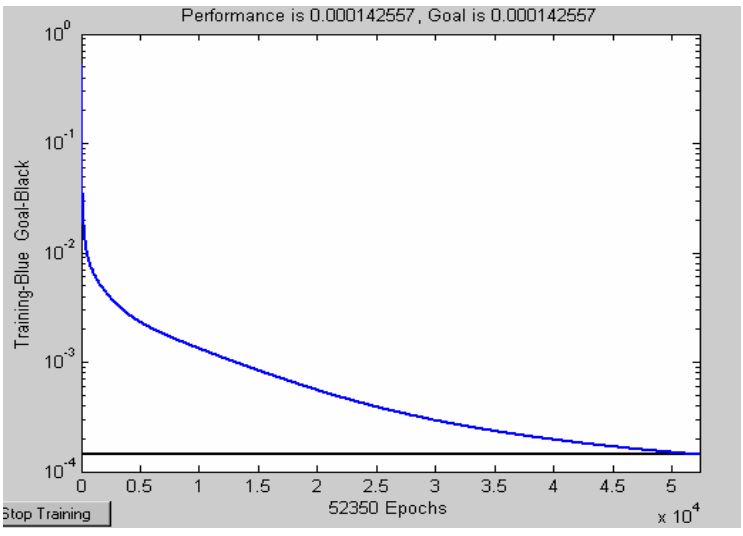

Figure 6.24: Epochs and performance of the training process for both simulators measured data (second iteration)

The results of the previous training process are shown in the next two figures.

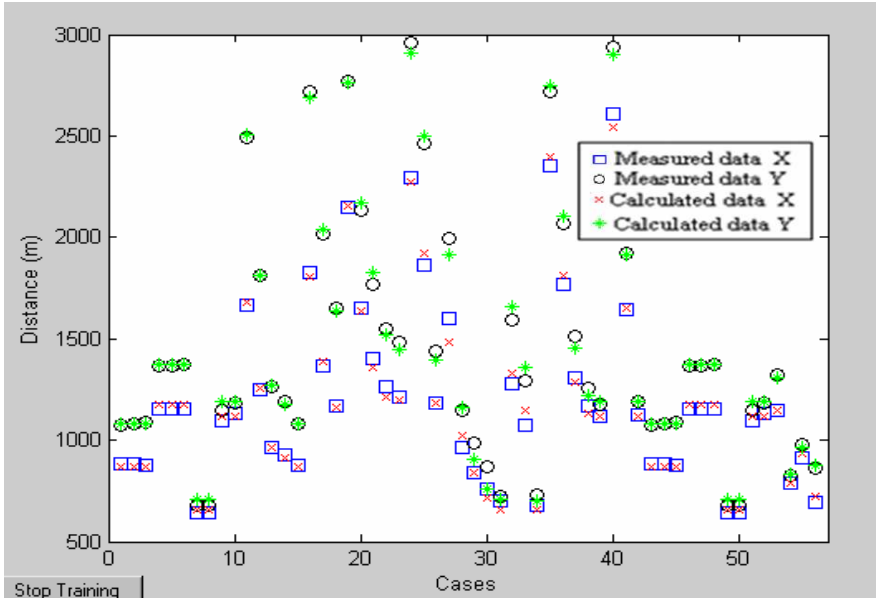

Figure 6.25: Results of the training performance of figure 23 Norcontrol Simulators and Ship Analytics Ship Simulators

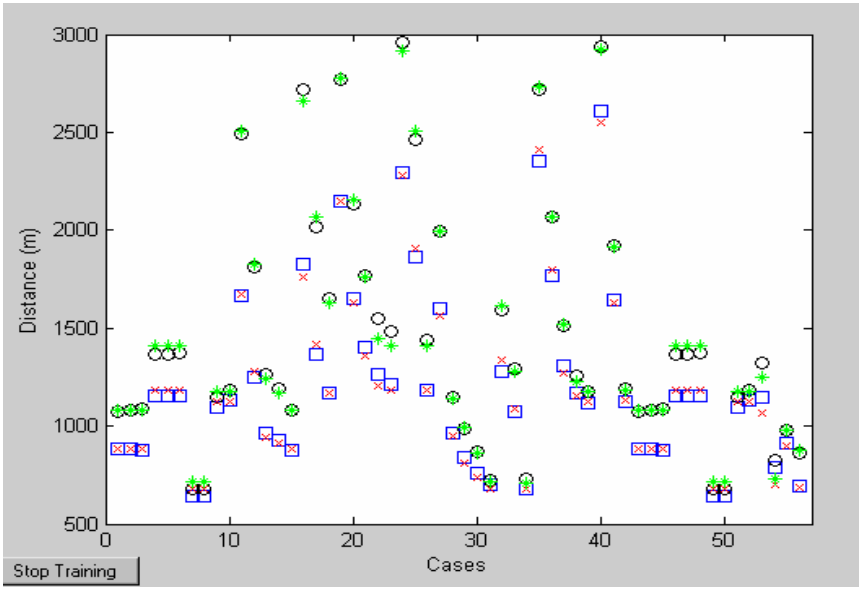

Figure 6.26: Results of the training performance of figure 24 Norcontrol Simulators and Ship Analytics Ship Simulators

F. 2

Figures of the testing results of Chapter 6: "Ship Analytics Ship simulators":

The results of the blind manoeuvres of four different ships (two Containerships, one Bulk carrier and one VLCC) of Ship Analytics Ship Simulators which are different in sizes, lengths and the other parameters from the four ships of Norcontrol simulators.

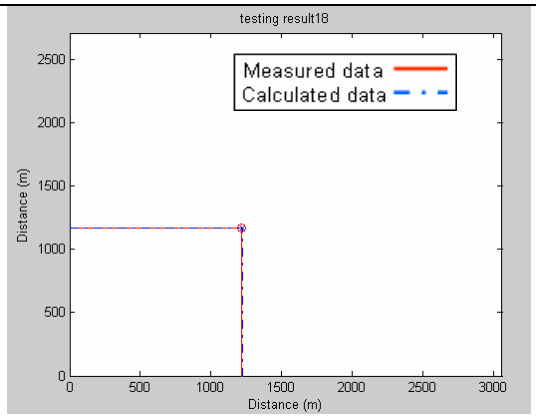

Fig. 6.27.1: Container 1, Δ = 48598.15, *LPP* = 206.96, Speed 22 *Kts* & δ_r = -27 ^{o}

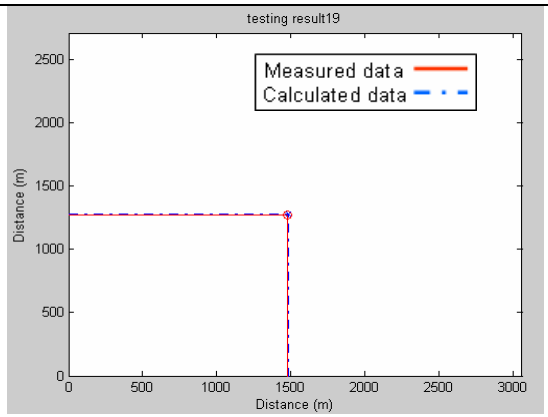

Fig. 6.27.2: Container 2, Δ = 71707.35, *LPP* = 274.76, Speed 18.8 *Kts* & δ_r = -30 ^{o}

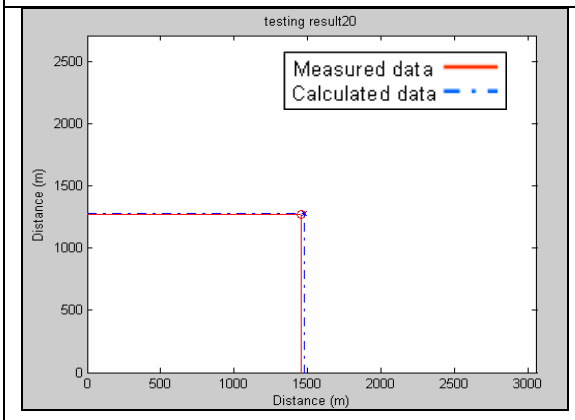

Fig. 6.27.3: Container 2, Δ = 71707.35, LPP = 274.76, Speed 14.7 *Kts* & δ_r = -35 ^{o}

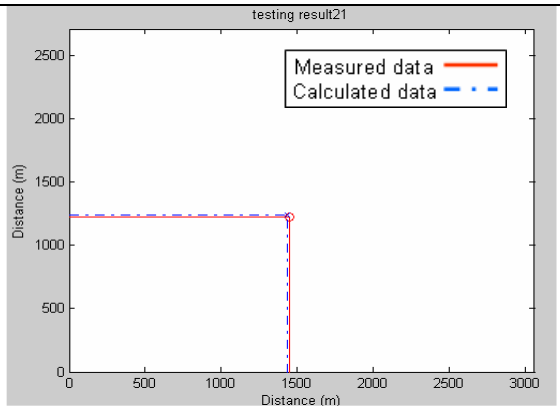

Fig. 6.27.4: Container 2, Δ = 71707.35, LPP = 274.76, Speed 7.88 *Kts* & δ_r = -35 ^{o}

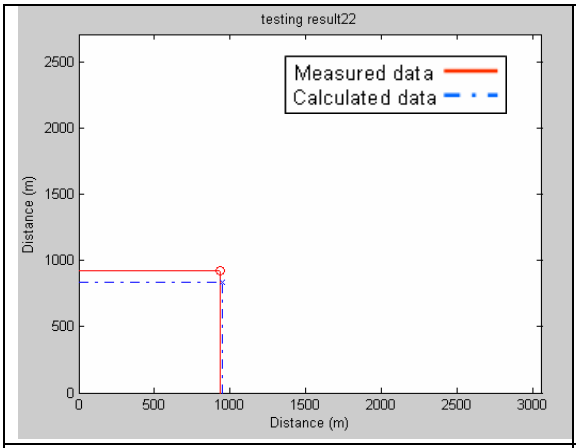

Fig. 6.27.5: Bulk Carrier, Δ = 90093.69, *LPP*= 226.65, Speed 12.97 *Kts*& δ_r = -25 ^{o}

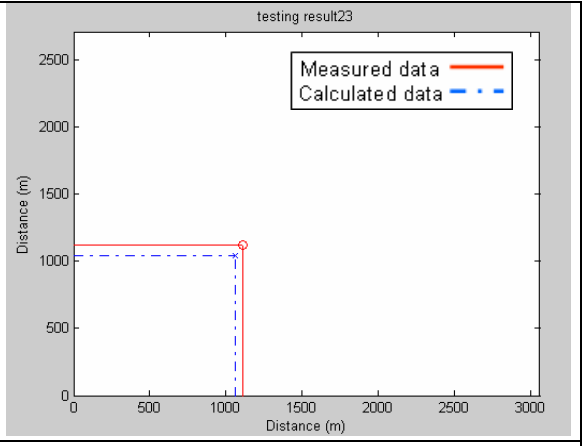

Fig. 6.27.6: VLCC, Δ = 347752.3, *LPP* =322.17, Speed 15.4 *Kts* & δ_r = -26 ^{o}

Figure 6.27: Test results of the maximum advance and total diameter using various rudder angles to starboard side (Direct Model), (Ship Analytics Ship Simulators)

F. 3

The results of the blind manoeuvres of "Ship Analytics Ship simulators" show the turning maneuvers tracks predication in figure 6.28 and the only good results of the simulation in figure 6.29.

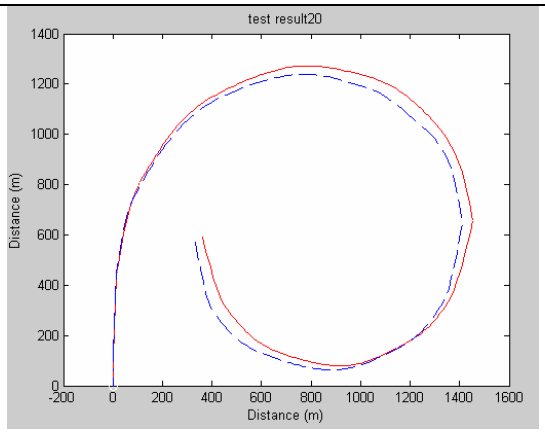

Fig. 6.28.1 Container 2, Δ = 71707.35, *LPP* = 274.76, Speed 14.7 *Kts* & δ_r = -35 ^{o}

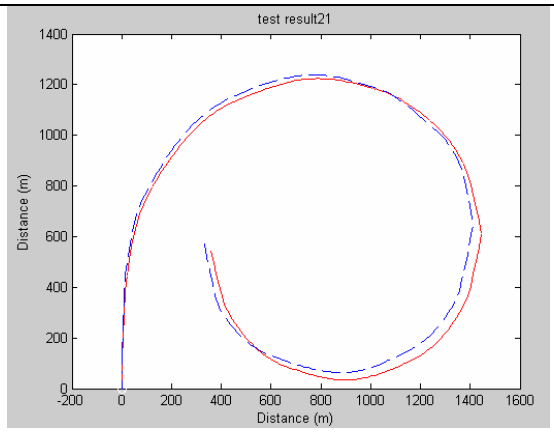

Fig. 6.28.2 Container 2, Δ = 71707.35, *LPP* = 274.76, Speed 7.88 *Kts* & δ_r = - 35 ^{o}

Figure 6.28: Test results of turning manoeuvre tracks of Container ship 2 at two different speeds with same rudder angles (Direct Model)
(Ship Analytics Ship Simulators)

F. 4

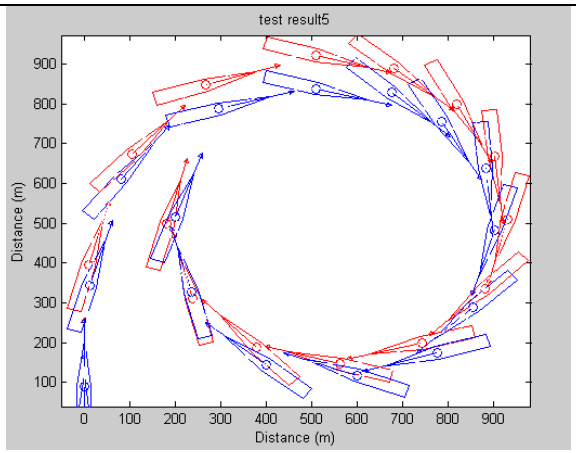

Fig. 6.29.1 Bulk Carrier, Δ = 90093.69, *LPP* = 226.65, Speed 12.97 *Kts* & δ_r = - 25 ^{o}

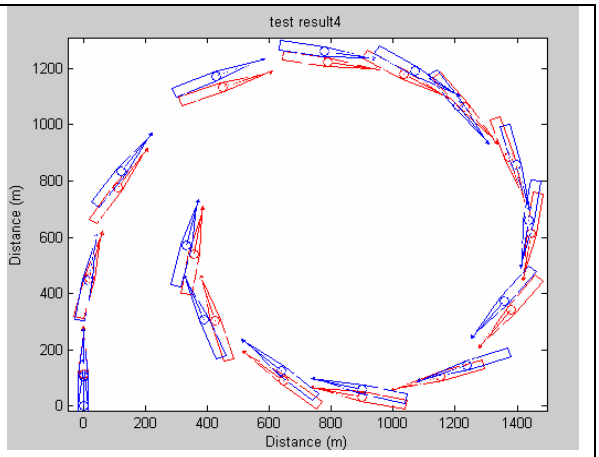

Fig. 6.29.2 Container 2, Δ = 71707.35, *LPP* = 274.76, Speed 7.88 *Kts* & δ_r = - 35 ^{o}

Figure 6.29: Test results, prediction of turning manoeuvre of two different ships' types using different rudder angles to starboard side (Direct Model)
(Ship Analytics Ship Simulators)

Appendix G

Table G.1: Main Ship Parameter and Input Data (Norcontrol Simulators)

Type of ship **Condition** **Ship No.**	**Container** **Loaded** **1281**	**Container** **Loaded** **3011**	**Bulk Carrier** **Loaded** **1225**	**Tanker** **Loaded** **1223**	**Input** **Data** **(*)**
Displacement m^3	42275	65,366	73096	269869	*
L.P.B. m	230,5	280.00	219.0	310	*
Length overall m	241.10	294.06	234	322	
Breadth moulded m	32.20	32.20	32.2	56	*
Draught m	10.15	11.45	12.8	20	*
Wetted Surface m^2	8021	11,436	10153	17721	
Wind area, side m^2	4633	1,004	2043	7101	
Wind area, front m^2	872	6,800	648	1706	
Block coefficient	0.561	0.63	0.810	0.7905	*
Trim by the stern, %	0	0	0	0	
LCB, % of LBP forward of LBP/2	.06	-3.27	2.42	-1.13	
Type of Engine	Diesel	Diesel	Diesel	Diesel	
Number of propellers	1	1	1	1	
Type of propellers	FP	FP	FP	FP	
Direction of rotation	R. Handed	R. Handed	R. Handed	R. Handed	
Propeller diameter	8.0	8.40	6.15	9.35	*
Pitch ratio at 0.7R	1.187	0.95	0.766	0.738	*
Area ratio	0.79	0.50	0.447	0.580	*
Shaft Power (Ahead) MW	37.08	36.80	5.00	17.87	*
Shaft Power (Astern) MW	37.08	36.80	5.00	17.87	
Number of rudders	1	1	1	1	
Type of rudders	Semi- Spade	Semi-Spade	Spade	Semi-Spade	
Position	In CL	In CL	In CL	In CL	
Area of each rudder, incl. ½ horn (m^2)	52.6	74.60	45.5	82.9	*
100 x total rudder area /LBP x T⊗	2.25	2.33	1.62	1.34	*
Turning velocity of rudder °/sec.	2.50	2.80	2.50	2.50	
Max. rudder angle °	35	35	35	35	*
Number of bow thrusters	1	1	0	0	
Nominal bow-thruster force(kN)	147	2.000	-	-	
Numbers of stern thrusters	1	0	0	0	
Nominal stern thruster force(kN)	98	-	-	-	

In addition to the input data mentioned above the following data are used as input to ANN:

Control data:

Rudder angle (δ_r), rudder moment, number of blades (z), propeller pitch (P_p), propeller diameter (D_p), blade area ratio, revolution per minute (RPM) and ship's speed (U),

Ship parameters:

Lateral area (A_{HL}), ship's pivot pint ($P.P$) and ship's main ratios. Inputs numbers and formations depend on the type of application.

G.2

NORCONTROL NAVSIM
(Models Documentation)

Doc. no. 1859a, Page 4 of 41 wrote: The realism of the simulated ship's behaviour depends upon the complexity and exactness of the mathematical model. Page 5 of 41 wrote: In NANSIM the real ship is replaced by a computer and a mathematical model. See illustration. Consequently the own ship can be navigated in the same way as a real ship.

Table G.3

Main Ship Parameter and Input Data (Ship Analytics Ship Simulators)

Type of ship **Condition** **Ship No.**	**Container** **Loaded** **30K**	**Container** **Loaded** **50K**	**Bulk Carrier** **Loaded** **70K**	**Tanker** **Loaded** **1223**	**Input** **Data** **(*)**
Displacement m^3	48598	71707.35	90093.69	347752.25	*
L.P.B. m	206.96	274.76	226.65	322.17	*
Length overall m	220	290	240.00	340.00	
Breadth moulded m	32	33	35	56.00	*
Draught m	11	13	14.00	22.00	*
Block coefficient	0.650	0.762	0.791	0.854	*
Trim by the stern, %	0	0	0	0	
Type of Engine	Diesel	Diesel	Diesel	Diesel	
Number of propellers	1	1	1	1	
Type of propellers	FP	FP	FP	FP	
Direction of rotation	R. Handed	R. Handed	R. Handed	R. Handed	
Propeller diameter	6.9	7.19	6.10	9.10	*
Pitch	6.15	6.4	4.38	6.51	*
Shaft Power (Ahead) MW	22.48	20.88	7.658	24.161	*
No. of blades	5				*
Number of rudders	1	1	1	1	
Type of rudders	Semi- Spade	Semi-Spade	Full. blanced	Full-Spade	
Position	In CL	In CL	In CL	In CL	
Area of each rudder, incl. ½ horn (m^2)	37.2	55.93	52.58	120.77	*
100 x total rudder area /LBP x T⊗	1.63	1.57	1.66	1.70	*
Max. rudder angle °	35	35	35	35	*

Note: *(This quality of ships figures of the following appendices were only available)*

Appendix H:

H. 1

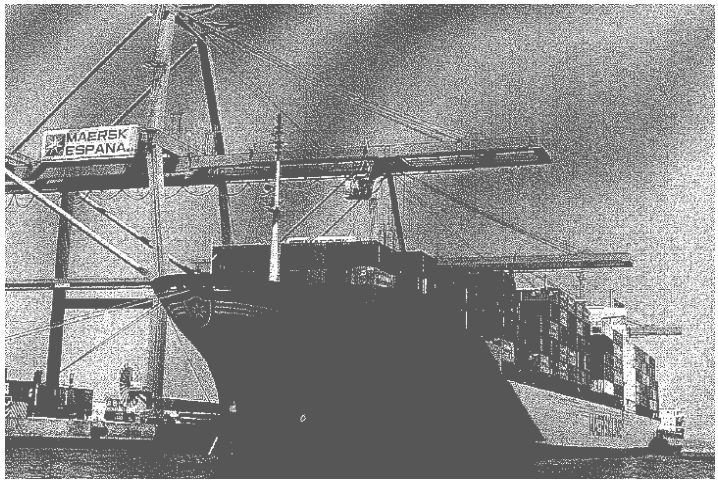

Figure H.1.1: Containership 1 (Luna), during cargo operation,
MDI (Danish Maritime Institute), simulator mathematical model updated in 2001

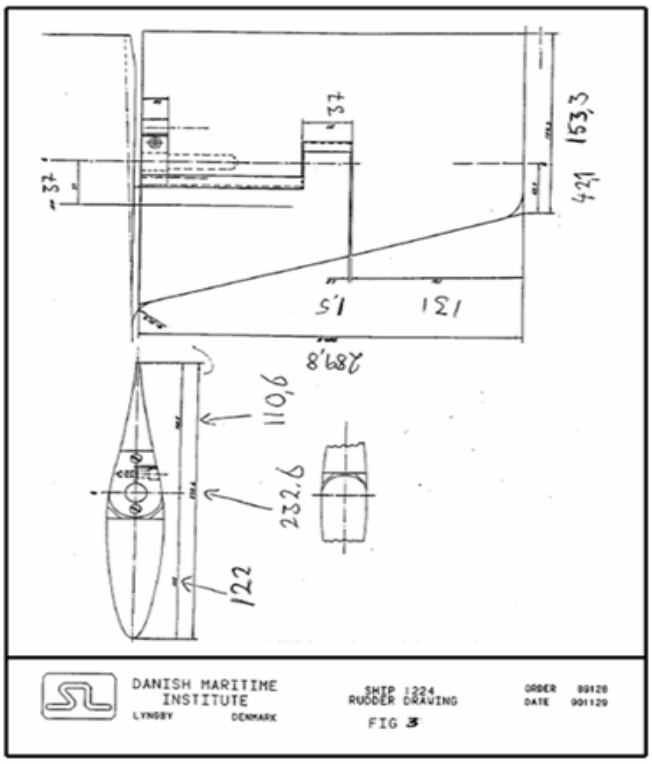

Figure H.1.2: Containership 1 (Luna), ship rudder drawing,
MDI (Danish Maritime Institute)

H. 2

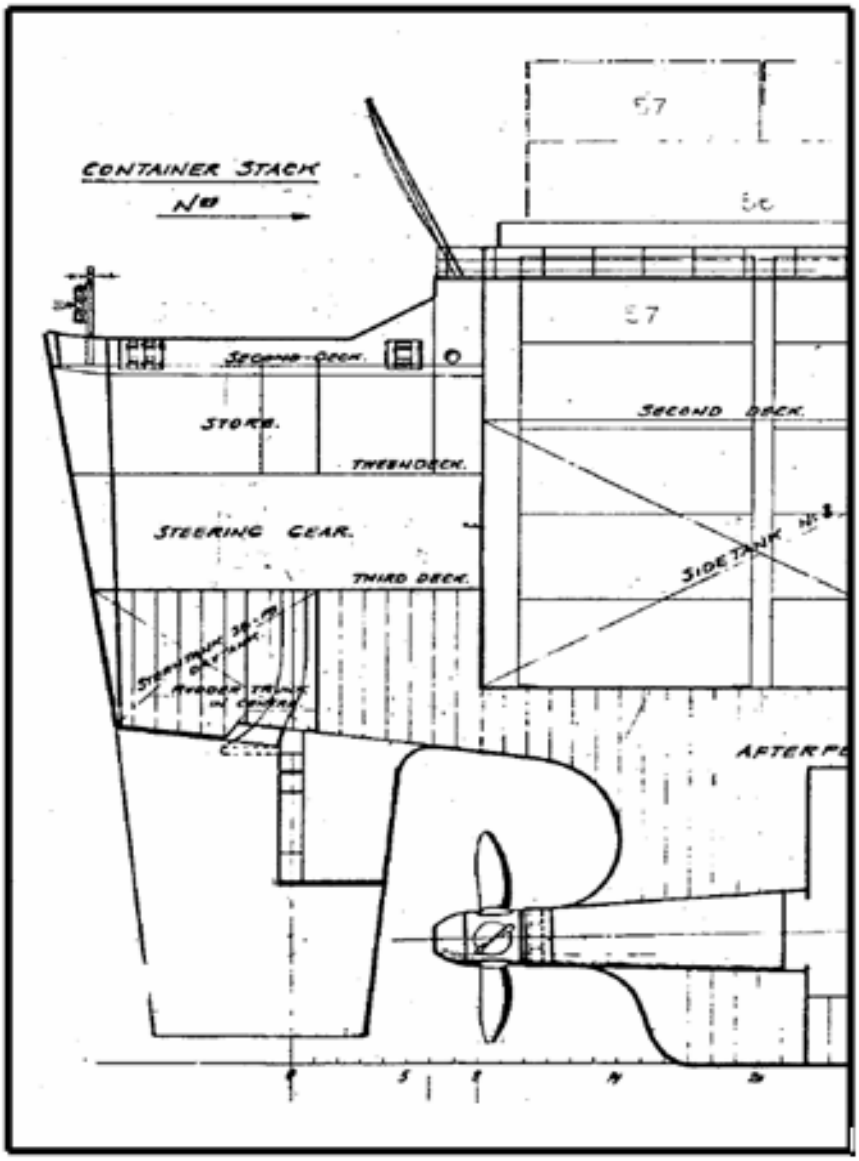

Figure H.2.1: Containership 2 (Jutlandia), a stern profile of rudder and propeller
MDI (Danish Maritime Institute), simulator mathematical model updated in 2001

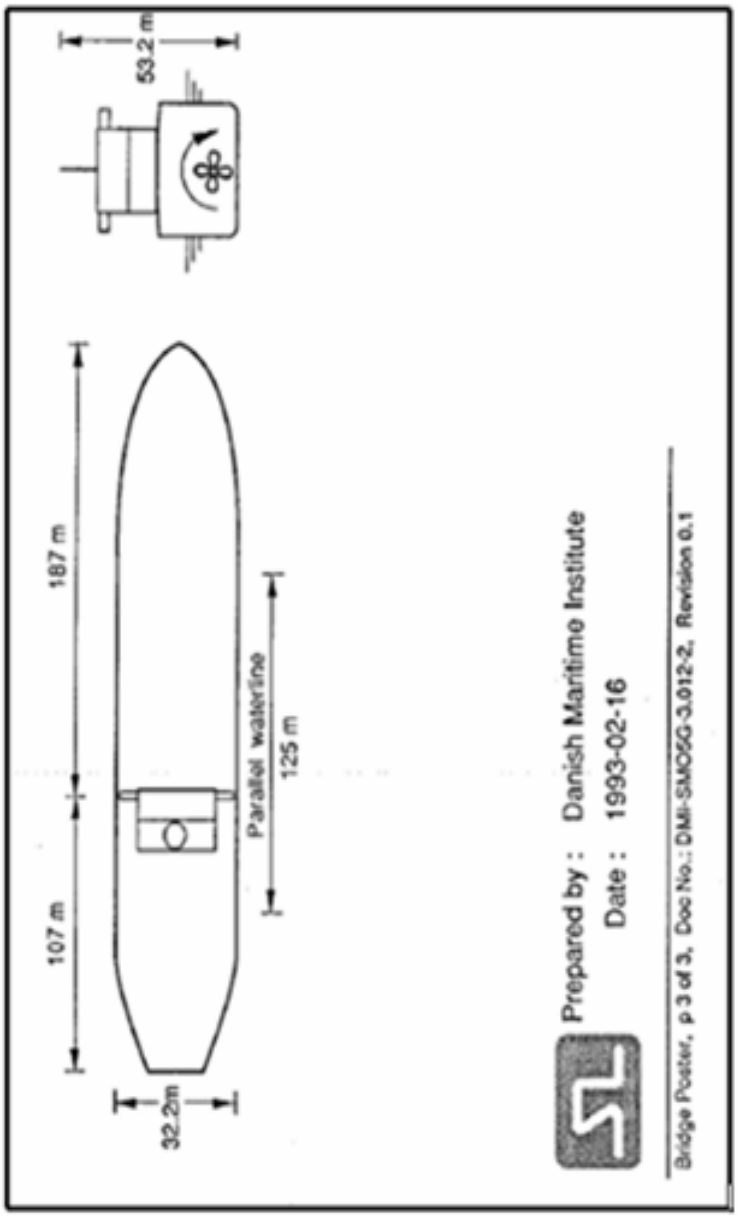

Figure H.2.2: Container ship 2 (Jutlandia), water plan at loaded draft. MDI (Danish Marin Institute)

H. 3

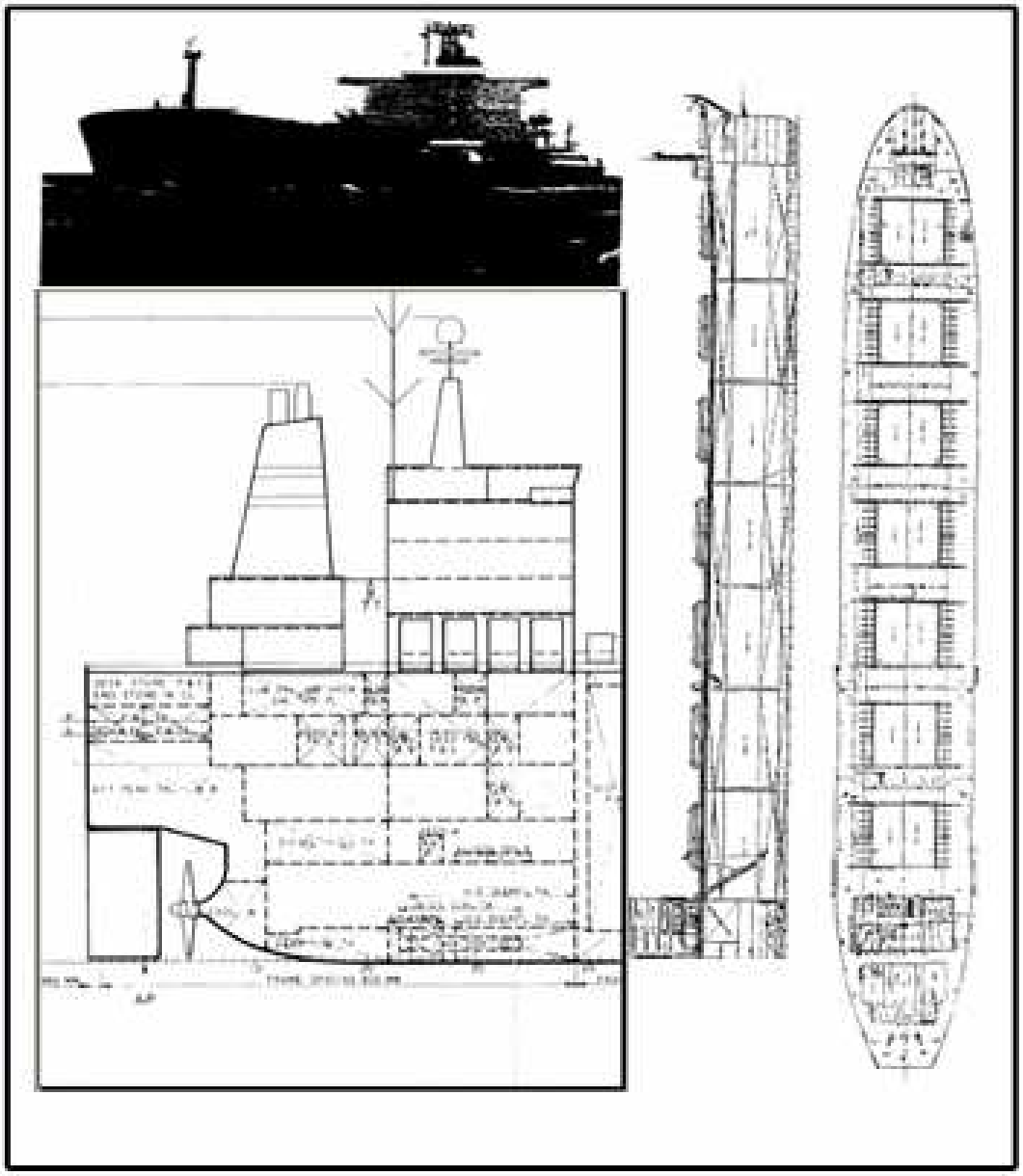

Figure H.3: Bulk carrier (Norseman), a stern, ship profile and plan view
MDI (Danish Maritime Institute), simulator mathematical model updated in 2001

H. 4

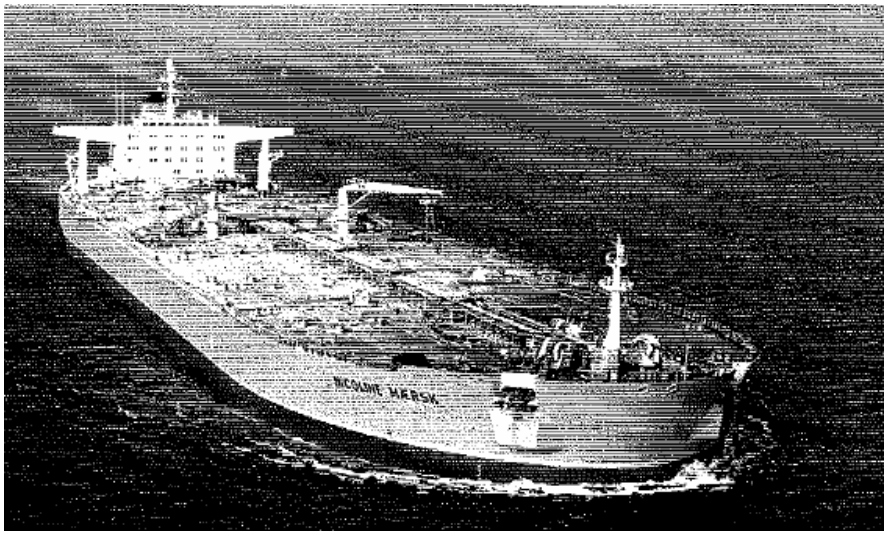

Figure H.4.1: VLCC (Nicoline), during sailing time,
MDI (Danish Maritime Institute), simulator mathematical model updated in 2001

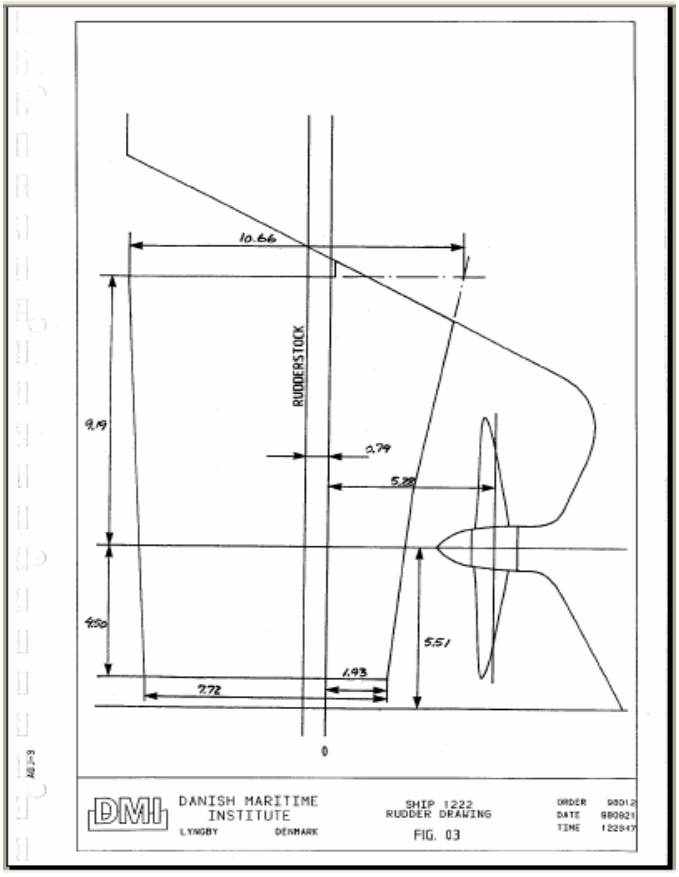

Figure H.4.2: VLCC (Nicoline)

A stern profile of rudder and propeller.

MDI (Danish Maritime Institute)

Appendix I

Ship Analytics Ship Simulators

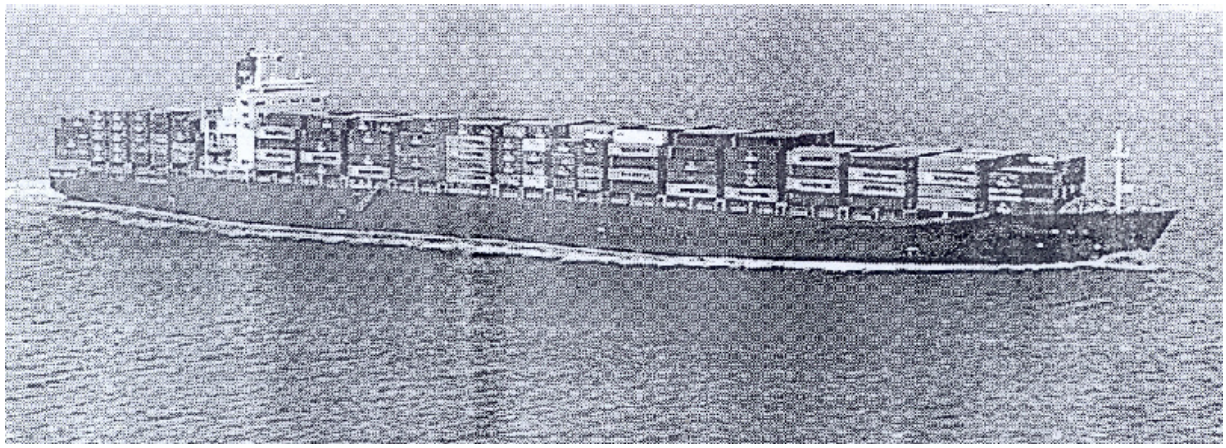

Figure I.1: Containership 2 (Code: C057L), Simulator Ship: GIN505F

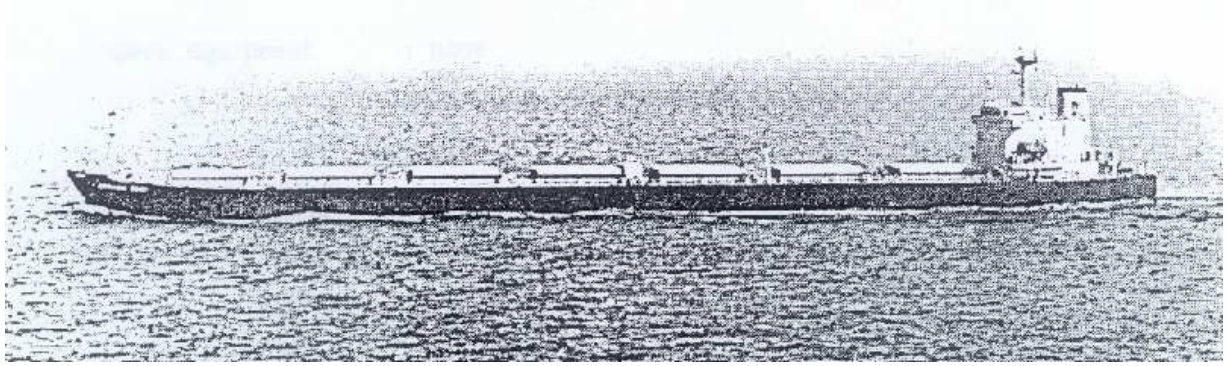

Figure I.2: Bulk Carrier (Code: K070L), Simulator Ship: GIN523F

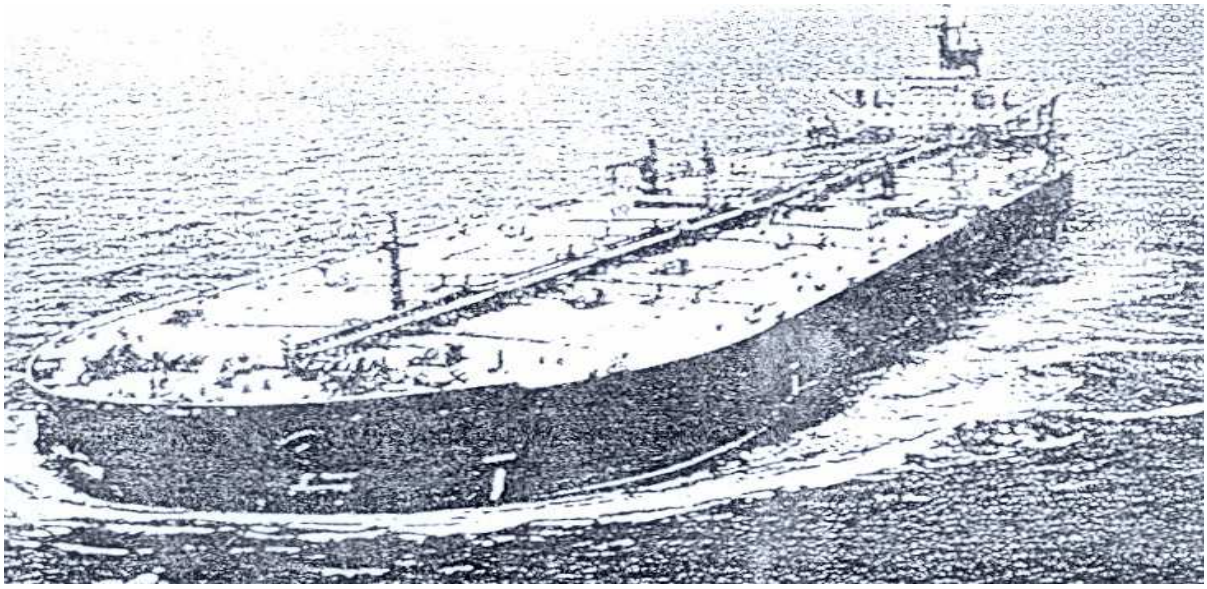

Figure I.3 VLCC (Code: T300L), Simulator Ship: GIN517F

Curricuclum Vitae (C.V.)

Personal Data

Name/Sir Name Adel Ebada

Address Institute of Ship Technology und Transport Systems (IST)
BK 118
Bismarckstr. 69
47057 Duisburg, Germany.

6 Omar Lotfy St. # 7 – Camp-Seizer, Alexandria, Egypt.

Arab Academy for Science and Technology and Maritime Transport (AAST) & (MT).
College of Maritime Transport & Technology
P.O. Box 1029
Miami, Alexandria, Egypt.
Fax: 0020-3-5623362

Tel. Handy (Egypt): 00-20-101635113 - Res: 00-20-3-5921624
Handy (Germany): 00-49-1797909861

E-mail adel_nav@yahoo.com

Language: English Good Command, Deutsch Learning & Arabic

Education

1994	Master Certificate, AAST & MT
1995	Marine Expert NO 807.
1998	Bachelor Degree (Nautical Technology), AAST & MT
1999	The High Diploma Degree in Advanced Navigation, AAST& MT

2001	Master of Science in Maritime Affairs, World Maritime University, Malmö – Sweden
2007	Ph.D. (Doctor-Engineer), University of Duisburg/Essen - Germany

Employment & Experiences (Last ten years)

1997 Till Present	AAST & MT. Marine Lecturer And Examiner.

Published Papers

Journal Paper

Ebada, A., *Hydrodynamics and ship Dynamics*, The Alumni Maritime Journal, World Maritime University, Malmö – Sweden, 2001.

Ebada, A., Abdel-Maksoud, M., "*Applying Artificial Intelligence (A.I) to Predict the Limits of Ship Turning Manoeuvres*", STG meeting, News from Hydrodynamics and Manoeuvring, Hamburg, September 2005.

Ebada, A., *Ship stability and parametric Rolling*, (Arab Academy for Science and Technology and Maritime Transport (AAST), Vol.30 No.60, July 2005.

Ebada, A. and Elbwab, M., *The Impact of New Technology on Education*, Magazine of Arab Institute of Navigation, Alexandria, Egypt, 2006

Conference Proceedings

Ebada, A., *Implementation of Satellite Navigation Enhance Marine Seismic Vessel*, International Navigation Conference on satellite Navigation Developments and Applications, Cairo, Egypt, April 13-15, 2004.

Ebada, A., Abdel-Maksoud, M., "*Applying Neural Networks to Predict Ship turning track manoeuvring*" , 8th Numerical Towing Tank Symposium, Varna, Bulgaria, October 2005.

Ebada, A., Abdel-Maksoud, M., "*Prediction of ship turning manoeuvre using Artificial Neural Networks (ANN)*" , 5th International Conference on Computer and IT Application in the Maritime Industries, Delft, Netherlands, May 2006.

.